Thresholds of Temperature and Time for Mars Sample Return: Final Report of The Mars Sample Return Temperature-Time Tiger Team

The Temperature and Time Tiger Team:

Mark A. Sephton[1], Kate Freeman[2], Lindsay Hays[3], Fiona Thiessen[4], Kathleen Benison[5], Brandi Carrier[6], Jason Dworkin[7], Mihaela Glamoclija[8], Raina Gough[9], Silvano Onofri[10], Ron Peterson[11], Richard Quinn[12], Sara Russell[13], Eva E. Stüeken [14], Michael Velbel[15,16], and Mikhail Zolotov[17]

1) Imperial College London, Earth Science and Engineering, South Kensington Campus, London, UK SW7 2AZ; 2) The Pennsylvania State University, Geosciences, 235 Deike Building, University Park, PA, US 16802-1503; 3) NASA Headquarters, Mars Sample Return Program, 300 E St. SW Headquarters, Washington, DC, US 20546; 4) European Space Research and Technology Centre, Noordwijk, South Holland, NL; 5) West Virginia University, Department of Geology and Geography, Morgantown, US; 6) Jet Propulsion Laboratory, California Institute of Technology, Pasadena, CA, US; 7) NASA Goddard Space Flight Center, Astrochemistry, Code 690, Greenbelt, MD, US 20771; 8) Rutgers University Newark College of Arts and Sciences, Earth and Environmental Sciences, Newark, NJ, US 07102; 9) University of Colorado, Department of Chemistry and Biochemistry, UCB 216, Boulder, CO, US 80309; 10) University of Tuscia, Department of Ecological and Biological Sciences, Largo dell'Università snc Viterbo, IT 01100; 11) Queens University, Kingston, ON, CA; 12) NASA Ames Research Center, Moffett Field, CA, US 94035; 13) Natural History Museum, Department of Earth Sciences, London, UK; 14) University of St Andrews, School of Earth & Environmental Sciences, St Andrews, Fife, KY16 9TS, UK; 15) Michigan State University, Earth and Environmental Sciences, East Lansing, MI, US 48824-1312; 16) Smithsonian Institution, Department of Mineral Sciences, National Museum of Natural History, Washington, US 20013-7012; 17) Arizona State University, School of Earth and Space Exploration, Tempe, AZ, US AZ 85287-1404

Address correspondence to:

Mark A. Sephton, Department of Earth Science and Engineering, Imperial College London, UK, SW7 2AZ. Tel: +44 (0)20 7594 6542; Fax: +44 (0)20 7594 7444; E-mail: m.a.sephton@imperial.ac.uk

Running title:

Report of The MSR Temperature-Time Tiger Team

Contents

Executive Summary

The Time-Temperature Tiger Team (T4) was chartered by NASA and ESA to evaluate the potential for degradation or alteration of the Mars Sample Return (MSR) samples if they are exposed to temperatures between +30 and +60 ^{0}C, and to what extent this alteration may reduce the scientific value of the samples. Thirteen scientists were selected to represent scientific disciplines expected to be most affected by sample heating. Team expertise helped in understanding whether exposing samples to temperatures between +30 and +60 ^{0}C poses risk to the sample integrity and, therefore, to future scientific investigations.

Key processes identified were as follows: the release of volatiles by desorption and sublimation and release from condensed phases (interiors, decomposition, dehydration); chemical reactions including gas-gas and gas-solid; deliquescence of hygroscopic salts; acid/base interactions (potential for extreme pH conditions); aqueous redox reactions, isotopic exchange (aqueous phases, minerals, gases, organic phases); condensation and freezing (in the after-heating cooling phase); and interactions with the sample tube materials. There is potential for multiple interactions and

overlapping effects.

For inorganic materials and their records, over both long time scales (hours to days) and short time scales (minutes to hours), no temperature excursion above +30 °C could be accommodated without loss of science. There would be some robust constituents (feldspars, quartz, pyroxenes, etc.) that are unaffected but also less robust constituents (salts, phyllosilicates, radicals, etc.) that would be affected across all temperature ranges ≤60 °C.

For organic materials, in particular organic biosignatures, the risks reflect that preservation is reliant on a number of processes, and a change in one component within a sample tube can affect another. For organic materials, over long timescales of hours to days no temperature excursion above +30 °C could be accommodated without loss of science, but over shorter time scales (minutes to hours), raising the temperature to 40 °C could be manageable without major disruption to science, whereas temperatures above 40 °C would lead to significant losses.

The consideration of these findings by the MSR team will help to maintain the fidelity of samples returned from Mars in the future and maximize scientific return when analyzed in Earth laboratories.

1. Introduction

Mars Sample Return (MSR) has been a top priority of the planetary science community for decades due to its potential to significantly advance our understanding of Mars, our solar system and beyond, including in diverse disciplines such as astrobiology, geology, geochemistry, and many others. The joint NASA-ESA MSR Campaign intends to collect samples of Mars rocks, regolith, and atmosphere and return them to Earth. Once samples have arrived in Earth laboratories, they would be subjected to analytical procedures that provide unprecedented levels of sensitivity, accurcy, and resolution. MSR is a multi-agency effort, and the first stage of the campaign is underway with the NASA Mars2020 *Perseverance* rover mission collecting and caching samples on the surface of Mars. Future stages will involve the collection of cached samples and the planned return of samples in the 2030s.

1.1. Temperature and Mars Sample Return

Each individual Mars 2020 (M2020) sample tube has an interior diameter of 1.3 cm and a maximum possible core length of 7.6 cm, which gives each a maximum capacity of 10 cm^3 of sample material (Moeller et al., 2021). An intact core of unaltered basalt (ϱ = 3.0 g cm^{-3}) fully occupying the tube would weigh ~30 g; porous rocks, fragmented samples, or regolith could fully occupy the tube with as little as ~10 g of solid sample; and tubes only partially filled could contain even less.

At certain times during the MSR Campaign, there is a possibility of the maximum allowable temperature, as defined by mission requirements, being violated for the Returnable Sample Tube Assemblies (RSTAs; Fig. 1). To minimize heating while exposed to sunlight, the tube surfaces are coated with a white "paint" to reduce thermal absorptivity. However, white paint was not applied to portions of the tube involved in tube manipulation. The heterogeneity in coating color will cause the tube to experience uneven heating. The modeled worst-case heating (WCH) of a sample tube cached at Jezero Crater is shown in Fig. 1 (Novak et al. 2022). The thicker end of the tube will achieve the highest temperatures, because of the unpainted surface present.

The maximum calculated temperature for the upper portion of the tube that is used for sample tube manipulation is +53.4 °C. However, the temperature of the tube will be significantly lower in much of the cylindrical portion that holds the sample, where the temperature increase will only be to about +30 °C in the modeled WCH. It remains unclear how tube temperature relates to sample temperature for different potential sample types and orientations inside the tube. These calculations also assume that no heat is transferred to the ground; in the more realistic scenarios described below there are operational parameters that could limit the maximum level of heating. To provide more realistic sample temperature estimates, additional thermal modeling of the sample temperature inside the cached tubes will be required now that the collected sample compositions and cached locations in the Three Forks depot are known.

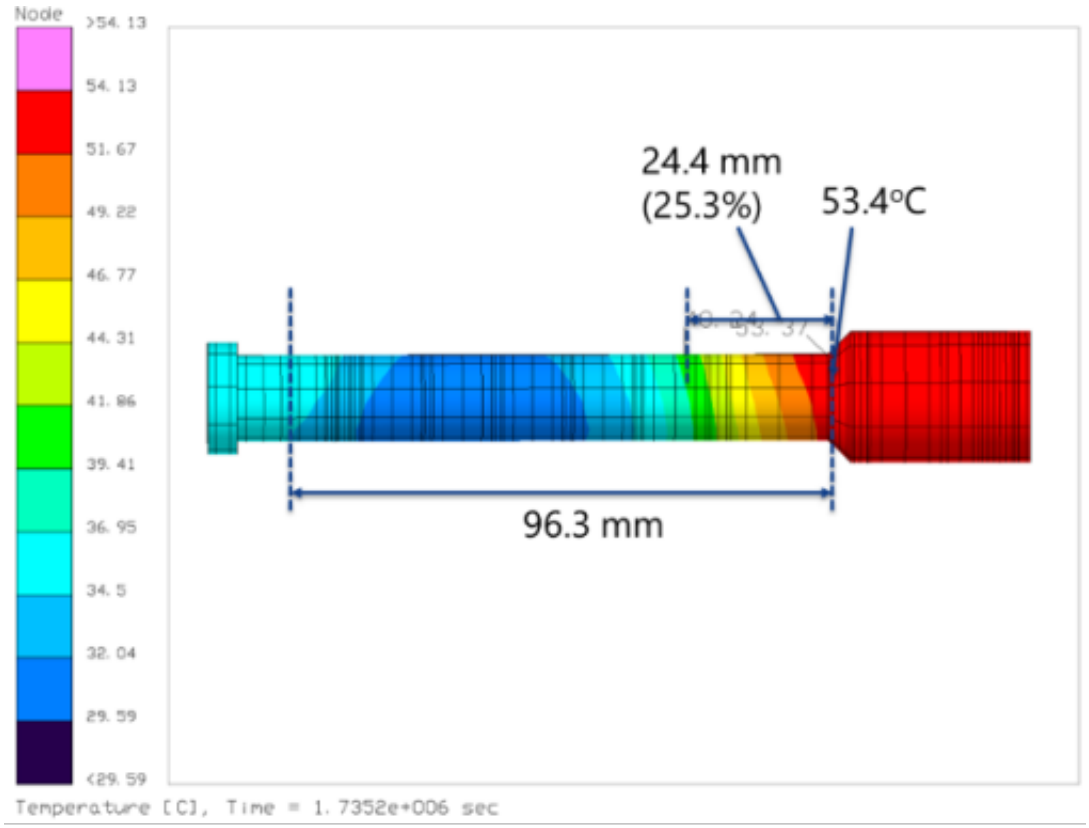

FIG. 1 Worst-case heating of an empty sample tube cached at Jezero Crater based on M2020 modeling (Novak et al. 2022). Approximately 25% of the tube could exceed 40°C but significant portions of the tube remain at <35 °C. It is unclear how tube temperature relates to the temperature of the collected sample for different potential sample types.

Based on the analysis by the Returned Sample Science Board (RSSB, 2018), M2020 accepted a requirement that no single point on any single sample would reach a temperature in excess of +60°C (with the possible exception of the outer 1 mm of cored samples during drilling due to frictional heating). While cached on the ground, the sample tubes will be subject to diurnal solar radiation. This will cause the temperature of the samples to increase during the day and decrease during the night. Whether the requirement will be met was assessed by worst-case modeling of the temperature of the samples when exposed to diurnal heating on the martian surface while cached (see Fig. 2).

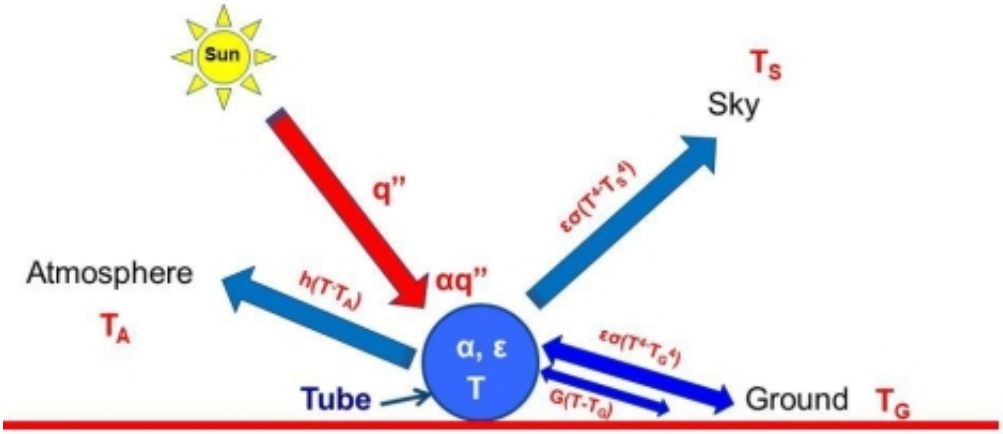

FIG. 2 Graphic illustration of the closed form thermal model used by Redmond et al. (2017) to model the temperature of the sample tubes in response to exposure at the martian surface.

With regard to the quantitative modeling described in the previous section, several factors that relate to the heat flux need to be considered. There are three primary aspects related to how the sample tubes are cached that affect their temperature: i) the thermal inertia of the substrate, ii) the albedo of the ground, and iii) the ground slope (which affects the solar insolation). Each of the three aspects can have an effect of about ±5 °C on the sample temperature. Taking advantage of all three factors would result in reducing the overall sample temperature by about 15 °C. The three aspects of sample cache location are under operational control and cannot be predicted in advance. Thermal modeling

has, therefore, typically taken the approach of assuming the worst-case scenario.

For a sand-rich location, the ground would have a lower thermal inertia and, therefore, would be a poor heat sink and would reach a higher peak ground temperature. However, thermal contact with the tube may be better. For a rock-rich location, there would be poor thermal contact, a higher thermal inertia, a lower peak ground temperature, and a better heat sink opportunity. In modeling sample tube temperature, previous work (Redmond et al. 2017) ignored thermal conduction into the ground, in large part because of uncertainties in heat flow between the tube and the sample, and the tube and the ground. However, for ground that has a high thermal inertia (TI = 350 J m^{-2} K^{-1} $s^{-½}$), the effect of heat loss to the ground could reduce tube temperature by up to 10°C (relative to a theoretical hovering tube). For a fine-grained ground that has a low thermal inertia (TI = 220 J m^{-2} K^{-1} $s^{-½}$), the effect of heat loss to the ground could be about -5°C. Thus, sample tubes cached on rock (or rocky regolith) rather than on sand (or soil) could experience an up to 5°C lower temperature.

Higher ground albedo would result in lower ground temperatures but also increased reflected solar flux on the tube. The tubes will experience higher temperatures on higher-albedo ground than on lower-albedo ground. Overall, it has been estimated that higher ground albedo will increase the temperature of the tube by up to 5°C (Redmond et al., 2017).

Modeling shows, as expected, that the effect of north- vs. south-facing ground slope is strongly latitude-dependent (Redmond et al., 2017). There is greater heating for the tubes placed along contour rather than perpendicular to the contour, but the difference is minimal. At the latitude of Jezero Crater (18.4 N), the south-facing slopes experience about 5-10°C lower temperatures than north-facing equivalents. In summary, placing the tubes perpendicular to contour on south-facing slopes would minimize heating.

1.2. Temperature and Returned Samples

The primary purpose of the MSR Campaign is to bring a diverse collection of scientifically selected martian samples to Earth for scientific investigation. A tenet of sample science is to avoid exposing the samples to novel environments prior to sample analysis. Therefore, the temperature history of the collected samples should not be outside of what was experienced on Mars before collection. The expected and unavoidable temperatures experienced by the samples are provided in Table 1. An example of an unavoidable temperature excursion is that experienced by a sample core boundary as it is being drilled. Given that thermal alteration at this boundary is already anticipated and that the transient heating is localized, it is not considered here. All considerations of loss of science owing to temperature excursions experienced following pickup and delivery to the Mars Ascent Vehicle (MAV) must be placed in the context of what unavoidable temperature changes have already been experienced.

TABLE 1. Range of estimated upper-temperatures likely to be experienced in a worst-case scenario, along with associated durations, by MSR samples (D. Beaty personal communication). Note that the higher temperature excursions are expected to be very transient, and the daily mean is expected to be only a few °C above the temperature of the martian surface.

Phase	Duration	Sample Temperature Range (°C)
Pre-collection	Eons	-20 to +10
Cached in M2020	Years	-65 to +10
Cached on Surface	Years	+5 to +53
Transfer to Orbiting Sample (OS)	Months	+30 to +53
Mars Ascent Vehicle (MAV) launch	Minutes	+30

OS Orbit	Weeks	-60 to -40
Capture, Containment, and Sterilization	Hours	
Return Cruise	2 Years	-40
Pre-Entry, Descent and Landing (EDL)	Days	-40
EDL	Minutes	-40 to +25
Recovery	Hours	< +30
Curation	Years	< +25

Beyond inevitable temperature and time encounters, there are existing temperature requirements (L1.5), which are expressed as follows:

- "The external temperature of the RSTAs over the allowable sample region as defined by D-101383 "Returnable Sample Tube Assembly (RSTA) Definition Document" shall be maintained below an Allowable Flight Temperature (AFT) of -20 °C except for periods of unavoidable operational transients for which the AFT is +30 °C."
- Note 1: A temperature history estimate based on ground and/or flight validated thermal models will be provided for transients during which the temperature is expected to exceed -20 °C. Accuracy goal is ± 5 °C when above -20 °C.
- Note 2: Transients which exceed +30 °C will be managed in the context of each Project's specific temperature requirements and be subject to review and approval by the MSR Program.

The above requirement statement is based on the long-standing conclusion that it is manageable to science for the RSTA temperature to be increased to as much as +30 °C. With regard to Temperature and Time Tiger Team deliberations, we assumed, conservatively, that the sample temperature equals the RSTA temperature. However, as per Note 2, the implementation engineers have identified several operational intervals during which it may be necessary to carry out an engineering step that results in a transient thermal event that heats the samples above this threshold.

Note 2 also states that requests to exceed +30 °C will be reviewed and discussed prior to a request for waiver approval. Waiver requests to exceed the temperature maximum of +30°C may involve different temperatures and different durations in the sample handling pathways as MSR moves forward. This report is intended to provide a response, grounded across the range of fields of relevant returned sample science, to inform upcoming decisions related to the sample temperature requirements for the MSR Program. The focus of this report is primarily on the science loss that would occur due to these temperature excursions, without specific implications for implementation.

1.3. The Temperature-Time Tiger Team

The Temperature-Time Tiger Team (T4) was chartered by NASA and ESA to provide some assessment of the possible loss of science for the returned samples if such heating between +30 and +60 ^{0}C for different amounts of time were to occur. The Statement of Task for the Temperature Time Tiger Team included the following questions:

- A question of highest priority is "how serious are the consequences to the highest priority science objectives (as provided in the International MSR Objectives and Samples Team - iMOST - report) of raising the sample temperature to values in the range of +30 to +40 °C and +40 to +50 °C for various amounts of time?"
- A question of medium priority is "how serious are the consequences of further raising the sample temperature to values in the range of +50 to +60 °C?

This team consisted of 13 scientists, who were selected based on their scientific background to represent the scientific disciplines that are expected to be the most affected if such heating were to occur. The team sought to understand whether exposing the MSR samples to temperatures between +30 and +60 ^{0}C will pose any risk to the sample integrity and, therefore, to future scientific investigations.

This publication is written and edited to accurately represent the information that was provided to MSR Campaign leadership on 1st March 2022, in response to the NASA/ESA charter and Statement of Task to T4 (Kminek and Meyer, unpublished two-page memorandum, 20th Dec 2021). How the information was used for decision support, advances in mission progress and scientific knowledge, and changes in Campaign architecture, since March 2022 postdate T4 and are all almost entirely outside the scope of this publication.

1.4. Science at risk in the 30 to 60 °C temperature range

The Tiger Team deliberated the potential science represented by the samples, the susceptibility of potential science to changes in temperature, and established a consequence-based risk-matrix to inform the review of potential waiver requests.

Most types of damage to the scientific value of samples are caused by a combination of time and temperature, so both variables were considered. To assist their deliberations, the Tiger Team made a number of practical assumptions:

- That there was no need to consider temperatures above +60 °C.
- The total scientific usefulness of the MSR samples will be a composite of multiple lines of scientific inquiry, but for the purpose of this analysis, it would be most helpful to focus on the sectors of science most impacted by exposure to elevated temperatures over time.

The science risk associated with Mars sample temperature excursions above the currently established 30 ºC upper-limit requirement varies and depends on both MSR objectives and sample type. An examination of mission objectives in the context of sample types allows for the identification and analysis of science risk related to the sample exposure to temperatures in the range of 30 to 60 ºC as a function of time.

A total of seven top-level objectives have been defined for MSR, and the corresponding sample types required to meet these objectives have also been established (International MSR Objectives and Samples Team (iMOST) report; Beaty et al. 2019).

In this section, iMOST science objectives and corresponding sample types are reviewed as a starting point for the evaluation of sample materials (components) and measurements that may be compromised if samples are heated between 30 °C < T < 60 °C (and for how long) and their impact on achieving corresponding iMOST science objectives.

This report considers the potential impact that would result from raising sample temperature to a range of +30 to +40 °C and a temperature range of +40 to +50 °C as a function of time. This report also considers the consequences of further raising the sample temperature to a range of +50 to +60°C. For each sub-objective, the iMOST report describes the objective's intent and importance along with the sample type needed to meet the sub-objective (Table 2).

TABLE 2. Summary of Objectives and Sub-Objectives for MSR Identified by iMOST:

Obj. #	Objective description
1	Interpret the primary geologic processes and history that formed the martian geologic record, with an emphasis on the role of water. Intent: To investigate the geologic environment(s) represented at the M2020 landing site, provide definitive geologic context for collected samples, and detail any characteristics that might relate to past biologic

processes

1.1 Characterize the essential stratigraphic, sedimentologic, and facies variations of a sequence of martian sedimentary rocks.

Intent: To understand the preserved martian sedimentary record.

Importance: Basic inputs into the history of water, climate change, and the possibility of life.

Samples: A suite of sedimentary rocks that span the range of variation.

1.2 Understand an ancient martian hydrothermal system through study of its mineralization products and morphological expression.

Intent: To evaluate at least one potentially life-bearing "habitable" environment

Importance: Identification of a potentially habitable geochemical environment with high preservation potential.

Samples: A suite of rocks formed and/or altered by hydrothermal fluids.

1.3 Understand the rocks and minerals representative of a deep subsurface groundwater environment.

Intent: To evaluate definitively the role of water in the subsurface.

Importance: May constitute the longest-lived habitable environments and a key to the hydrologic cycle.

Samples: Suites of rocks/veins representing water/rock interaction in the subsurface.

1.4 Understand water/rock/atmosphere interactions at the martian surface and how they have changed with time.

Intent: To constrain time-variable factors necessary to preserve records of microbial life.

Importance: Subaerial near-surface processes could support and preserve microbial life.

Samples: Regolith, paleosols, and evaporites.

1.5 Determine the petrogenesis of martian igneous rocks in time and space.

Intent: To provide definitive characterization of igneous rocks on Mars.

Samples: Diverse suites of ancient igneous rocks.

Importance: Thermochemical record of the planet and nature of the interior.

2 Assess and interpret the potential biological history of Mars, including assaying returned samples for the evidence of life.

Intent: To investigate the nature and extent of martian habitability, the conditions and processes that supported or challenged life, how different environments might have influenced the preservation of biosignatures and created nonbiological "mimics," and to look for biosignatures of past or present life.

2.1 Assess and characterize carbon, including possible organic and pre-biotic chemistry.

Importance: Any biologic molecular scaffolding on Mars would likely be carbon-based.

Samples: All samples collected as part of Objective 1.

2.2 Assay for the presence of biosignatures of past life at sites that hosted habitable environments and could have preserved any biosignatures.

Importance: Provides the means of discovering ancient life.

Samples: All samples collected as part of Objective 1.

2.3 Assess the possibility that any life forms detected are alive or were recently alive.

Importance: Planetary protection, and arguably the most important scientific discovery possible.

Samples: All samples collected as part of Objective 1.

3 Quantitatively determine the evolutionary timeline of Mars.

Intent: To provide a radioisotope-based time scale for major events, including magmatic, tectonic, fluvial, and impact events, and the formation of major sedimentary deposits and geomorphological features.

Importance: Quantification of martian geologic history.

Samples: Ancient igneous rocks that bound critical stratigraphic intervals or correlate with crater-dated surfaces.

4 Constrain the inventory of martian volatiles as a function of geologic time and determine the ways in which these volatiles have interacted with Mars as a geologic system.

Intent: To recognize and quantify the major roles that volatiles (in the atmosphere and in the hydrosphere) play in martian geologic and possibly biologic evolution.

Importance: Key to understanding climate and environmental evolution.

Samples: Current atmospheric gas, ancient atmospheric gas trapped in older rocks, and minerals that equilibrated with the ancient atmosphere.

5 Reconstruct the processes that have affected the origin and modification of the interior, including the crust, mantle, core, and the evolution of the martian dynamo.

Intent: To quantify processes that have shaped the planet's crust and underlying structure, including planetary differentiation, core segregation, and state of the magnetic dynamo, and cratering.

Importance: Elucidate fundamental processes for comparative planetology.

Samples: Igneous, potentially magnetized rocks (both igneous and sedimentary) and impact-generated samples.

6 Understand and quantify the potential martian environmental hazards to future human exploration and the terrestrial biosphere.

Intent: To define and mitigate an array of health risks related to the martian environment associated with the potential future human exploration of Mars.

Importance: Key input to planetary protection planning and astronaut health.

Samples: Fine-grained dust and regolith samples.

7 Evaluate the type and distribution of in-situ resources to support potential future Mars exploration.

Intent: To quantify the potential for obtaining martian resources, including use of martian materials as a source of water for human consumption, fuel production, building fabrication, and agriculture.

Importance: Production of simulants that will facilitate long-term human presence on Mars.

Samples: Regolith.

For the purposes of this report, as defined by the Statement of Task provided to the Temperature-Time Tiger Team by the NASA and ESA Mars Sample Return Program, MSR Objectives 1 and 2 have been designated as highest priority (iMOST, 2018; Beaty et al., 2019), namely:

- Objective 1. Geological environment(s): Interpret the primary geologic processes and history that formed the martian geologic record, with an emphasis on the role of water.

- Objective 2. Life: Assess and interpret the potential biological history of Mars, including assaying returned samples for the evidence of life.

The intent of objective 1, as described in the iMOST report, is to investigate the geological environment(s) of the landing site, provide definitive geologic context for collected samples, and detail any characteristics that might relate to past biologic processes.

The intent of objective 2 is to investigate the nature and extent of martian habitability, the conditions and processes that supported or challenged life, how different environments might have influenced the preservation of biosignatures and created nonbiological "mimics," and to look for biosignatures of past or present life.

Objectives 1 and 2 are divided into sub-objectives. For each of the sub-objectives, the iMOST report describes both the objective's intent and importance along with the sample type needed to meet the sub-objective.

The importance of understanding sample exposure to the +30 to +60 °C temperature range links directly to meeting the MSR mission objectives and is evaluated on a Mission Risk Consequence Criteria scale (Table 3).

TABLE 3. Mission Risk Consequence Criteria.

Level	Description	Definition	Criteria
4	High	Significant reduction in mission return	Acquires significant science (or objectives) but does not achieve minimum mission success per project Level-1 requirements
3	Moderate	Moderate reduction in mission return	Achieves minimum mission but does not achieve baseline success per project Level-1 requirements
2	Low	Small reduction in mission return	Achieves baseline mission success per project Level-1 requirements
1	Very Low	Minimal reduction in mission return	Only minor loss of mission science (or objectives)

Heating may affect sample materials through a significant number of different processes including (Table 4):

TABLE 4. The different processes, initiated by changes in temperature, which may affect samples.

Process	Effects on sample materials
Physical integrity changes	May, among other effects, result in a loss of stratigraphic information (Obj. 1.1).
Hydration and dehydration	May impact the ability to evaluate the role of water in the environment (Obj. 1.3) and trigger reactions that alter carbon chemistry (Obj. 2.1).
Changes in redox state	May impact the ability to characterize Mars "oxidants" (Obj. 1.4) and trigger reactions that alter carbon chemistry (Obj. 2.1).
Isotopic fractionation	Would broadly impact both objectives 1 and 2.
Organic alteration	May be induced by direct heating or in combination with changes in water availability (e.g., hydration, #2 above) which may broadly affect objective 2.

The iMOST defined MSR sample types and their components are considered. The impact of sample heating depends on sample type (Tables 5 and 6) and ultimately their temperature sensitive mineral and chemical abundances (Table 7). The iMOST report concluded that a carefully selected suite of different sample types would allow MSR objectives to be achieved and identified the specific sample types needed to meet MSR objectives (Table 5).

TABLE 5. Sample types needed to meet MSR objectives.

Sedimentary	Hydrothermal	Deep-Subsurface	Sub-Aerial	Igneous	Volatile-Bearing	Other
Stratigraphy	Vent Distal Range	Leaching/ Sedimentation	Soil/Paleosol Alteration	Diverse Collection	Clay-minerals Hydrated Minerals	Orientated Samples
Lithification	Chemistry W/Mineralogy Range	Fluid Chemistry Evolution	Precipitated Minerals	Ancient Crust	Clay-mineral-Free Dune Material	Impact Melts
Weathering	Stratal Relationships		Coatings or Rinds	Lava Flow	Fluid Inclusions	Impact Breccias
Grain Compositions	Age Model		Redox Conditions	Basalts	Highly Shocked Rock	Rocks W/Trapped Fluid Inclusions
Clastic Rocks	Late Stage Diagenetic Processes		Ultramafic Igneous Rock W/ Basaltic Igneous Host			Shocked Rock w/Impact Melt Pockets or Veins
Stream Channel						Hydrothermally Altered Impact Breccia
Lithified Aeolian						

Each of these sample types map onto mission objectives (Table 6), and impact of time/temperature excursions on these samples can be examined in the context of their chemical and mineralogical compositions (Table 7).

TABLE 6 Potential significance of heating MSR sample types. Effect of heating to 60 °C - Likely Insignificant (Grey) to Potentially Significant (White). Sample types: 1) Sedimentary; 2) Hydrothermal; 3) Water-rock interaction materials; 4) Regolith/Dust; 5) Paleosols; 6) Evaporites; 7) Igneous materials; 8) Atmospheric gases; 9) Trapped gases; 10) Atmosphere-equilibrated minerals; 11) Impact generated materials.

iMOST Objective Intent Understand, Characterize or Assess	Physical Integrity	Hydration/ Dehydration	Redox State	Isotope Fractionation	Organic Alteration
1.1 Sedimentary record	1	1	1	1	1

1.2 Habitable environment	2	2	2	2	2
1.3 Role of subsurface water	3	3	3	3	3
1.4 Biosignature preservation	4,5,6	4,5,6	4,5,6	4,5,6	4,5,6
1.5 Petrogenesis	7	7	7	7	7
2.1 Carbon	1,2,3,4,5,6,7	1,2,3,4,5,6,7	1,2,3,4,5,6,7	1,2,3,4,5,6,7	1,2,3,4,5,6,7
2.2 Presence of biosignatures	1,2,3,4,5,6,7	1,2,3,4,5,6,7	1,2,3,4,5,6,7	1,2,3,4,5,6,7	1,2,3,4,5,6,7
2.3 Extant life	1,2,3,4,5,6,7	1,2,3,4,5,6,7	1,2,3,4,5,6,7	1,2,3,4,5,6,7	1,2,3,4,5,6,7
3 Event time history (Radioisotope)	7	7	7	7	7
4 Volatiles geologic/biologic evolution	8, 9, 10	8, 9, 10	8, 9, 10	8, 9, 10	8, 9, 10
5 Planet interior	7, 11	7, 11	7, 11	7, 11	7, 11
6 Environmental hazards	4	4	4	4	4
7 In-situ resource utilization	4	4	4	4	4

Returned samples are expected to include a range of material types, including minerals and some amorphous inorganic materials. Some returned materials may contain preserved biosignatures. Table 7 shows a summary of the potential sampled materials and the potential effects of alteration of those samples if heated to ~60 °C. Detailed descriptions of potential processes for the various materials are provided below.

TABLE 7 Materials and potential effects of heating to ~60 °C. Greater number of check marks indicate progressive significance, while question marks designate uncertainty.

Material Types	physical integrity	hydration/ dehydration	oxidation /reduction	isotopic fractionation
carbonates	✓	✓	✓	✓ to ✓✓✓
sulfates	✓✓	✓✓ to ✓✓✓	✓	✓ to ✓✓✓
sulfides	✓	✓	✓✓✓	?
chlorides	✓	✓ to ✓✓	✓	?
nitrates	✓	✓✓✓	✓	✓✓✓

phosphates	✓	✓	✓✓	✓✓
phyllosilicates	✓✓	✓✓✓	✓	✓
anhydrous silicates	✓		✓	✓
amorphous silica	✓	✓	✓	✓
oxides (magnetite, hematite, silica, opaline silica, manganese oxide, etc.)	✓	✓✓	✓✓	✓✓
Amorphous materials	✓✓	✓	?	?
Organics	✓	✓	✓✓✓	?
perchlorate/ chlorate		✓✓✓		
[1]*Viking* "oxidants"	✓✓		✓✓✓	

[1]Includes possible presence of chlorite, hypochlorite, trapped oxygen

1.5. Risk to MSR mission requirements/objectives

In summary, there are potential risks to MSR objectives if temperatures of the samples are raised before analysis back on Earth. These risks are present for the two high priority objectives: namely geological environment(s) and biology. Examples of susceptible information would include loss of information about modern/recent Mars that is currently preserved in the form of radical species, strong oxidants, modern atmospheric gases, and exogenic oxidized mineral phases near the surface. Paleoenvironmental records could also be lost in the form of specific mineral phases and their spatial arrangement, isotopic ratios, and fluid/gas inclusions. Raising temperatures also has the potential to affect organic biosignatures in the form of biomarkers, isotopic ratios, and textures.

The approach used by the team was to draw on mineralogical and geochemical data available from the following sources:

- Studies of terrestrial analogues of the martian surface. These provide information on textures and mineral associations that allow understanding of the processes that created these phase assemblages. It is important to predict whether these mineral textures will survive sample return.
- Experimental studies of phase transformations in chemical systems that are thought to be relevant to processes on the martian surface. These provide information on temperature ranges and reaction rates that may take place within the containers during sample return.
- Experimental studies of microbial survivability set onboard the International Space Station (ISS). These studies provide valuable insight into organismal resistance to temperature changes under Mars simulated conditions.
- Geochemical and isotopic experimental studies on relevant analogue samples, especially for volatile species such as hydrogen that may be affected by heating up to 60 °C.
- Spectroscopic data obtained from orbiting spacecraft, which identify mineral species present on the martian surface.
- Direct observations made by the *Viking*, Mars Exploration Rovers (MER), *Phoenix Mars Lander* (PHX), Mars

Science Laboratory (MSL), and M2020 missions that provide evidence of minerals and mineral behavior on the martian surface.

The team used these data to explore the effects of temperatures between +30 and +60 ^{0}C and their impact on samples that would limit future scientific investigations. The team considered generic processes initiated by heating and then the consequences of those processes on the physical and chemical constituents of samples.

2. Processes

2.1. Temperature and time

When samples are collected and transported back to Earth, any chemical modifications that take place will reduce the fidelity of the samples' records of Mars. While temperature is important, it must be considered alongside time because these two variables can be somewhat interchangeable. The rates of many chemical reactions double with every 10 °C increase in temperature. The breaking of carbon-carbon bonds occurs naturally in Earth's subsurface at temperatures close to 100 °C over many years but similar effects can be achieved at 300 °C in the laboratory at durations of days, or at 500 °C for durations of seconds or less. The accessibility of chemical consequences in days at higher temperatures rather than millions of years at lower temperatures has allowed experimentally derived predictions about organic preservation for different types of Mars analogues (Tan and Sephton 2020; Tan et al. 2021; Tan and Sephton 2021). Other variables that increase the rate of reactions include concentration of the reactants, physical state (e.g., surface area), and the presence of catalysts. In addition, water is a key component when considering organic matter. The presence of water can suppress the thermal metamorphism of organic matter, and its repressive effects have been recognized in Earth rocks (Price 1993) and fragments of extraterrestrial organic-rich asteroids presented in the meteorite collection by carbonaceous chondrites (Sephton et al. 2000).

2.2. Physical and chemical processes

When samples are heated, physical and chemical processes are initiated, and these processes include transformation of condensed phases (minerals, amorphous, and organic compounds), the release of volatiles from different sources, reactions between gases and condensed phases, as well as aqueous reactions and phase transformations that are enabled by the formation of liquid water and brines. These processes are described below.

Oxidation-reduction (redox) reactions could occur during many of the listed processes, and such redox interactions also are listed and described in Table 8. Synergistic processes also occur and involve multiple linked transformations.

TABLE 8. Redox processes that could proceed during heating of samples.

Process	Notes and consequences
Decomposition of H_2O_2; $2H_2O_2 \rightarrow O_2 + 2H_2O$	Proceeds in the gas phase, on the mineral surface, and in aqueous solution. Complete loss of H_2O_2 is likely.
H_2O_2, O_2, O_3 + ferrous Fe → ferric species	Proceeds on the mineral surface and in aqueous solution (with aqueous Fe^{2+}). Release of H^+ in reaction with O_2. Release of hydroxyl radicals in rection with H_2O_2. Loss of oxidants.
H_2O_2, O_2, O_3 + sulfide S → sulfate + H^+	Proceeds in the gas phase with H_2S, on the sulfide mineral surface, and in aqueous solution with aqueous H_2S and/or HS^-. Release of H^+ in solution. Loss of H_2O_2 etc.
H_2O_2, O_2, O_3 + organic compounds (CH_4, etc.) → H_2O, CO_2	Loss of H_2O_2, O_2, O_3, trace organic gases; a minor loss of other organic compounds.

Nitrate + Fe^{2+} in solution → ferric species + ammonium (+ minor N_2 and NOx gas)	In aqueous phase. Loss of nitrate.
Nitrate + sulfide S in solution → sulfate + ammonium or N_2	In aqueous phase. Loss of nitrate.
Nitrate + organic matter → CO_2, N_2	Loss of nitrate and organics.
Chlorate + ferrous Fe → ferric species	In aqueous phase. Loss of chlorate.
Chlorate + sulfide S → sulfate	In aqueous phase. Loss of chlorate.
Chlorate + organic matter → CO_2, chloride	In aqueous phase. Loss of organics and chlorate.
Mn oxides + organic matter → Mn^{3+} and Mn^{2+} species, CO_2	MnO may not interact below 60 °C.
Decomposition of oxychlorine compounds (e.g., perchlorates)	Perchlorates and chlorates are stable at 60 °C. Hypochlorite, ClO^- ion, decomposes at ~50 °C or lower depending on cation type and water availability. Decomposition results in generation of active chlorine compounds. Organic compounds, especially amines, are subject to attack.
Ferric iron + sulfide —> ferrous iron + sulfate	Loss of sulfide, generation of sulfuric acid
Ferric iron + organics → ferrous iron + CO_2	This reaction may not proceed fast below 40-60 °C but could be biomediated.

2.2.1. Processes during heating

2.2.1.1. Physical arrangements, architectures and fate of inclusions

Increasing the temperature of a sample can lead to a change in the physical arrangement and architecture of constituents. Heating of some minerals can deform or destroy fluid inclusions (Fig. 3). Carbonates, sulfates, chlorides, and other minerals that precipitate from aqueous solutions can entrap fluid inclusions as they grow in a container. Nitrates, perchlorates, and phosphates tend to be too finely crystalline for fluid inclusions to be detected or studied. As the host mineral may stretch or flow due to temperature (and/or pressure), fluid inclusion shapes and arrangements can indicate the amount of deformation of the host mineral. Carbonates, sulfates, and chlorides are sensitive in different ways to increases in temperature. Calcite, gypsum, and halite are known to alter slightly, altering fluid inclusion shapes and volumes during heating (Goldstein and Reynolds, 1994; Roedder, 1984). The temperatures at which most carbonates and chlorides stretch are higher than +60 °C on Earth and are typically noticed as temperatures approach ~90 °C. In contrast, gypsum and related sulfates may begin to deform at relatively lower temperatures, especially in the ~40 - 60 °C range. The structural deformation of fluid inclusions has been witnessed mainly in these minerals after being buried in the subsurface at elevated temperatures for millions of years.

Evidence of stretching includes primary fluid inclusions with: (1) shapes not consistent with crystal habit, (2) rounded corners, (3) inconsistent liquid:vapor ratio in an inclusion population within a growth band (or other fluid inclusion assemblage), and (4) elongated or necked shapes (e.g., Goldstein and Reynolds, 1994). Shorter time periods (hours-

days) of exposure to temperatures of ~60 °C (while minerals are prepared in laboratories) has not yielded such stretching. Regardless, this stretching of fluid inclusions is not known to alter chemical or organic compositions of included materials. It does negatively affect some analyses that rely on volume of liquid:gas, such as homogenization microthermometry, which would be used to determine parent water temperatures.

Halite and other chloride minerals are likely to be returned from Mars and may act as good potential repositories for martian biosignatures (e.g., Benison, 2019). On Earth, halite flows plasticly when placed under high temperatures and pressures, especially when buried at depths of greater than ~ 2,000 m below the surface. In these conditions, temperatures are at, or higher than, 60 °C for millions of years. However, even at temperatures of ~60 °C for long geological time spans, halite can be well-preserved, as indicated by unaltered primary fluid inclusions that contain microorganisms and organic compounds. In addition, halite tends to insulate heat, so that, at temperatures greater than ~ 60 °C, only the other edges of the crystals show signs of slight alteration (stretched fluid inclusions) or clear halite. Unaltered fluid inclusions remain in crystal interiors.

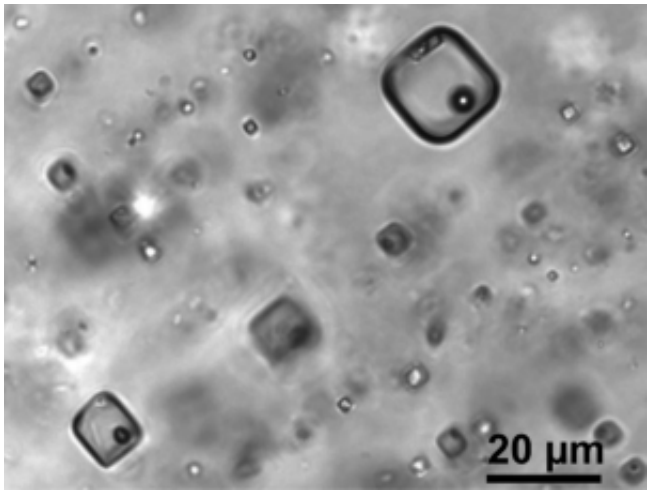

FIG. 3. Primary fluid inclusions in the ~260 million year-old Permian Opeche Shale from ~2500 m depth in the subsurface of North Dakota (Image: K. Benison). Rounded corners and consistent vapor:liquid ratio suggest slight stretching due to temperatures slightly higher than 60 °C for millions of years. Liquid composition, organic compound composition, and imaging of microorganisms was still possible from these fluid inclusions.

Gypsum and some other sulfate minerals dehydrate to less hydrated forms (i.e., gypsum dehydrates to bassanite and anhydrite). As a result, fluid inclusions are destroyed, but solid inclusions are preserved. Some solid inclusions preserved may include microbial cells and solid organic compounds. Sulfide minerals, found in association with some chemical sediments, are easily oxidized, which leads to a change chemical composition and crystal or grain size. For example, pyrite oxidizes to hematite, and native sulfur can oxidize to a sulfate mineral. Besides yielding byproducts such as acids and brines, these oxidation processes commonly decrease crystal sizes, which results in a powdered product. Phyllosilicates deform by stretching and shrinking during hydration and dehydration, respectively.

2.2.1.2. Thermal maturation and mineral structure transformation

Amorphous and semi-amorphous compounds are very abundant in martian materials. For instance, amorphous and semi-amorphous compounds have been recognized in Mars Science Laboratory (MSL) X-ray diffraction data (Bish et al., 2013), and heating may increase the crystallinity of those phases and produce additional abundances of similar material by dehydration of crystalline hydrous phases. No major effects on crystallization of silicates (e.g., semi-amorphous clay-like phases) are expected at even 50-60 °C because of the slow diffusion rate. Thermal structuring of non-silicate phases (e.g., ferric hydroxides) could be notable at 50-60 °C (e.g., Cornell et al., 1989; Cornell and Schwertmann, 1996). The occurrence of ferric OH-bearing phases in martian near-surface materials within 10^8-10^9 years could have led to a structural maturation. In such a case, a short-time heating of them up to 60 °C could not lead to further major/complete conversion of semi-crystalline hydroxides/oxyhydroxideso Fe_2O_3 (hematite or maghemite). Some structural maturation of condensed organic matter is possible. Although thermal structural transformation of some crystalline phases is also conceivable, the major transformation of crystalline phases would involve loss of

volatiles (e.g., dehydration).

2.2.1.3. Release of volatiles

The amount of sorbed gases in the martian materials (mainly adsorbed on surfaces of solids but possibly also absorbed within solids) depends on the time of day, location, season, grain size, and mineralogy of the samples. Low temperature favors adsorption of gases on mineral surfaces. Winter- and night/morning-sampled, fine-grained (soil), and phyllosilicate-rich materials would contain the highest amounts of adsorbed gases. Major sorbed gases are likely CO_2 and H_2O, and minor species are N_2, Ar, O_2, H_2O_2, and O_3. In sealed containers, an establishment of gas-adsorbed gas equilibration is likely to occur during heating episodes that exceed several minutes. Because the heating could cause an additional supply of volatiles (e.g., through salt dehydration), surfaces of heated samples may contain even more sorbed volatiles (mostly water) than at the surface of Mars. Desorbed reactive gases (H_2O, CO_2, O_2, H_2O_2, and O_3) could be involved in chemical reactions and be at least partially consumed during heating episodes. Other released volatiles will be preserved in cooled returned samples and available for laboratory investigations.

One source of volatiles that is not expected for samples returned from the Mars2020 cache, owing to the latitude of sampling, but may be important for future missions at higher latitudes, is the presence of frozen water. Winter-, night/morning-, and in shade-sampled materials may contain water ice (frost). The fraction of frost could be higher in fine-grained (soil) materials rich in phyllosilicates. Sublimation of ice occurs after any increase in temperature of samples. Captured ice could sublimate to the atmosphere befre and/or during sealing a container. In either case, no direct action of water ice is expected at temperatures between +30 °C and + 60 °C. The majority of martian inorganic materials are not subjected to any significant sublimation below 60 °C. However, sublimation of condensed low molecular weight organic compounds (e.g., alkanes) could be significant, especially at temperatures above ~40 °C.

The amount of interlayer water in phyllosilicates (*e.g.*, in smectites) depends on temperature and relative humidity. Neither *Viking* nor MSL/SAM data indicate release of interlayer water from phyllosilicates below 60 °C. This is consistent with desiccation of martian clay minerals exposed during several Ga to dry surface environments. Therefore, the effect of thermal release of interlayer water from phyllosilicates is likely minor. Note that clay mineral hydration-dehydration cycles are possible in containers if water will initially be released from hydrated salts. It is not clear how many volatiles could be released upon heating to 40-60 °C of amorphous silicates, though *Viking* and SAM data do not indicate a major release. The release of volatiles from micro-cracks, structural defects, and gas/fluid inclusions in solid inorganic phases is possible, but the release is likely minor compared to possible loss of volatiles through structural thermal decomposition of solids.

Structural decomposition and related devolatilization of martian solid phases mainly include dehydration of salts (sulfates, chlorides, carbonates, perchlorates, and nitrates) (e.g., Fig. 4). Dehydration of hydrated oxides/oxyhydroxides (amorphous silica, etc.) is less likely below 60 °C. Some structural decomposition of organic compounds is also possible, for example, release of low-molecular weight compounds (CH_4, etc.) from warmed macromolecular organic matter (polymers). Mobilization of H and O by structural dehydroxylation of OH-bearing silicates is not expected within the temperature range of interest (30 °C < T < 60 °C) (Velbel and others, 2022). However, other OH-bearing phases (*e.g.*, Fe sulfide tochilinite, some metal hydroxides such as ferric hydroxides) may dehydrate.

The process of heating a sample within a closed container that contains hydrated sulfates or other hydrous phases may cause partial or complete dehydration. The evolved water vapor will alter the partial pressure of water vapor (pH_2O) in the container. The degree to which the water vapor pressure increases will be a function of (i) what hydrate is present (for example, kinetically persistent kieserite ($MgSO_4 \cdot H_2O$) would have little effect, while conversion of epsomite ($MgSO_4 \cdot 7H_{2O}$) to hexahydrite ($MgSO_4 \cdot 6H_2O$) would release H_2O), (ii) the amount of dehydrating phase, (iii) other hydrates in the sample that may buffer this increase in pH_2O by rehydrating (*e.g.*, existing starkeyite, $MgSO_4 \cdot 4H_2O$, hydrating to hexahydrite), and (iv) a larger proportion of the gas phase within the container. With a limited gas volume, pH_2O will rise, and further dehydration will be suppressed because of a H_2O(g)-hydrate equilibration. With a larger gas volume, a larger proportion of the hydrated compounds will dehydrate before equilibrium is achieved, and more water vapor will be contained in the container's atmosphere. The rate and extent of dehydration will depend on the permeability of the sample. Loosely packed regolith will have a much larger surface area in contact with the atmosphere. The surface layers of core samples may have already been disturbed by heating and abrasion during drilling. The interaction of a solid core with the atmosphere in the sample tube will be limited to the surface of the core during reasonably short exposures. The surface at the end of the solid core may be exposed to the higher temperature atmosphere created at the end of the tube during sample

sealing. The sample cores may also have different hydration levels along their length that reflect the hydration level below the martian surface.

An appreciation of the potential effects of temperature change on dehydration of minerals can be provided by numerical assessments. For example, gypsum and bassanite have been reported in martian surface materials. Up to 25% gypsum has been observed in *Curiosity*-collected samples (Rampe et al., 2022). By making some assumptions, it is possible to calculate the relative humidity of the atmosphere within a gypsum-bearing sample tube for various heating temperatures. For our example assessment, we made the following assumptions: i) 1300 mm^3 sample tube volume, ii) 13 mm × 76 mm maximum sample dimension, iii) volume of gypsum present in the sample, iv) the percent of gypsum that dehydrates and to what phase (bassanite).

With the known composition and density of gypsum, it is possible to calculate the number of moles of water vapor that are released for given amounts of gypsum. The water pressure in a saturated volume as a function of temperature is known, and when using this, it is possible to calculate the percentage saturation of H_2O within the volume (relative humidity, RH) in the sample tube surrounding the sample that is created by gypsum dehydration. For example, if one assumes (i) 50% success in retrieving core material (this leaves a significant volume of headspace to accommodate pH_2O), (ii) 1% volume of gypsum exists in the entire core volume, (iii) only 1% or 5% of this gypsum actually dehydrates (which is likely to take place on the surface of the core), then the following % water saturations (relative humidity) can be calculated (Table 9).

TABLE 9. Relative humidity of the atmosphere within a gypsum-bearing sample tube for various heating temperatures.

Temperatures (°C)	1% reaction	5% reaction
0	Saturated	Saturated
5	Saturated	Saturated
10	Saturated	Saturated
20	Saturated	Saturated
30	78% RH	Saturated
40	47% RH	Saturated
50	29% RH	Saturated
60	18% RH	91% RH

Gypsum dehydrates when the relative humidity is less than approximately 40% over the temperatures of interest here. Above 40%, RH gypsum is stable. Therefore, the calculated atmosphere within the sample tube becomes saturated with water vapor with only a very small amount of gypsum dehydrated. However, the atmosphere will not reach total saturation because, as gypsum dehydrates, the relative humidity will rise until it reaches approximately 40% at which point the gypsum is in equilibrium with the water vapor in the sample tube and no further dehydration will occur. Small amounts of gypsum dehydration on grains surfaces may cause disaggregation of the core sample and loss of textural details.

On a fast cooling, this very small amount of water vapor will condense as water or ice. This volume may be calculated. It is possible that the water vapor could rehydrate any bassanite that was created by gypsum dehydration. If

gypsum/bassanite are the only hydrous phases, any pH_2O created will not be high enough to cause deliquescence of any halite or epsomite but may cause the deliquescence of other materials that are prone to deliquescence below a RH of 40%, as outlined below.

A similar numerical assessment can be performed for epsomite. If epsomite is present in the sample, it will dehydrate more readily than gypsum, but the equilibrium vapor pressure created will again arrest further dehydration of epsomite. At 50 °C, epsomite, hexahydrite, and a brine exist with a relative humidity of 85% (Chipera and Vaniman 2007). This is a high enough humidity to cause deliquescence of many other salts. Assuming (i) 50% sample retrieval, and (ii) 1% epsomite by volume of which 1% or 5% is converted to hexahydrite, saturations can be calculated (Table 10).

TABLE 10. Relative humidity of the atmosphere within an epsomite-bearing sample tube for various heating temperatures.

Temperatures (°C)	1% reaction	5% reaction
0	Saturated	Saturated
5	Saturated	Saturated
10	83% RH	Saturated
20	45% RH	Saturated
30	26% RH	Saturated
40	15% RH	76% RH
50	9% RH	47% RH
60	6% RH	30% RH

In this scenario, at approximately 35 °C, epsomite (and 1% reaction) will be in equilibrium with $H_2O(g)$ at 83% RH in the sample tube and hexahydrite (Chipera and Vaniman, 2007). Once the atmosphere above the sample is saturated with respect to water vapor, the possibility exists for a small amount of brine to exist, given the assumptions for the calculation of how much epsomite exists in the sample and what % of this is exposed to the atmosphere in the tube. With additional heating, more epsomite will dehydrate, and the relative humidity will increase until, at about 50 °C, when a mixture of epsomite, hexahydrite, and brine will coexist in three-phase equilibrium. If all the epsomite is consumed before this triple point is reached, then hexahydrite will be in equilibrium with the $H_2O(g)$. If all the epsomite is not consumed, additional heating will result in a two-phase (binary) equilibrium mixture of magnesium sulfate brine and epsomite.

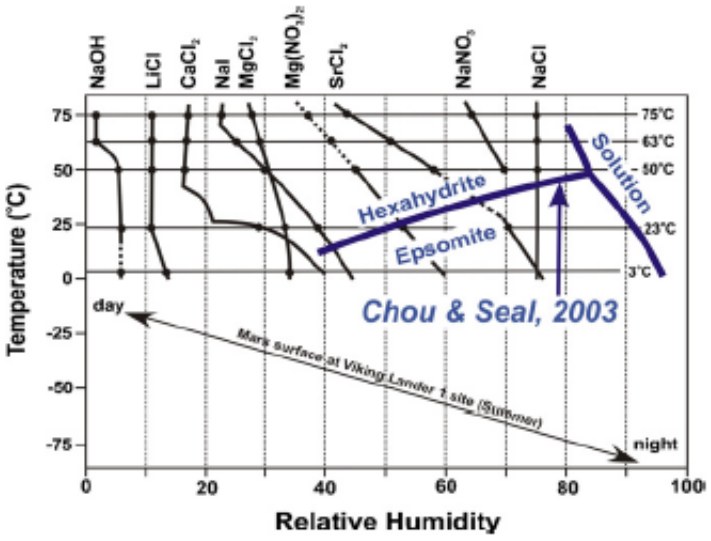

FIG. 4. Stability fields of Mg sulfates and deliquescence conditions (black curves) of other species (Chipera and Vaniman, 2007).

The extent to which these reactions take place is dependent on how exposed the magnesium sulfate is to the sample tube atmosphere. The volume of material that is dehydrated and any possible brine that is created would be quite small in a sealed container.

If other sulfates such a pickeringite or mirabilite are present, they may dehydrate and increase the relative humidity of the sample tube atmosphere to the point where lower hydrated sulfates may deliquesce to form brine. This effect is limited by the volume of sulfate involved as well as the available atmosphere within the sample tube. Amorphous hydrated sulfate material will release water vapor into the sample tube atmosphere. This material, which has most likely been exposed to the martian atmosphere, will likely contain less H_2O than gypsum or epsomite, and the effect on the sample tube atmosphere will be lessened.

With so many unknown factors controlling the partial pressure of water vapor within the sample container, it is impossible to be specific about the effects different maximum heating temperatures will have. Some of these processes may already have taken place at temperatures below 30 °C.

In summary, the dehydration of hydrous phases within the sealed sample tube (and possible creation of very small amounts of liquid H_2O on subsequent cooling) could be limited by the increase in pH_2O of the small volume of atmosphere contained in a sample tube. This arrests further dehydration.

2.2.1.4. Reactions between gases and condensed phases

Gas-gas type reactions

Both warming and corresponding release of volatiles to the gas phase (Table 7) could lead to gas-gas type chemical reactions. The rate of gas-gas reactions exponentially increases with temperature, and yields of high-temperature reactions increase because of higher partial pressure of gases in higher-temperature containers. Some redox gas-gas type reactions (*e.g.*, $O_2 + H_2$; $CO_2 + H_2$) are sluggish at the considered temperatures, while interactions of strong gaseous oxidizers (O_3, H_2O_2, O_2, N oxides) with reduced species (*e.g.*, H_2S, CH_4 and other volatile organic compounds) are expected. In addition, hydrogen peroxide (H_2O_2) readily thermally decomposes to O_2 and H_2O ($2H_2O_2 \rightarrow 2H_2O + O_2$). The reaction could be catalyzed by compounds of transition metals (e.g., MnO_2). It follows that H_2O_2 may not survive heating because of this and heterogeneous redox reactions (Table 8).

Gas-solid chemical reactions

The gas-solid type chemical reactions during heating could include interactions of major chemically active headspace gases (CO_2, H_2O, O_2) and multiple redox reactions that include strong minor oxidants released to the gas phase from

materials surfaces (H_2O_2, O_3), as listed in Table 8. Any prolonged heating will cause complete consumption of these oxidants in reactions with reduced mineral phases, mainly ferrous, sulfide, and organic compounds. Reactions with relatively abundant Fe sulfides (pyrrhotite, pyrite) in martian materials could be mainly responsible for consumption of strong gaseous oxidants. Moisture on sulfidesurfaces strongly accelerates the oxidation that affects both sulfide sulfur and ferrous iron.

Gas-liquid exchange reactions

CO_2 gas is present in the sampled martian atmosphere and may be released from a potential fluid phase if it reacts with carbonates. Fluids may be acidic and corrosive due to the dissolution of acid-sulfate minerals or oxidation of sulfides and/or ferrous compounds (Table 8). If such acidic fluids contact carbonates, the latter should undergo at least some dissolution. Dissolved inorganic carbon (DIC) includes carbonate ions (CO_3^{-2}), bicarbonate (HCO_3^-) and carbonic acid (H_2CO_3), whose relative abundance is a function of fluid pH. At lower pH, carbonic acid rapidly converts to aqueous CO_2, which is the dominant form of inorganic carbon. Aqueous CO_2 exsolves from the fluid as CO_2 gas. An additional DIC source may be oxidation of CH_4 and/or organic molecules.

The solubility of CO_2 in pure water decreases by a factor of ~3 as temperature is raised from +5 °C to +60 °C (Fig. 5a). Salinity and alkalinity play an additional role in constraining the exact solubility. Exsolution of CO_2 gas from the fluid may lead to an increase in the pH of the residual fluid, an increase in the headspace pressure of the sample container, as well as a decrease of the pH of other fluids in which CO_2 dissolves.

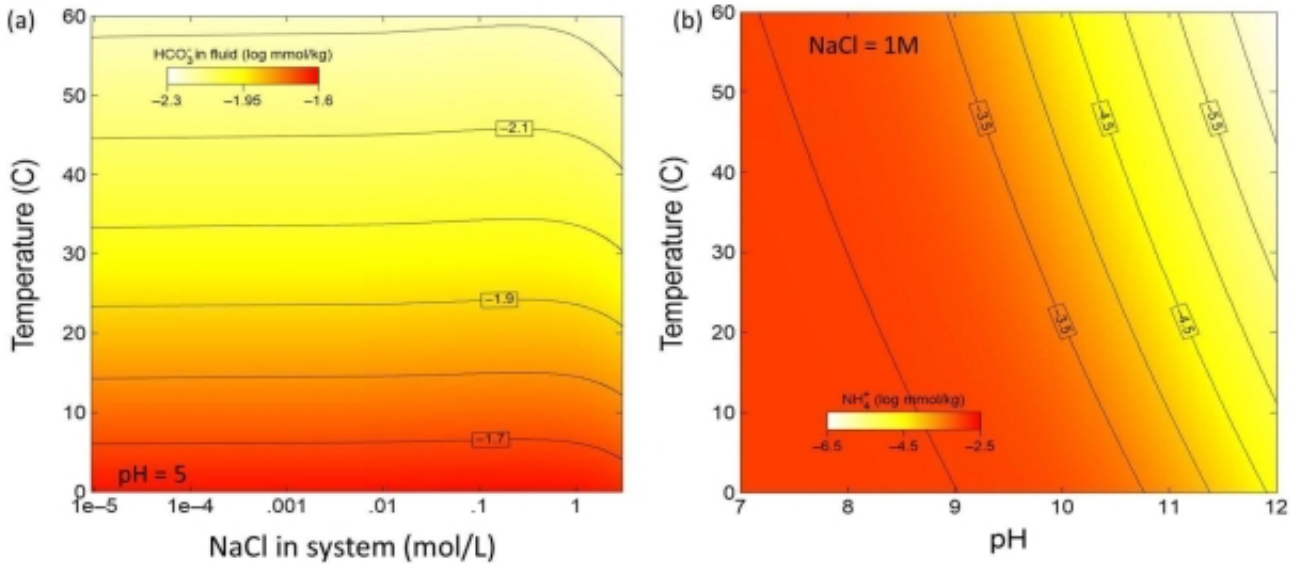

FIG. 5. (a) CO_2 solubility in water as a function of salinity (x-axis) and temperature (y-axis). In this model, pCO_2 was held constant at a log fugacity of -3.5, and pH was set to 5. Aqueous DIC is expressed as HCO_3^-. (b) NH_4^+ speciation as a function of pH and temperature, with salinity (molarity of NaCl) set to 1 mol/kg. The initial concentration of NH_4^+ was set to 1 μM. Dissolved NH_4^+ decreases with increasing pH and temperature due to conversion to NH_3, which is volatile. Models were generated in Geochemist's Workbench, using the Phase2 module and the standard thermodynamic database.

Clay mineral-bound or organic-bound ammonium (NH_4^+) that is released into fluids during thawing may convert into ammonia (NH_3) gas if the fluid has an alkaline pH (see Section 2.1.1.4) (Fig. 5b). The pKa of the reaction $NH_4^+ = NH_3 + H^+$ is 9.2 at 25 °C and standard pressure, but it shifts to lower pa values with increasing temperature (Li et al. 2012). At 50 °C, the pKa is below 9, and at 100 °C it is below 8. Hence more reduced nitrogen could be lost from a heated sample. The conversion from NH_4^+ to NH_3 occurs instantaneously. The loss of NH_3 gas can induce large isotopic

fractionations, rendering the residual NH_4^+ enriched in $^{15}N/^{14}N$ (α = 42 ‰ at 25 °C, Li et al. 2012), and hence this process may hinder accurate reconstructions of the original $\delta^{15}N$ composition of the sample prior to heating.

Radical-initiated reactions

Radiation-induced formation of radical species in martian surface materials, including reactive oxygen species (ROS), has long been anticipated (Zent and McKay 1993). The results of the *Viking* Biology Experiments have been extensively linked to several hypotheses that invoke the presence, and perhaps long-term stabilization, of various types of radicals. Perturbation of collected *Viking* samples from ambient temperatures along with an increase in water availability drove decomposition of organics that were added to the samples. Similarly, organics that may be present and persevered through physical segregation or other means would potentially be vulnerable to attack if redistribution of water occurs due to sample heating. While dynamic formation of radicals may be most prevalent on the uppermost surface of Mars resulting from solar ultraviolet (UV) irradiation, ionizing radiation in the form of Galactic Cosmic Rays and Solar Energetic Particles penetrate to the meter scale, which can result in the formation and low-temperature preservation of radical species.

The UV-induced formation of reactive oxygen Mars analogs has been demonstrated with superoxide (O_2^-) shown to be thermally stable (in the absence of water) with a 10% population reduction after heating to 100 °C for 1 hr, while other radical species including O^- and O_3^- do not survive (Yen et al., 2000). In fact, superoxide is the source of the oxygen release observed in the *Viking* Gas Exchange experiment. It may be possible for it to survive heating in the 50-60 °C range or above during MSR and remain preserved. However other ROS, including O^- and O_3^-, are unlikely to survive short-term elevation to 50 °C, or even the current 30 °C MSR upper temperature limit requirement. In addition to UV formation of ROS, the formation of superoxide in gamma-irradiated Mars-*Phoneix* analogs has been demonstrated along with a corresponding formation of H_2O_2 and hydroxyl radicals (·OH) upon wetting (Georgiou et al., 2017). Formation of perhydroxyl radicals would also be expected as a result of wetting (Yen et al., 2000).

Redistribution of water within the RSTA upon heating may initiate reactions of radicals with preserved organic species, with perhaps carboxylic acids being most vulnerable to ROS attack. In addition to the formation of ROS, the presence of active chlorine-bearing species is expected in Mars samples that contain perchlorate. These species, including ClO^-, would react with organic compounds through various mechanisms, some of which include the generation of radical intermediates. In the case of active chlorine compounds, amino acids and other amines would be partially vulnerable to attack (Quinn et al., 2013). Based on the results of the *Viking* Biology experiments, in which excess organics were added to the martian samples, total decomposition of organics would be expected to be limited to no more than ppm levels (Zent and McKay 1993).

2.2.1.5. Aqueous processes

Aqueous processes may or may not occur during heating. They are more likely to occur if water ice was present in the samples. Abundant water-rich salts (*e.g.*, $CaCl_2{\cdot}6H_2O$, Ca and Mg perchlorates) could also favor formation of brines through deliquescence. Aqueous processes are less likely in core samples of igneous and dense sedimentary rocks collected in summer, at mid-day, and in sun-exposed environments. Upon heating, partial pressure (p) of H_2O(g) in the head space would increas due to sublimation of the frost (if it was present), and/or decomposition of hydrated solids (e.g., salts). At a certain temperature and partial pressure of H_2O(g), liquid water may condense to form the liquid phase. Initial condensation of liquid water, if any, is expected in pores, cracks in mineral grains, and grain boundaries, in which pH_2O could be elevated locally.

Salt deliquescence

Deliquescence occurs through absorption of water vapor by hygroscopic salts. Increase in relative humidity in water-rich samples during heating can cause deliquescence of some salts. Because of heating of hydrous phases, pH_2O and RH in sealed containers could be higher than on Mars, and this would increase the chance of deliquescence. If water ice is not sampled (a likely event), deliquescence could be the main process that causes the formation of an aqueous (briny) phase in the sample tubes. The formation of brines through deliquescence is more likely in interior parts of

samples (*e.g.*, at grain boundaries and close pores where humidity could be higher than in the container headspace).

The martian salts that could be affected by deliquescence (Fig. 6) are chlorides, perchlorates, and chlorates of Ca, Mg, and Na (*e.g.*, Brass et al., 1980; Davila et al., 2010; Gough et al., 2011, 2014, 2016; Fischer et al., 2014, 2016; Nuding et al., 2014; Zorzano et al., 2009; Wang et al., 2019; Primm et al., 2017; Toner and Catling, 2018).

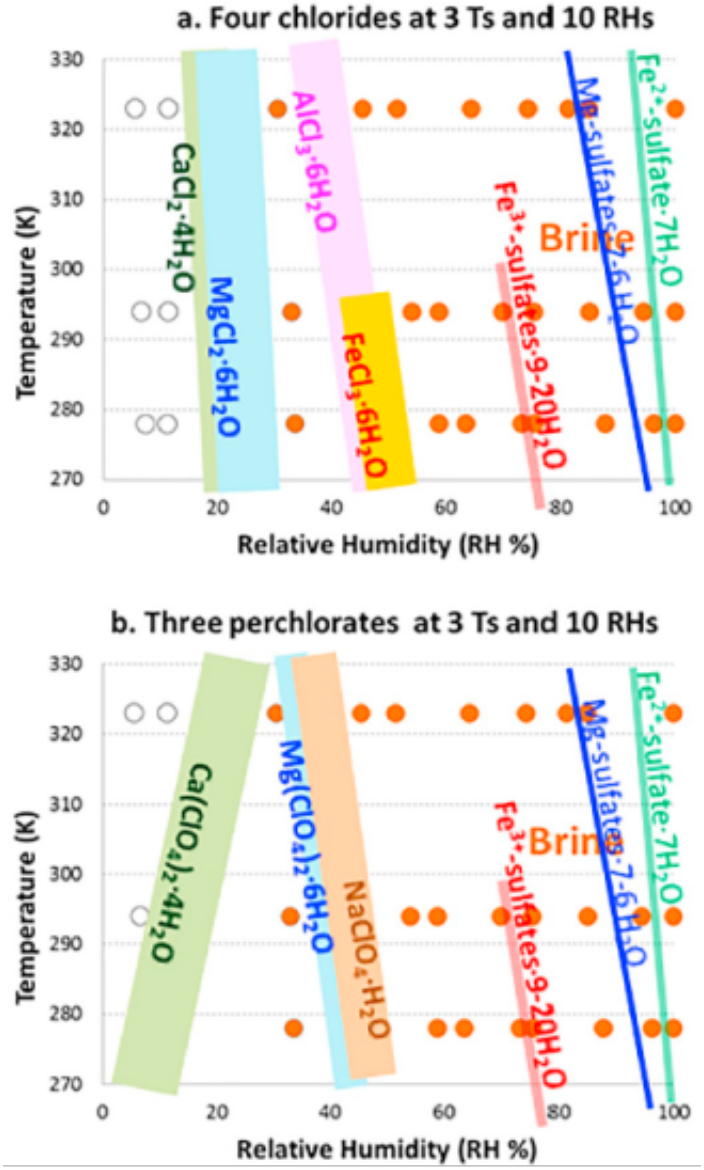

FIG. 6. Deliquescence phase boundaries of some Mars-related salts (Wang et al., 2019). The deliquescence occurs at higher RH (to the right-hand side of the phase boundaries).

At ~+25 to +45 °C, deliquescence of $CaCl_2 \cdot 4H_2O$ occurs at RH > ~15-20% (Wang et al., 2019; Gough et al., 2016) (Fig. 6). Antarcticite, $CaCl_2 \cdot 6H_2O$, dehydrates to $CaCl_2 \cdot 4H_2O$ and then to $CaCl_2 \cdot 2H_2O$ at elevated temperature and/or lower RH (Fig. 7). Above 45 °C, deliquescence of $CaCl_2 \cdot 2H_2O$ occurs at RH > 2-4% (Gough et al., 2016), though larger deliquescence RH values (~15%) are reported based on experimental data.

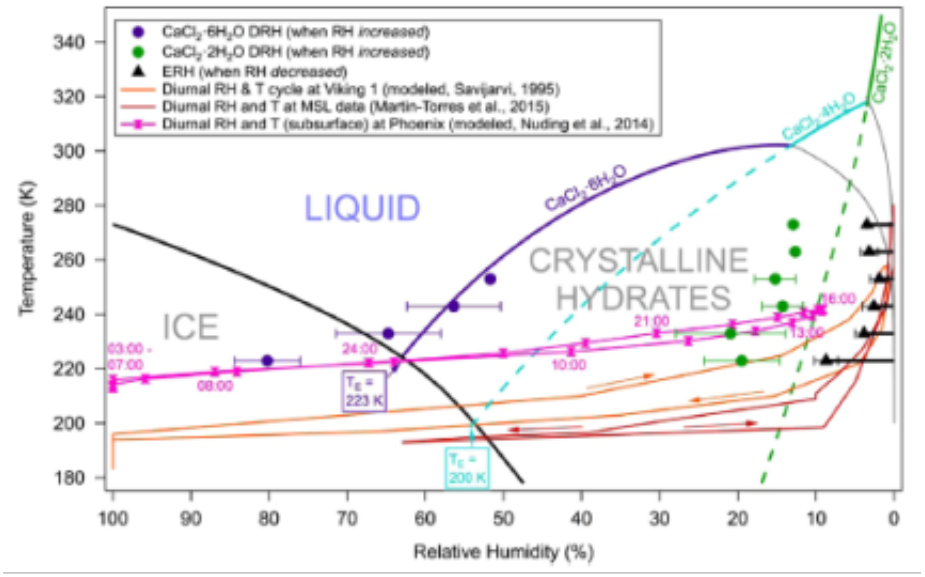

FIG. 7. Stability diagram of the $CaCl_2$-H_2O system (Gough et al., 2016). T: Temperature; TE: eutectic temperature; RH: relative humidity; DRH: deliquescence relative humidity; ERH: efflorescence relative humidity.

Bischofite ($MgCl_2 \cdot 6H_2O$,) can convert to liquid at elevated RH and temperature (*e.g.*, Davila et al., 2010; Primm et al., 2017; Wang et al., 2019). At 25 °C, the conversion occurs at RH > ~33%. The same or slightly lower RH (~33-25 %) is likely needed for deliquescence at 25-60 °C (Primm et al., 2017) (Figs. 8) and 9), though bishopite dehydrates to $MgCl_2 \cdot 4H_2O$ at these temperatures at RH < 6% (Xu et al., 2021) (Fig. 9).

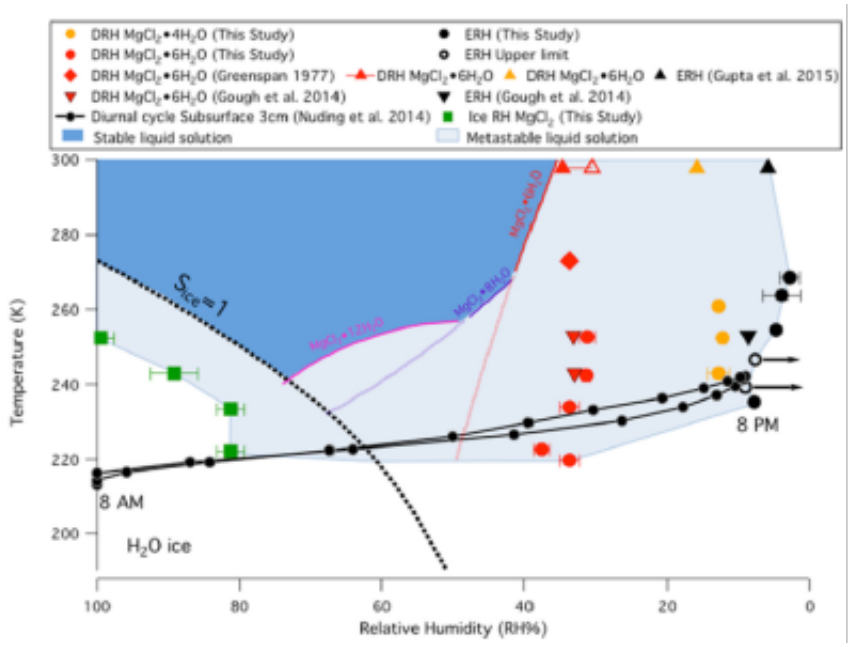

FIG 8. Stability diagram of Mg chlorides at Mars-related conditions (Primm et al., 2017). T: Temperature; TE: eutectic temperature; RH: relative humidity; DRH: deliquescence relative humidity; ERH: efflorescence relative humidity.

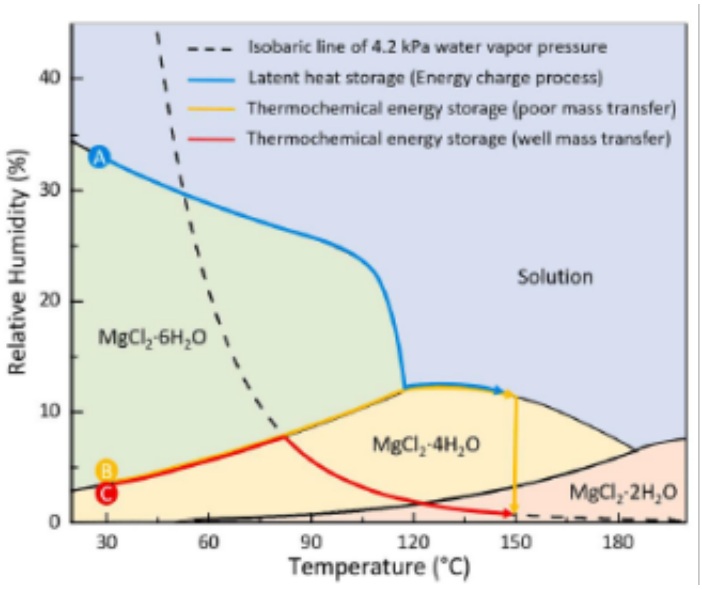

FIG 9. Relative humidity-temperature phase diagram of $MgCl_2$-H_2O (Xu et al., 2021). The letters A, B, and C are related to energy storage applications and are not relevant to this main context of this publication.

Eutectic temperature of water with Ca perchlorate is among the lowest among possible martian salts (198 K), and the deliquescence of hydrated Ca perchlorate $Ca(ClO_4)_2 \cdot 4H_2O$ occurs at 30-60 °C if RH > 10-20%, respectively (Wang et al., 2019) (Fig. 6). Lower deliquescence RH is needed at T > +25 to +60 °C. At 0 °C, $Mg(ClO_4)_2 \cdot 6H_2O$ is subjected to deliquescence at RH > ~40% (*e.g.*, Gough et al., 2011). At temperatures up to 60 °C, the deliquescence HR is 30-35% (Fig. 6).

At 0 to +50 °C, $NaClO_4 \cdot H_2O$ is subjected to deliquescence at RH above ~51-38%, respectively (Fig. 10). Deliquescence of $NaClO_4$ occurs at RH > ~38% and T > ~50 °C and slightly changes with temperature (Figs. 6 and 10). In even moderately water-bearing samples, deliquescence of perchlorates of Ca, Mg, and Na, and chlorides of Ca and Mg is likely upon heating of samples up to 30-0 °C. Note that deliquescence of these hygroscopic salts could maintain RH in a container that will buffer HR at a low level (*e.g.*, 30-40%) that does not allow deliquescence of less hygroscopic salts discussed below.

Chlorates could be affected by deliquescence as well. Toner and Catling (2008) evaluated the stability of chlorates with respect to delinquency and found that $Mg(ClO_3)_2 \cdot 6H_2O$ is much more deliquescent (RH > 20%) than $Mg(ClO_4)_2 \cdot 6H_2O$ (RH > 40.1%) at 25 °C.

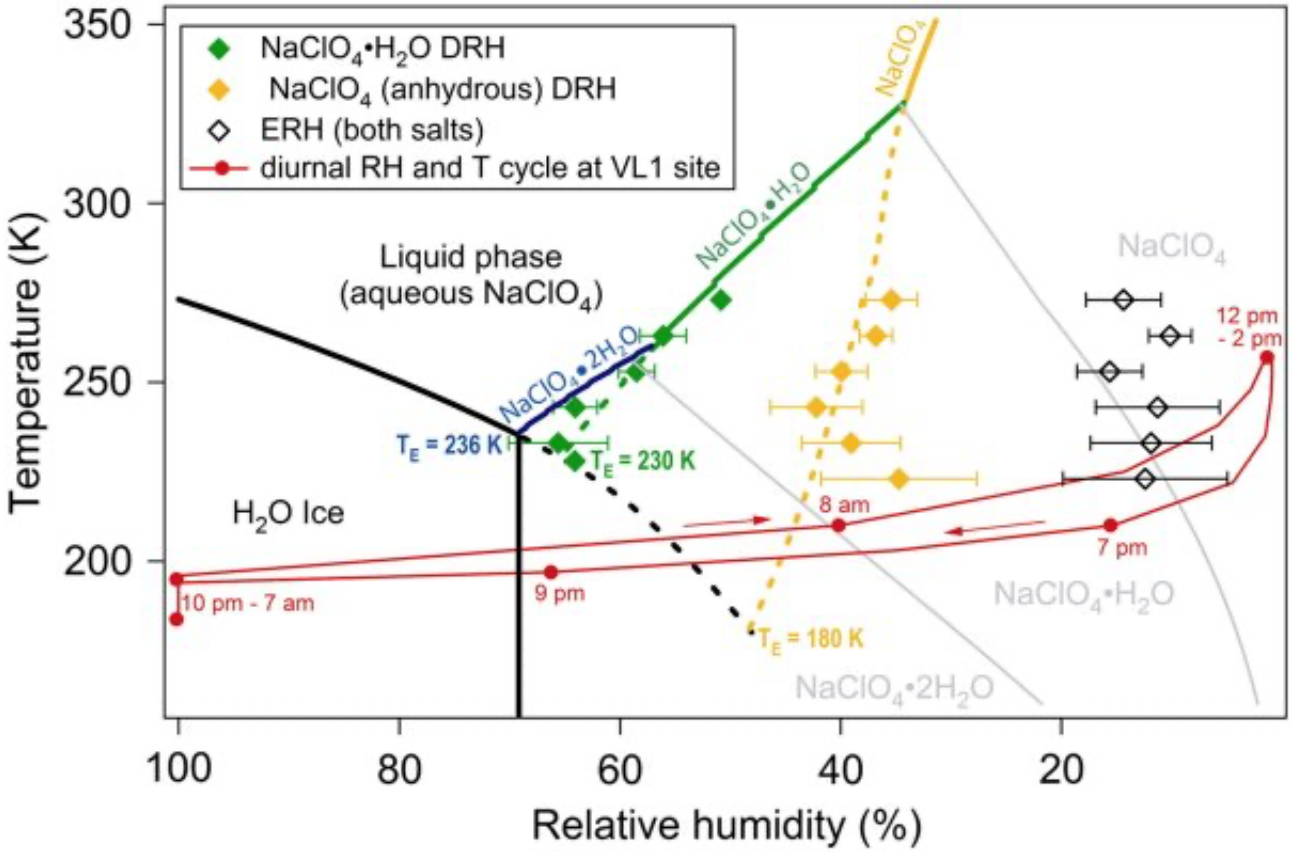

FIG 10. Stability fields of Na perchlorates as functions of temperature and relative humidity (Gough et al., 2011). Liquid phase is stable at elevated Relative Humidity (RH) and temperature (T). DRH: deliquescence relative humidity; ERH: efflorescence relative humidity.

Magnesium and iron (Fe^{2+} and Fe^{3+}) sulfates require higher RH for deliquescence in the considered temperature range (Fig. 6). The deliquescence of these salts is less likely, especially in water-deficient samples with a large headspace. Meridianiite ($MgSO_4 \cdot 11H_2O$) is only stable at sub-freezing temperatures, though epsomite ($MgSO_4 \cdot 7H_2O$) is subjected to deliquescence at ~30-50 °C if RH > 85-90 % (Figs. 4, 6, and 11). Epsomite dehydrates to hexahydrite ($MgSO_4 \cdot 6H_2O$) above ~50 °C. Hexahydrite is subjected to deliquescence at HR > 85% at 50 °C and at HR > 80 % at 70 °C. Fig. 11 illustrates a possibility of sequential thermal dehyration of Mg sulfates if HR is less than ~80%: $MgSO_4 \cdot 7H_2O \rightarrow MgSO_4 \cdot 6H_2O \rightarrow MgSO_4 \cdot 4H_2O$. The higher the HR, the higher the temperature of dehydration of a Mg sulfate salt.

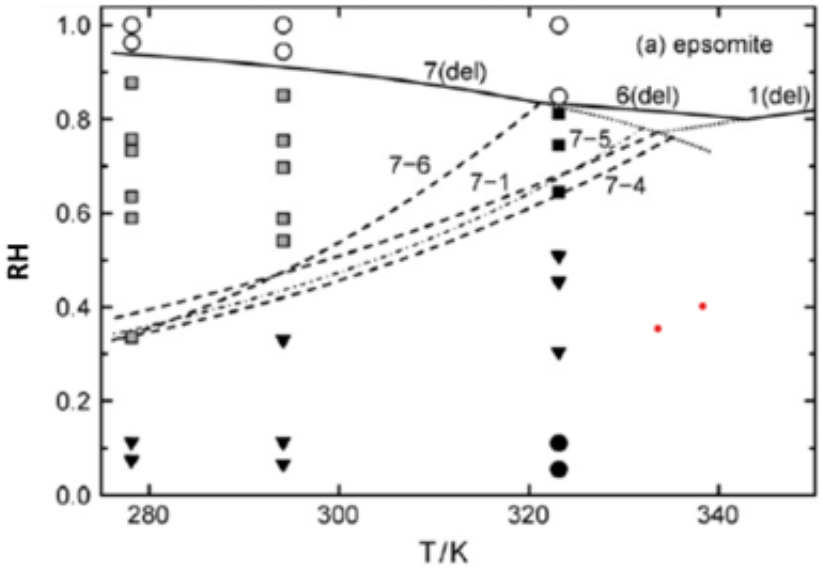

FIG. 11. Experimental and calculated deliquescence humidities (solid line) and hydration–dehydration equilibrium humidities in the system $MgSO_4$–H_2O (Steiger et al., 2011). (7), $MgSO_4 \cdot 7H_2O$; (6), $MgSO_4 \cdot 6H_2O$; (4), $MgSO_4 \cdot 4H_2O$; (1) $MgSO_4 \cdot H_2O$.

Processes that include brines

Chemical interactions of brines with other materials of heated samples can alter the affected materials and brines. One possible interaction is cation (Ca^{2+}, Na^+, K^+, etc.) exchange between clay minerals and brines. As an example, interaction of Ca-bearing clay minerals with Mg-sulfate rich brine includes Ca-Mg ion exchange, formation of Ca sulfates, and incorporation of Mg to the clay structure (Wilson and Bish, 2012). Such interactions could have occurred during the diagenesis (*e.g.*, Bridges et al., 2015) of martian clay minerals and are likely in heated brine-bearing samples. Another process is dissolution of solid and/or amorphous phases in contact with brines. The latter process is important in the case of low-pH[MZ1] brines (next section).

The composition of brines depends on the amount and composition of salts in samples, temperature, and RH in containers. The lower the RH, the higher the salinity of brines and the higher relative concentration of high-solubility salts, such as perchlorates and bromides. Solubility of bromides is comparable with that of perchlorates (Marion et al., 2009, 2010), and they all could be mobilized (*e.g.*, through deliquescence) and deposited through evaporation and freezing in a similar manner.

Bromine is a trace element in martian materials, and bromides likely exist as admixtures in chlorides. Bromides Ca, Mg, and Na are more soluble in water than corresponding chlorides. The bromide ion (Br^-) is preferentially concentrated in brines that approach salt-water eutectic compositions due to freezing or evaporation. Therefore, bromine could be preferentially mobilized through freezing/thawing and evaporation of brines at low RH. The Opportunity rover data and corresponding chemical equilibrium models for brines suggest preferential occurrence and mobility of Br^- in cold near-eutectic brines at the Meridiani Planum (Marion et al., 2009). Near-eutectic brines that could form in heated martian samples through deliquescence or water vapor condensation would be enriched in Br^-. Existence of corresponding brines at low RH implies preferential mobility and re-deposition of bromide(s). At low-RH aqueous conditions in heated containers, high solubility of bromides (*e.g.*, $CaBr_2$) suggests higher mobility than chlorides and sulfates of Ca, Mg, and Na. The expected aqueous mobilization, mobility, and re-deposition of bromides during heating and subsequent freezing of samples will moderately affect the science goals related to martian water history.

Physical processes include migration of brines and subsequent re-deposition of salts. Migration of brines in a gravity field may not be a concern because of low gravity and the overall water-deficient nature of samples. However, migration in humidity and/or temperature gradients is likely to occur and cause preferential accumulation of first brines and then salts in veins and at the surfaces exposed to the container atmosphere. Analogous processes are common on Earth (Bing et al., 2015) and could lead to accumulation of salts on the surfaces of soil. These processes occur in salt-bearing terrestrial soils in arid areas and are responsible for accumulation of salts (mostly Mg sulfates) in salt-rich carbonaceous chondrites in the meteorite collection (Gounelle and Zolensky, 2001). Several freeze[MZ2]-thaw cycles during the sample journey to Earth could contribute to brine migration and re-deposition of salts through efflorescence (liquid to crystalline solid transition).

Acid-generating reactions

If an aqueous fluid develops within the sample, several reactions may occur subsequently that can lower the pH of this fluid. These reactions include mineral dissolutions and/or redox interactions.

The mineral jarosite ($(K,Na,H_3O)Fe_3(SO_4)_2(OH)_6$) has been detected on Mars and may be present in potential samples. Jarosite forms in acidic environments (pH < 3), where dissolved ferric iron (Fe^{3+}) and sulfate (SO_4^{2-}), bisulfate (HSO_4^-), as well as cations such as K^+ or Na^+, are freely available. For example, jarosite has been described from acid mine drainage sites on Earth *(e.g.*, Hudson-Edwards 1999). It can be classed as an evaporite mineral that is readily soluble in liquid water. The most soluble variety is the hydronium (H_3O^+) endmember (Alpers et al. 1989). If the dissolving fluid has an elevated pH (> 3 at standard pressure and temperature), where jarosite would be unstable, the mineral may

convert into other iron oxy-hydroxides and release protons into solution: $KFe_3(SO_4)_2(OH)_6 = FeO(OH) + K^+ + 2SO_4^{2-} + 3H^+$ (Smith et al. 2006). Hence, the dissolution of jarosite not only increases the salinity (see above) but the acidity of a fluid as well.

Another important process that can generate acidity is the oxidation of sulfide minerals and sulfide species in solution (*e.g.*, H_2S, HS^-). On Earth, these reactions are typically coupled to O_2 reduction via the reaction $FeS_2 + 7/2\ O_2 + H_2O \rightarrow Fe^{2+} + 2SO_4^{2-} + 2H^+$ (*e.g.*, Dos Santos et al. 2016). However, under anoxic conditions, Fe^{3+} (see details below) and NO_3^- can act as oxidants instead of O_2 (Hayakawa et al., 2013; Moses et al., 1987), though oxidation of Fe^{2+} by O_2 is needed to form Fe^{3+} in the solution at the first place. On Mars, other species such as H_2O_2 and ClO_4^{2-} could also serve as oxidants (Lasne et al. 2016). In either case, sulfuric acid is generated from the oxidized sulfide, and the pH of the resulting solution can be very low (below 2), depending on the total amount of sulfide (pyrrhotite, pyrite) oxidized and the buffering capaciy of other minerals and gases in the environment. Fe^{3+} is abundant on the surface of Mars and may act as a sulfide oxidant if it is mobilized in acidic liquid water. Reaction rate of Fe^{+3}-sulfide interaction has been shown to increase if temperature is raised from 20 to 70 °C (Boogerd et al., 1991). Significant sulfide oxidation thus occurs within a few hours. Even on Earth, where pyrite oxidation is ultimately linked to O_2, Fe^{3+} is an important intermediate oxidizing agent, especially in subsurface O_2-depleted environments (Moses et al. 1987). Hence, Fe^{3+}-driven sulfide oxidation on Mars is a plausible scenario, and the increasing reaction rate with increasing temperature increases the risk of sulfuric-acid generation in sample containers. However, the latter process could be limited because of deficiency of strong oxidants (O_2, H_2O_2, Fe^{3+}, nitrate) compared to sulfide minerals.

Nitrate has been detected in the martian surface materials (Stern et al., 2015), and while on Earth the reaction between nitrate and sulfide is usually biologically catalyzed, it may also proceed abiotically, though at much slower rates (Hendrix et al., 2022). The effects of temperature on the reaction between nitrate and sulfide are yet to be determined; however, it is likely that elevated temperature enhances the reaction rate, like what has been described for the reaction between nitrate and ferrous iron (Summers and Chang, 1993). Here, an increase in temperature from 20 to 60 °C raises the reaction rate by several orders of magnitude with significant reduction occurring on timescales of minutes to hours. If the same is true for the nitrate-sulfide reaction, and if significant amounts of both substrates are present in the martian samples, then a significant amount of acidity may be generated through this process.

Thermal decomposition of martian materials explored by the SAM instrument on the MSL suggests formation of HCl (g) upon heating beyond ~25 to 30 °C (Clark et al., 2020). HCl is a strong acid. Therefore, the released HCl could affect aqueous phase and solid samples. With or without an aqueous phase, the presence of HCl (g) and H_2O (g) in the headspace will cause some alteration of the exposed carbonate surfaces and formation of corresponding (mainly Ca) chlorides.

Alkalinity-generating reactions

Some alkalinity may be generated if formed acidic fluids described above react with silicate materials and carbonates. Carbonates have a strong pH-buffering capacity. However, additional reactions can occur, independent of the initial acidity of the fluid. Even at neutral pH, aqueous fluids, which are generated more abundantly with increasing temperature of the sample (see above), may react with silicate materials and generate alkalinity over timescales of weeks to months (Gislason and Eugster 1987), and the rate of the reaction increases slightly with temperature. Volcanic glass and fine-crystalline volcanic rock, in particular rocks of mafic and ultramafic composition, can act as a strong base, that is,they absorb protons and release cations into solution during water-rock reactions (Garrels and Mackenzie 1967). The pH of the resulting solution may be as high as 9 or 10, especially if it is associated with subsequent evaporation of the fluid and precipitation of carbonate minerals.

A related reaction is serpentinization, that is, the reaction between water and olivine and pyroxene minerals. This reaction can proceed at temperatures as low as 30 °C if given sufficient time (on the order of months), and serpentinization of ferrous minerals can lead to the formation of abiotic H_2 and, possibly CH_4 (Neubeck et al. 2011), but may not produce these gases at considered temperatures and time of heading (McCollom and Donaldson 2016). The pH of fluids involved in serpentinization can reach high pH values of 9-11 (Moody 1976; Holm et al. 2015),

though water deficiency in sample containers would limit these processes.

Aqueous redox reactions

As noted before for some acid-generating reactions, redox processes are expected to occur because the modern martian surface is oxidized, whereas igneous rocks and some subsurface sediments may have formed under anoxic conditions. Physical mixing between modern (or relatively recent) oxic surface materials and anoxic subsurface materials may, therefore, lead to chemical disequilibrium, which can drive reactions and ultimately obliterate specific environmental and biological signatures. Importantly, this may include signatures of past and present (or recent) surface conditions. The major oxidizing agents to consider are radical species, O_2, H_2O_2, ferric iron, sulfate, oxychlorine compounds, including perchlorate, and minor nitrate as well as manganese oxides. Major reductants are likely to be ferrous iron, sulfide, organic matter, as well as trace levels of CH_4, H_2 (see above), or ammonium (see above) that may be released from the sample. Reactions between some of these reagents are of concern, because they may destroy certain phases (*e.g.*, organic matter or sulfides becoming oxidized), alter isotopic compositions, and/or generate acidity (see above), which may further impact the integrity of the sample.

As an example, we consider the reaction between martian nitrate (Stern et al. 2015) and ferrous iron. Under aqueous anoxic conditions, nitrate may spontaneously react with Fe^{2+} and convert to nitrite and then to ammonium with the reaction accelerated by an increase in temperature (Summers and Chang 1993). Hence, a significant amount of the original nitrate may be lost as it reacts with ferrous iron.[MZ3] The ferrous iron ion (Fe^{2+}) could be derived from ferrous clay phases or from primary mafic silicates and sulfides (pyroxene, olivine, amphibole, pyrrhotite) that are contained in the sample. Isotopic effects (see also next section) of these reactions have so far not been investigated, but they are likely to be significant, given the large isotopic effects associated with biological nitrate reduction. Hence, any efforts of constraining the primary N isotopic composition of the ammonium-bearing organic matter, ammoniated clay minerals and primary nitrate deposits could be compromised. Losing nitrates from the sample may further impact our ability to reconstruct atmospheric processes on Mars that lead to the formation of nitrates in soils.

Reactive oxygen species and radicals that are informative of photochemical reactions on Mars may be lost from the sample if they react with reductants such as ferrous iron, sulfide sulfur, ammonium, organic matter, H_2, or CH_4. Hence, our ability to measure these radicals after the sample has been returned to Earth may be severely impacted.

Sulfates can theoretically be reduced to elemental sulfur or sulfide, coupled to the oxidation of organic matter, H_2 or CH_4. However, on Earth, these reactions are typically catalyzed by microbes, because the abiotic reaction rate is very low below 100 °C (Machel 2001). Significant abiotic sulfate reduction, also known as thermochemical sulfate reduction, only occurs at temperatures in excess of 150 °C (Ohmoto and Lasaga 1982) and is therefore not relevant for this study. Manganese oxides have also been detected on Mars (Lanza et al. 2014; Arvidson et al. 2016), and they, too, may undergo reduction if they are brought into contact with aqueous Fe^{2+}, H_2, CH_4, or sulfides (HS^-, H_2S). Abiotic reduction of Mn^{4+} to Mn^{3+} and Mn^{2+} can occur on timescales of hours at room temperature (Johnson et al. 2016*)*. Hence, primary Mn oxides may be lost from the samples.

Isotopic exchange reactions

Even if phases are not entirely lost from the record during sample storage, it is possible for them to undergo isotopic exchange reactions and thus lose some primary environmental information. For example, the dissolution of sulfate minerals may homogenize their stable isotope ratios ($\delta^{34}S$, $\Delta^{33}S$, $\Delta^{36}S$). Similarly, oxygen isotope ratios ($\delta^{18}O$, $\delta^{17}O$) of various salts and hydrated oxides (Mn^{4+}, Fe^{3+}) may undergo homogenization upon prolonged heating in aqueous media. For hydrous iron oxides, for example, isotopic exchange occurs rapidly and is therefore considered to reach equilibrium with the new fluid phase almost instantaneously (Bao and Koch 1999). The isotopic composition of primary atmospheric CO_2 gas ($\delta^{13}C$) may become homogenized with that of carbonates if the latter undergo (partial) dissolution. Isotopic equilibration between aqueous and gaseous inorganic carbon is reached on timescales of hours at room temperature, limited by diffusion kinetics (Zhang et al. 1995).

2.2.1.6. Interactions with container materials

Given the coating of the container with titanium nitride (TiN), there might be some concern about contamination of nitrogen and possibly even titanium in the sample. Titanium nitride is almost insoluble in liquid water, but corrosion of TiN by sulfuric acid has been demonstrated (Chyou et al. 1993). For samples where sulfuric acid generation is a possibility (*e.g.*, samples containing soluble acid sulfate salts or oxidizable sulfides), some corrosion of TiN needs to be considered. As more sulfuric acid is expected to be generated with increasing temperatures (see above), the prolonged heating of the sample containers could enhance corrosion intensity. A consequence of such corrosion would be the release of N and Ti into the sample, which may hinder accurate analyses of primary Ti and N abundances and isotopic compositions. The magnitude of this effect would depend on the sample's original Ti and N contents, as well as on the length of time for which the container is exposed to acid attack.

2.2.2. Processes after heating

Cooling of heated samples will lead to sorption of gases that are either survived or produced in chemical reactions that occur at elevated temperatures. Deposition of sublimated organic compounds is expected after lowering the temperature. Therefore, those organic compounds will not be lost but could condense in different locations (including walls) in the container.

High relative humidity in the head space maintained during cooling of water-rich samples could cause incorporation of H_2O(g) into the interlayer space of clay minerals (*e.g.*, saponite, montmorillonite, kaolinite). The process is more efficient in a liquid water-rich environment. The incorporation of H_2O into the interlayer space of phyllosilicates would compete with other processes that affect the amount of H_2O present, including absorption, condensation, and hydration of solid phases (mainly salts), which could occur more rapidly.

Rates in chemical reactions exponentially decrease as temperature decreases. Rapid cooling of water-poor samples to temperatures below 0 °C would mainly preserve mineralogy that was formed at elevated temperatures.

Cooling of water-rich samples may cause condensation of H_2O(g) followed by formation of water ice. If an aqueous phase existed at the highest temperature, more water would condense. The decrease in temperature will decrease the H_2O(g)/H_2O(l) and H_2O(g)/H_2O(ice) ratios. Water would predominantly condense on colder materials in the container (Fig. 1) and may sink to lower levels by the gravitational force. A rapid cooling would lead to condensation of water rather than formation of hydrated phases (e.g., salts) from which water was initially released. Later, if the temperature remains above freezing point, new-formed hydrated salts (*e.g.*, Ca-, Mg-chlorides and Mg-, Ca-, Na-sulfates) will equilibrate with the H_2O(g) in the head space and with aqueous phase, if it is present.

If an aqueous phase exists during heating, subsequent cooling and freezing of brines will cause precipitation of salts (carbonates, sulfates, and halogenides). As noted above, newly precipitated salts may differ from original salt hydrates. Physical-chemical modeling of freezing of martian water solutions (*e.g.*, Marion and Kargel, 2008; Marion et al., 2009; Toner and Catling, 2015) suggests precipitation in the following sequence, Ca sulfates and/or Mg/Ca carbonates, Mg sulfates, Na chloride(s), Mg chlorides/perchlorates, Ca chlorides, perchlorates, and bromides. As temperature decreases, the salinity and chloride/sulfate ratio in the remaining diminishing volume of brines increases. In originally water-rich samples, migration of brines enriched in high-solubility salts (Ca/Mg chlorides, bromides and perchlorates) and corresponding re-deposition of salts is possible well below 0 °C. In water-poor samples, the salts could be deposited near the places where the salts experienced deliquescence and were dissolved by liquid water during heating. In such samples, salt materials will not be lost, though aqueous alteration of silicates and other phases during higher-temperature periods would modestly change the composition of precipitated salts. In water-rich samples (*e.g.*, soil with abundant hydrated salts and water ice), the salt composition could be more chemically altered during the heating-cooling episode(s). Salts, especially high-solubility chlorides, perchlorates, and bromides will be deposited in places where brines migrated. In both cases, the composition of salts will be more altered in cases of prolonged (months) and high-temperature (40 to 60 °C) warming.

Fluid inclusions can be formed as a secondary phase ("secondary fluid inclusions") when exposed to volatiles. These secondary fluid inclusions can contain various liquid and gaseous phases. Ancient chemical sediments and diagenetic features commonly host both primary and secondary fluid inclusions in the same crystals. However, petrographic criteria have been established to distinguish them from one another (*e.g.*, Goldstein and Reynolds, 1994). On Earth, secondary fluid inclusions most commonly form during burial. In the case of Mars return samples, any secondary fluid inclusions may be the result of diagenetic events on Mars and/or due to heating and exposure to volatiles within

sample tubes.

Redox reactions are much less efficient than they are at higher temperatures. Rates of redox reactions increase with increasing temperature, and oxidants may be completely consumed at high temperatures.

2.3. Synergistic effects

Each RSTA is a closed system, and water evolved from hydrous phases is not only lost from its host phases but will be retained in the closed system as vapor that may condense and catalyze mineral-water reactions and even hydrate other phases. Reactions that would be catalyzed by molecular water or consume and incorporate the water's elements and isotopes into newly formed reaction products include oxidation-reduction of any redox-sensitive element that would be the desired measurement for any number of other iMOST Investigation Strategies. Consequently, any measurable attribute of the sample that would be changed by being exposed to free molecular water in the RSTA would be compromised by the water evolving from any phases that even partially dehydrate in the 30 to 50°C range for more than a limited duration of time. Timescales for individual mineral and amorphous phases likely to occur in samples from Mars are reported in the literature discussed below.

3. Inorganic compounds

Numerous iMOST investigation strategies and their supporting samples and measurements (iMOST, 2018; Beaty et al., 2019) refer to mineral groups (*e.g.*, carbonate, evaporite, clay minerals, etc.), mineral properties (*e.g.*, hydrated, hydrous, etc.), and broad categories of reaction types (*e.g.,* dehydration, oxidation, hydrothermal, etc.). Specific minerals in these groups are expected to contain evidence of paleoenvironments, potentially habitable niches, and the geologic context of life-science observations, and many are likely host phases for morphological and molecular biosignatures. The occurrences of these minerals individually and as phases in mneral assemblages, and the abundances and isotopes of H and O in their structural molecular water, and C and S in their anionic groups, constrain the ranges of temperature and the solute composition (e.g., pH) of the aqueous solutions from which they formed. Microscopic studies of mineral habits (crystal shape), fluid inclusions, spatial associations, and textures are indicative of reaction relationships, paragenetic assemblages, and temporal sequences of reactions of mineral formation and alteration. All these types of information are crucial to meeting iMOST objectives of characterization of paleofluids and paleoenvironmental conditions conducive to past habitability and preservation of potential biosignatures. The iMOST report made the case for more than 200 anticipated measurement types for a wide range of landing-site geologies (iMOST, 2018; Beaty et al., 2019).

3.1. Hydrated minerals at risk of heating events

Hydrous/"hydrated" minerals in general, or one or more specific hydrous salt-mineral groups, or phyllosilicates and other hydrous silicates (examples shown in Fig. 12) are host phases of volatiles and may ~~content~~ contain redox-sensitive (including mixed valence) elements. They are explicitly stated as phases to be sought for analytical studies of isotopy, dehydration/hydration, polymorphs, transitions, and redox state of carbon, hydrogen, nitrogen, oxygen, phosphorous, and sulfur (CHNOPS) elements and first row transition elements (FRTE) in support of high-priority iMOST Objectives 1 and 2 (and most other iMOST Objectives), Sub-objectives, Investigation Strategies (Table 11), and Measurement types. Explicit callouts in iMOST Objectives 1 and 2 by mineral type (*e.g.*, sulfate, carbonate, phyllosilicate, clay mineral), stable isotopes of elements hosted by such minerals (especially H, O, C, and S), genesis (*e.g.*, evaporite, diagenesis, weathering), or host material *(e.g.*, soil/paleosol) are included and underlined in Supplemental Table S1. Many more measurement-sample pairs are referred to implicitly, by seeking evidence of specific processes (*e.g.*, diagenetic alteration of sedimentary deposits) rather than specific minerals; these are also underlined, but only some of these are included in Supplemental Table S1; many more are in the iMOST report (iMOST, 2018; Beaty etl., 2019).

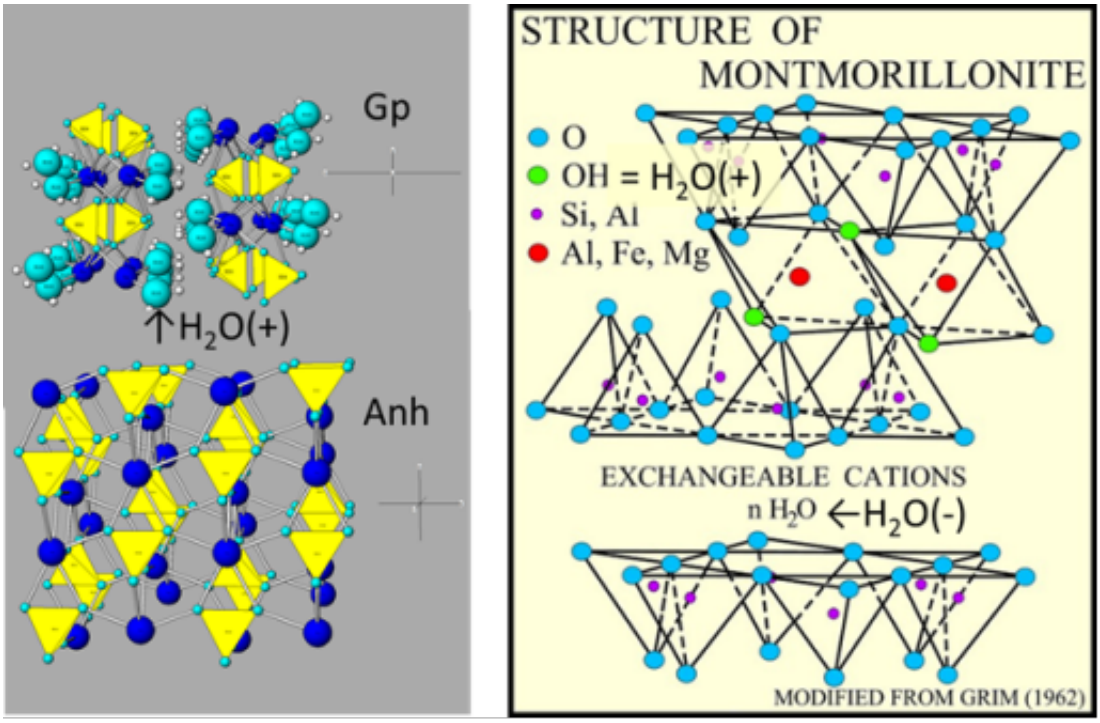

FIG. 12. Crystal structure diagrams of minerals that contain scientifically important volatile and oxidation-reduction (redox)-sensitive elements (O, H, S, Fe): (left) sulfate minerals gypsum (Gp) ($CaSO_4 \cdot 2H_2O$) and anhydrite (Anh) ($CaSO_4$) (drawn using ATOMS), (right) the smectite-group clay mineral, montmorillonite (~ $Ca_{0.25}(Al(Mg,Fe^{2+})_2(Si,Al)_4O_{10}(OH)_2 \cdot nH_2O$). (modified from Poppe et al., 2001; modified from Grim, 1962). $H_2O(+)$ – so-called "structural water" – includes molecular H_2O that is part of the mineral's structure (for example, in gypsum) and hydroxyl (OH) that is part of the mineral's structure (for example, in montmorillonite). Both structural H_2O and structural OH can be removed from the structure by, for example, heating, with dehydration and dehydroxylation evolving molecular water and producing a different mineral. $H_2O(-)$ includes molecular water sorbed at any mineral's surface and molecular water weakly bound to exchangeable interlayer cations in some common and widespread clay minerals (for example, montmorillonite). See Velbel and Zolensky (2021), footnote 1.

EIC's NOTE TO THE COPY EDITOR: Please reduce the row-spacing height in Table 11 to reduce its overall size in the published article. Thanks, Sherry

Table 11. Summary of high-priority iMOST sample-related investigation strategies calling for analyses of hydrous minerals.

Investigation Strategies (IS) for Objectives 1 and 2		
IfObjective 1	Geological environment(s)	Interpret the primary geologic processes and history that formed the martian geologic record, with an emphasis on the role of water.
Sub-Obj. 1.1	Sedimentary System	Characterize the essential stratigraphic, sedimentologic, and facies variations of a sequence of martian sedimentary rocks.
Why is this objective critical?	*A key input into quantifying and interpreting the history of water on Mars; search for life.*	
IS 1.1B	Investigate sediment diagenesis, including the processes of cementation, dissolution,	

	authigenesis, recrystallization, oxidation/reduction, and fluid-mineral interaction	
IS 1.1C	Investigate the mechanisms by which sediment is/was generated on Mars, by understanding the weathering and erosional processes.	
Sub-Obj. 1.2	Hydrothermal	Understand an ancient martian hydrothermal system through study of its mineralization products and morphological expression.
Why is this objective critical?	*A key input into interpreting the history of water on Mars; search for life.*	
IS 1.2D	Determine the age of the hydrothermal system and the duration and rate of water flow.	
IS 1.2E	Investigate the possibility of post-depositional modification/fluids and interpret those processes.	
Sub-Obj. 1.3	Deep subsurface groundwater	Understand the rocks and minerals representative of a deep subsurface groundwater environment.
Why is this objective critical?	*A key input into interpreting the history of water on Mars; search for life.*	
IS 1.3A	Interpret the morphologic features and minerals resulting from groundwaters in igneous and sedimentary host rocks to understand the extent of groundwaters, their transport, and their episodicity.	
IS 1.3B	Determine the physical-chemical conditions of water-rock interaction and assess habitability.	
IS 1.3C	Determine the source of fluids and abiotic or biotic reactions governing mineral precipitation.	
IS 1.3D	the absolute time-evolution of the groundwater system and chemical reactions.	
Sub-Obj. 1.4	Subaerial	Understand water/rock/atmosphere interactions at the martian surface and how they have changed with time.
Why is this objective critical?	*A key input into interpreting the history of water on Mars; search for life.*	

IS 1.4A	Investigate weathered materials such as soils, paleosols, weathering rinds or rock coatings to investigate the duration and nature of past climates and both ancient and modern habitable surface environments.	
IS 1.4B	Assess the history of surface water at the site, including the chemistry, source, and longevity of the waters, and their role in the formation of wetlands, ponds, and springs.	
IS 1.4C	Assess the diagenetic history of the site, including the chemistry and redox state of past near-surface waters and groundwaters, how water sources may have interacted, and how they have changed through time.	
IS 1.4D	Determine sediment provenance and transport history.	
Sub-Obj. 1.5	Igneous terrane	Determine the petrogenesis of martian igneous rocks in time and space.
Why is this objective critical?	*Key input into the mechanisms for formation of igneous rocks and the evolution of Mars on a planetary scale*	
IS 1.5A	Determine the compositional and textural diversity of igneous rocks and the time-resolved geological processes which relate them to each other and to martian meteorites.	
Objective 2	Life	Assess and interpret the potential biological history of Mars, including assaying returned samples for the evidence of life.
2.2	Biosignatures-ancient	Assay for the presence of biosignatures of past life at sites that hosted habitable environments and could have preserved any biosignatures.
Why is this objective critical?	*The search for life is one of the driving objectives for Mars exploration in general, and sample studies are an essential component of astrobiology strategy.*	
Which are the most important samples?	*All of the samples collected as part of Objective 1 are of interest*.	
IS 2.2A	Characterize aspects of the environment that are conducive to the preservation or degradation of biosignatures.	

IS 2.2F	Identify any chemical evidence of life that is different from that specified above.

Secondary minerals (alteration products of various paleoenvironmental chemical reactions of aqueous solutions with pre-existing minerals) observed by orbital spectroscopy of Jezero crater were among the main criteria used to select the M2020 landing site (Grant et al., 2018). The first Earth year of *Perseverance* rover operations at Jezero crater has already yielded provisional identifications of all the aforementioned mineral groups. Minerals including gypsum, monohydrated Mg-sulfate, polyhydrated Mg-sulfate, unspecified carbonate, and smectite-group clay minerals have been tentatively identified in Jezero crater from *Perseverance* SuperCam Visible and Near InfraRed (VisNIR) spectroscopy (Mandon et al., 2021). Planetary Instrument for X-ray Lithochemistry (PIXL) data lend additional support to the occurrence of Ca-S-rich surface crust or cement (Schmidt et al., 2021).[MZ4][VM5][MS6]

Most of the minerals listed in the preceding paragraphs are known to be heat-sensitive upon heating to above their formation temperatures. A sample is heat-sensitive if heating to above its formation temperature changes the attribute(s) of one or more of the minerals or other amorphous solid phases that must be measured to implement and inform the corresponding iMOST investigation strategy. The deleterious effects of heating a sample to sterilization temperatures (sterilization sensitivity) for a variety of measurable attributes were explored in depth by Velbel and others (2022) and are illustrated for this report in Fig. 13. iMOST investigation strategies and their associated saples and measurements are revisited here for their sensitivity to heat within the temperature range of concern to this study (30 to 50° C).

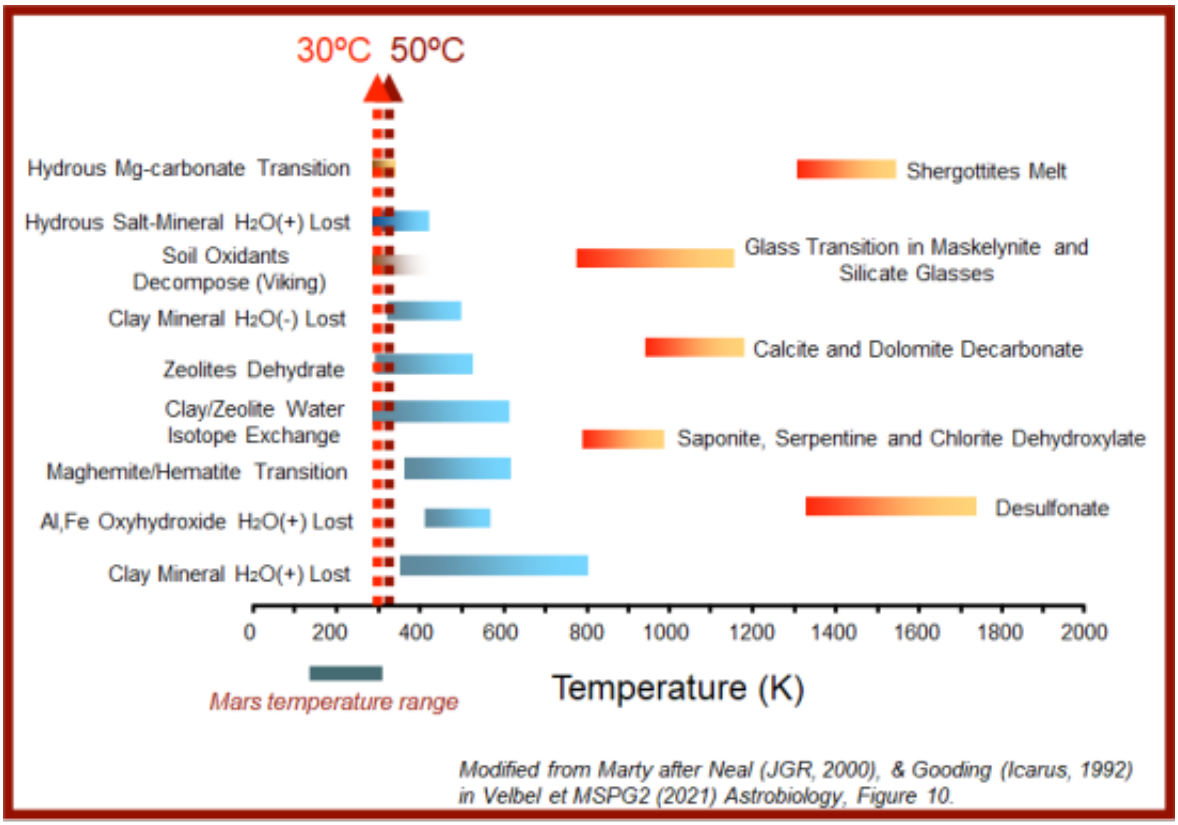

FIG. 13. Phase transition temperatures for MSR Campaign-relevant minerals and amorphous materials. The dashed lines indicate the range of temperatures of concern to this study. $H_2O(+)$ and $H_2O(-)$ are defined in Figure 12. Modified by B. Marty after Gooding (1992) and Neal (2000) for, and adapted for this report from, Velbel and others (2022).

3.2. Deleterious effects on hydrous minerals owing to dehydration and rehydration

Dehydration causes loss of information important for interpretation of the sample's paleoenvironment, the potential habitability of the paleoenvironmental, the preservation potential of potential biosignatures, and the geologic context of life-science observations. Specific categories include phase change (loss of knowledge of pristine mineral

occurrence on Mars) with corresponding loss of information about thermodynamic stability and metastable persistence of the water's as-sampled host mineral, loss of molecular water from the as-sampled host mineral and addition of that water to other pases in the closed system of the sealed RSTA with corresponding information degradation and loss in other phases ("sharing water" – blurring of stable isotope differences between different minerals). Rock fabric may be disrupted by volume change during (i) dehydration and rehydration of salt hydrates and (ii) expansion of swelling clay minerals, causing degradation and loss of microscopic and spatially resolved (host phase-specific) microanalytical observations of mineral habit (crystal shape), associations, paragenetic assemblages, pseudomorphism, textures indicative of reaction relationships, and fluid inclusions, with corresponding loss of information about temporal sequences of reactions and host environments, and loss of stable H and O isotopes of molecular water hosted in the as-sampled hydrous sulfates, eliminating the possibility of spatially resolved *in situ* microanalyses of phase- and grain-/crystal-specific water abundance and stable H and O isotopes.

Rehydration would redistribute water molecules and their isotopes from their as-sampled host phase to other phases in the closed RSTA system, with similar loss of information. With the possible exception of very finely crystalline clay minerals such as smectite (Bish and Duffy, 1990), mobilization of H and O by dehydroxylation of OH-bearing minerals (*e.g.*, phyllosilicates) is not expected within the temperature range of interest (30 to 50 °C) (Kawano and Tomita 1991, Gooding, 1992; Huang et al., 1994; Frost et al., 2000; Neal, 2000; Che et al., 2011).

3.3. Sulfates

All the first 15 samples of fluviolacustrine sedimentary rocks analyzed as bulk drill-fine powders by MSL's Chemistry and Mineralogy (CheMin) X-ray diffractometer (XRD) at Gale Crater contain at least one hydrated sulfate mineral (Rampe et al., 2020). Sulfate minerals were not spectroscopically detected from orbit at Jezero Crater (Ehlmann et al., 2008a; Goudge et al., 2015; Horgan et al., 2020) or mentioned specifically by advocates for landing and operating the M2020 rover in Jezero Crater (Golombek et al., 2012; Grant et al., 2018). Nevertheless, sulfates are expected in Jezero crater. Literature supporting such expectations is cited where specific groups of minerals are discussed below.

3.3.1. Ca-sulfates

3.3.1.1. Ca-sulfates and iMOST objectives

The probable occurrence of hydrous Ca-sulfates in returned Mars samples is anticipated based on the following observational evidence:

- Ca-sulfates occur in at least some individual meteorites from each of the abundant groups of meteorites from Mars – shergottites, nakhlites, and chassignites (SNCs; see review by Velbel, 2012, references therein, and more recent references). Some may be part of the meteorite's mineral inventory on Mars (martian), but many are demonstrably terrestrial (formed by terrestrial weathering after the meteorite's fall). Ambiguity about this mineral group's origin in meteorites from Mars is one reason for the MSR Campaign.
- At least one of the Ca-sulfates gypsum ($CaSO_4 \cdot 2H_2O$; Figure 12), bassanite ($CaSO_4 \cdot 0.5H_2O$), and anhydrite ($CaSO_4$, anhydrous; Figure 12) has been detected and quantified in 12 (80%) of the first 15 samples of fluviolacustrine sedimentary rocks analyzed as bulk drill-fine powders by MSL's CheMin XRD at Gale Crater (Rampe et al., 2020).
- Unspecified sulfate minerals have been detected from orbital Mars Global surveyor (MGS) Thermal Emission Spectrometer (TES) data in the Jezero watershed and Jezero crater (Salvatore et al., 2018).
- Bassanite has been detected by Compact Reconnaissance Spectrometer for Mars (CRISM) orbital spectroscopy in the North Polar dunes of Mars (Parente et al., 2022).
- Recent data from *Perseverance* instruments in Jezero crater include the following:
    - Gypsum has been tentatively identified from early SuperCam VisNIR spectroscopy (Mandon et al., 2021).
    - Early PIXL data lend additional support to the occurrence of a Ca-S-rich mineral and intermixed Ca- and Mg-sulfates occurring as a surface crust or cement (Schmidt et al., 2021; Meslin et al., 2022).
    - SHERLOC-WATSON Raman spectroscopic detections of a widely distributed sparsely abundant Ca-S-rich mineral in the Guillaume target (Scheller et al., 2022).

The MSR Campaign science to be built upon analyses of these minerals: High-priority iMOST Objectives, Sub-Objectives, Investigation Strategies, and associated Measurement types – 1.1B, 1.2E, 1.3B, 1.3C, 1.3D, 1.4A, 1.4B,

1.4C, 1.5A, 2.2A, 2.2F.

Paleoenvironmental conditions of the water, such as the thermodynamic activity of the solvent water (aH_2O) and the saturation state of the aqueous solution from which the Ca-sulfates initially precipitated with respect to the precipitated salt mineral, can be determined from equilibrium chemical thermodynamics. The temperature and pre-precipitation natural history of the solvent water can be inferred from the stable H and O isotopes of the Ca-sulfate minerals precipitated from that water. Two thirds (66%) of the first 15 samples of fluviolacustrine sedimentary rocks analyzed as bulk drill-fine powders by MSL's CheMin XRD at Gale Crater contain two or more of the Ca-sulfates (Rampe et al., 2020). Textural (microscopic) observations and associatedpatially resolved isotope microanalysis of intact samples containing more than one Ca-sulfate mineral would be required to establish (from crystal habits, cross-cutting or superposition relationships, or pseudomorphic replacement) whether the multiple Ca-sulfates coexist in the sample because they formed at the same time, formed initially as one that was then consumed by a reaction that formed the other, or formed completely independently of one another. Evolving paleoenvironmental conditions of the long-absent aqueous solutions can be inferred in support of establishing the context within which potential biosignatures in associated rocks may have been incorporated and preserved.

3.3.1.2. Ca-Sulfates - Deleterious effects of heating to (30 °C < T < 50 °C)

Dehydration

In a vacuum oven with pH_2O maintained at ~0.7 Pa, the onset and completion of gypsum dehydration to bassanite (sub-mm coarse silt to fine sand size natural White Sands, New Mexico, U.S.A.) occur after tens and hundreds of hours, respectively, at 297 K (24 °C) and after ~ 1 hour and several tens of hours, respectively, at 323 K (50 °C) (Vaniman et al., 2008). An apparent Arrhenius activation energy calculated from their experiments (19.9 kcal mol^{-1}, 83 kJ mol^{-1}) permits interpolation (Table 12) of the experimental results of Vaniman et al. (2008) from the range of their experimental temperatures (24 °C < T < 50 °C) to temperatures in the range considered in this study (30 °C < T < 50 °C). Temperatures of 30 °C for less than several days are unlikely to induce gypsum dehydration, whereas granular gypsum is unlikely to persist intact for longer than a few tens of hours at 50 °C, possibly within the range of concern for this study (Table 12). In Western Australia, gypsum occurs at the surface as large (up to ~10 cm) bottom-growth crystals, as well as in smaller crystals and as re-worked sand and silt. There, it has been exposed to temperatures of 50 °C over several days at a time, and has remained as gypsum (Benison et al., 2007).

Estimated amount of water evolved

The amount of molecular water that could be released by complete dehydration of gypsum to bassanite in fluvio-lacustrine sedimentary rock samples from Jezero crater after the RSTA is sealed can be estimated. The preliminary estimate here uses the weight % of water in gypsum (~21 wt.%), [MZ7][VM8]the maximum known abundance of gypsum detected in similar rocks by CheMin at Gale crater (7 wt%; Rampe et al., 2020), estimated densities of sedimentary rock types from uncompacted mudstone through compacted mudstone and moderately porous mafic sandstone to low-porosity mafic sandstone (2.0 – 2.8 g/cm^3), and the volume of a nominal cylindrical sample in an RSTA (dimensions 1.3 cm diameter, 8.1 cm length = ~8 cm^3 not including a nominal 25% margin; Moeller et al., 2021). From these values and assumptions, complete dehydration of the gypsum in mudstones and mafic sandstones to bassanite would evolve ~250 – 350 mg of water into other phases in the sealed, closed-system RSTA. Higher proportions of gypsum in the rock would yield higher abundances; the recently acquired CheMin sample Zechstein hit a gypsum-rich vein that was not exposed at the surface and contained 25% gypsum (Rampe et al. 2022). Complete dehydration of the vein gypsum in Zechstein would evolve ~610 – 850 mg of water into other phases in the sealed, closed-system RSTA.

Rehydration

Rehydration of sub-mm (coarse silt to medium sand grain size) bassanite to gypsum by vapor over H_2O ice can begin in ~1 hour and proceed approximately one-third of the way to completion in ~10 hours at 271 K (Vaniman et al., 2008). Vaniman et al. (2008) performed similar experiments at 243 K and 223 K. An apparent Arrhenius activation energy calculated from their experiments (9.6 kcal mol^{-1}, 40 kJ mol^{-1}) permits extrapolation of the experimental results of Vaniman et al. (2008) over the range of the experimental temperatures (-50 °C < T < -2 °C) to temperatures in the range considered in this study (30 °C < T < 50 °C; Table 12 herein). Bassanite would be fully rehydrated to gypsum on a timescale on the order of one day in the closed-system RSTA by water of hydration evolved from any mineral in the

RSTA that dehydrates over the temperature range of interest to this study. On this basis, the hydration states of Ca-sulfates are expected to differ as a consequence of heating such samples particularly in the 40 °C < T < 50 °C range. These timescales are in the same range (hours to days) estimated for room-temperature laboratory conditions by Tosca et al. (2021). The ability to perform the science investigations described in the preceding paragraph on Ca-sulfates would be impaired by mobilization of water molecules between host phases during heating in the same temperature range.

Gypsum and perhaps bassanite are excellent and most likely candidates to contain fluid inclusions that could reflect fluid compositions at the time of crystal growth. These inclusions will be lost during any dehydration/rehydration process. Also, these fluid inclusions would likely be 100% filled if they are trapped at surface pressures and temperatures. As such, significant increases in temperature will cause expansion of any high-density brines that they contain, and that may cause the rupture of the fluid inclusion (especially in gypsum that has an excellent cleavage). It should be noted that halite (NaCl) is a more robust host for fluid inclusions and examples exist on Earth of Precambrian halites with unaltered fluid inclusions.

Gypsum and bassanite convert to anhydrite at around 50 °C. The exact temperature is variable, depending on the exact composition of the solution (if the minerals are in it) and mineral phase (Hill 1937). The reactions seem to proceed on timescales of months. Gypsum (Langevin et al. 2005) and bassanite (Wray et al. 2010) have been detected on the martian surface, and it has been hypothesized that they may contain trapped organic matter (Aubreyt al. 2006). Therefore, the stability of these minerals during the sampling process needs to be considered.

The effects of temperatures between ~6 °C < T < 30 °C on the preservation of martian gypsum and the scientifically useful attributes it preserves (*e.g.*, phase stability/metastability, H and O isotopes, fluid inclusions) can be extracted from Ca-sulfate abundances in X-ray diffraction results from *Curiosity*'s CheMin instrument. The daily temperature cycle inside CheMin ranges from ~6 to 30 °C (Vaniman et al., 2018). During the 150 sols in which a suite of five gypsum-bearing samples were analyzed, daily surface temperatures around *Curiosity* increased from -12 to 10 °C and maximum air temperature increased from around -17 to -5 °C; the temperature inside CheMin cycled diurnally between 7 and ~30 °C throughout this interval (Vaniman et al., 2018). Gypsum- and anhydrite-rich and bassanite-free sample Oudam was initially analyzed four times over 37 sols. It is important to note that Vaniman et al. (2018) only used the first night of analysis, within a few hours of sample delivery into CheMin, to estimate the initial gypsum:bassanite ratio. This is too short a period for significant transition of gypsum to bassanite. Evidence to corroborate this assumption is in their analysis of the sample Oudam, which had 3.3% gypsum and no bassanite in the first night of analysis. Bassanite was first seen in Oudam at very low abundance (0.1%) after 4 sols inside CheMin and was still forming from gypsum at least 8 sols into the set of analyses (Vaniman et al., 2018). By the 37th sol, no gypsum was detected and the Ca-sulfates in the sample consisted entirely of bassanite and anhydrite. The prompt, first-sol analysis raises the possibility that all bassanite detected by the CheMin XRD (Rampe et al., 2020, and references therein) may have been formed prior to the XRD measurements after many sols in *Curiosity's* onboard environment and may thus preserve at best only minimal information about conditions of the pre-acquisition sample and the sample site (Vaniman et al., 2018).

The Ca-sulfate assemblage in this sample changed from its as-sampled gypsum-anhydrite assemblage at the temperatures of the CheMin sampling depth (2 – 6 cm) and the local relative humidity when acquired to an artificial bassanite-anhydrite assemblage in 37 sols when stored in CheMin at temperatures fluctuating between ~6 to 30 °C (Vaniman et al., 2018). This is at the short end of the timescales for gypsum dehydration to bassanite at higher tmperatures determined by Ritterbach and Becker (2020). The hydrous phase and the Ca-sulfate phase assemblage present after 37 sols between ~6 to 30 °C were artefacts of the temperatures inside CheMin, and 75% of the molecular water in the sample on the sol of acquisition was lost from the solid sample– along with it the H and O isotope information about the fluid from which the gypsum formed.

Timescales of deleterious effects

The timescales of deleterious effects on the fidelity of Ca-sulfates subject to heating are available in the literature (Vaniman et al. 2008) and tabulated below (Table 12).

TABLE 12. Estimated timescales of gypsum dehydration and bassanite rehydration in Mars sedimentary rock samples (Vaniman et al. 2008).

Reaction	Details	Units	10	20	30	40	50

			°C	°C	°C	°C	°C
Dehydration	vacuum oven pH_2O ~0.7 Pa, t to complete dehydration						
Gypsum to anhydrite	$CaSO_4 \cdot 2H_2O \rightarrow CaSO_4 + 2H_2O$	days	67	20	7	2	1
		hours	1616	485	158	55	20
Rehydration	vapor over H_2O ice, t from n = ~0.2 to ~1.8						
Bassanite to gypsum	$CaSO_4 \cdot 0.5H_2O + 1.5H_2O \rightarrow CaSO_4 \cdot 2H_2O$	days	6	3	2	1	1
		hours	133	74	43	26	16
Dehydration	vacuum oven pH_2O ~0.7 Pa, t to complete dehydration	Units	10 °C	20 °C	30 °C	40 °C	50 °C
Gypsum to anhydrite	$CaSO_4 \cdot 2H_2O \rightarrow CaSO_4 + 2H_2O$	days	67	20	7	2	1
		hours	1616	485	158	55	20
Rehydration	vapor over H_2O ice, t from n = ~0.2 to ~1.8						
Bassanite to gypsum	$CaSO_4 \cdot 0.5H_2O + 1.5H_2O \rightarrow CaSO_4 \cdot 2H_2O$	days	6	3	2	1	1
		hours	133	74	43	26	16

Notice that dehydration of gypsum is much (> ~4×) slower than rehydration of bassanite to gypsum below 30 °C, but nearly equal at 50 °C. Heating in the range of concern to this study could change the proportions of gypsum and bassanite in a heated sample in a matter of hours.

3.3.2. Mg-sulfates

Considerations of Mg-sulfates are similar to Ca-sulfates in some ways, but there are many more hydrous Mg-sulfates ($MgSO_4 \cdot nH_2O$) with a much larger range of hydration states; kieserite, n = 1; sanderite, n = 2; starkeyite, n = 4; pentahydrite, n = 5; hexahydrite, n = 6; epsomite, n = 7; and the recently discovered meridianiite, n = 11 (Peterson and Wang, 2006; Peterson et al., 2007).

3.3.2.1. Mg-sulfates and iMOST objectives

The probable occurrence of hydrous Mg-sulfates in returned Mars samples is anticipated based on the following observational evidence:

- Mg-sulfates occur in at least some individual meteorites from each of the abundant groups of meteorites from Mars – shergottites, nakhlites, and chassignites (SNCs; see Wentworth et al., 2005; the review by Velbel (2012) and references therein; and more recent references such as Stopar et al., 2013). Some may be part of the meteorite's mineral inventory on Mars (martian), but many are demonstrably terrestrial (formed by terrestrial weathering after the meteorite's fall), and/or aqueously mobilized and re-deposited during museum storage as are Mg-sulfates in curated carbonaceous chondrite meteorites (Gounelle and Zolensky, 2001). Ambiguity about this mineral group's orgin in meteorites from Mars is one reason for the MSR Campaign.
- The *Mars Express* orbiter's OMEGA spectrometer detected kieserite (monohydrate) and polyhydrated Mg-sulfates at numerous localities on Mars (Gendrin et al., 2005).
- The former presence of Mg-sulfate was inferred from the morphological crystallography of euhedral moldic secondary porosity imaged by MER *Opportunity's* Microscopic Imager (MI) in ancient sedimentary rocks exposed in the walls of Eagle crater in Meridiani Planum (Herkenhoff et al. 2004; McLennan et al. 2005). It was inferred that the euhedral moldic pores formed by selective dissolution of a former, euhedral mineral of preferential solubility relative to the rest of the sediment (Squyres et al. 2004; Herkenhoff et al. 2004; McLennan et al. 2005). Motivated by this finding, a targeted search for terrestrial environments with conditions suitable for the formation of such a mineral was undertaken and succeeded – a terrestrial counterpart was discovered and named meridianiite (Peterson and Wang, 2006; Peterson et al., 2007). (See the review by Velbel, 2018.)
- The *Mars Reconnaissance Orbiter* (MRO) CRISM spectrometer detected kieserite and polyhydrated Mg-sulfates in the proposed operations area of MSL *Curiosity* (Milliken et al., 2010). The ubiquitous and abundant amorphous material detected by the CheMin XRD instrument in the fluvio-lacustrine strata of Gale crater may include amorphous Mg- and Fe-sulfates (Rampe et al., 2020).
- Unspecified sulfate minerals have been detected from orbital MGS TES data in the Jezero watershed and Jezero crater (Salvatore et al., 2018).
- Chipera et al. (2023) documented the first definitive case for the occurrence on Mars of starkeyite ($MgSO_4 \cdot 4H_2O$), a specific hydration state among Mars' environmentally and climatically relevant hydrous Mg-sulfate minerals, and co-occurring amorphous hydrous Mg-sulfate, using CheMin to determine crystal structure. CheMin can distinguish the hydrous Mg-sulfates from one another from their crystal structures and has at last encountered a specimen in Gale crater with sufficiently abundant hydrous Mg-sulfate to exceed the detection limit of XRD. Chipera et al. (2023) thoroughly interpreted the occurrence of both of the Mg-sulfate phases detected, especially starkeyite. The manuscript follows its thorough characterization of starkeyite and co-occurring amorphous Mg-sulfate with excellent discussions of how such a mineral can be fundamental to constraining environmental (climatic) conditions and their history on Mars when the mineral is preserved in its as-sampled state in sample material from a well-characterized context. Chipera et al. (2023) also pointed out several aspects of their findings that are relevant to Mars Sample Return (MSR).
- Although Mg-sulfates were not detected from orbit at Jezero crater (see numerous references in Velbel and others, 2022), minerals including both monohydrated and polyhydrated Mg-sulfate, some intermixed with Ca-sulfate, have been tentatively identified in Jezero crater from early *Perseverance* SuperCam VisNIR spectroscopy (Mandon et al., 2021; Meslin et al., 2022).

The MSR Campaign science to be built upon analyses of these minerals: High-priority iMOST Objectives, Sub-Objectives, Investigation Strategies and associated Measurement types –1.1B, 1.2E, 1.3B, 1.3C, 1.3D, 1.4A, 1.4B, 1.4C, 1.5A, 2.2A, 2.2F.

Paleoenvironmental conditions of the water such as the thermodynamic activity of the solvent water and the saturation state of the aqueous solution from which the Mg-sulfates initially precipitated with respect to the precipitated salt mineral can be determined from equilibrium chemical thermodynamics. The temperature and pre-precipitation natural history of the solvent water can be inferred from the stable H and O isotopes of the Mg-sulfate minerals precipitated from that water. Textural (microscopic) observations and associated spatially resolved isotope microanalysis of intact samples containing more than one Mg-sulfate mineral would be required to establish (from crystal habits, cross-cutting or superposition relationships, or pseudomorphic replacement) whether the multiple Mg-sulfates coexist in the sample because they formed at the same time, formed initially as one that was then consumed by a reaction that formed the other, or formed completely independently of one another. Evolving paleoenvironmental conditions of the long-absent aqueous solutions can be inferred in support of establishing the context within which potential biosignatures in

associated rocks may have been incorporated and preserved. Furthermore, the relative ease with which hydrous Mg-sulfates can take on or evolve water molecules may, if hydration numbers of sulfates formed by surface-atmosphere exchange can be preserved in the samples, enable isotope analyses of the waters of hydration to characterize the influence of surface-atmosphere exchange on the present Mars water cycle.

3.3.2.2. Mg-sulfates - Deleterious effects of heating to (30 °C < T < 50 °C).

Mg sulfates are present in the martian soil, which has a relatively uniform composition over the planet, and were first suggested from elemental data obtained by the *Viking* missions (Clark et al. 1982).

Dehydration

Dehydration and rehydration of hydrous magnesian sulfates at a variety of temperatures and relative humidities, including many relevant to Mars, have been studied experimentally (*e.g.*, Chipera and Vaniman, 2007; Wang et al., 2009a, 2011; Chou et al., 2013) (see also Figs. 4 and 11). Of specific relevance to this study, Wang et al. (2011) performed experiments at three temperatures for each of eight dehydration and rehydration reactions. All eight reactions were investigated at 21 °C, and seven at 50 °C; relative humidities ranged from <<0.1% to 100%.

Estimated amount of water evolved by dehydration

The amount of molecular water that could be released by complete dehydration of hydrous Mg-sulfates in fluvio-lacustrine sedimentary rock samples from Jezero crater after the RSTA is sealed cannot be estimated as for gypsum, because crystalline Mg-sulfates were not detected (and therefore were not quantified) by CheMin at Gale crater (Rampe et al., 2020), although X-ray amorphous Mg-sulfates cannot be ruled out. However, most hydrous Mg-sulfates contain higher proportions of water than gypsum (from 23 wt.% for sanderite to 51% for epsomite), so a few wt.% of a hydrous Mg-sulfate in a *Perseverance* core could produce an appreciable fraction of the amount of water gypsum would evolve. The work on Mg,Ni-sulfate concretions (Rampe et al. 2020) may be informative regarding crystalline vs. amorphous Mg-sulfates (Vaniman, written communication, Feb. 13, 2022). The drill sample at Mojave2 did not target a concretion, but when the CheMin mineralogy is compared with the Alpha Particle X-Ray Spectrometer (APXS) data from drill tailings, it appears that enough of such concretion material was collected that a Mg,Ni-sulfate phase would have been detected if it was crystalline. This means that the Mg-Ni sulfate is either amorphous or a mixture of crystalline sulfates that were individually below the CheMin detection limit (Vaniman, written communication, Feb. 13, 2022).

Rehydration

Rehydration of large desiccated amorphous Mg-sulfate (n = 1.2) pseudomorphs after hexahydrite (itself pseudomorphic after epsomite; Vaniman and Chipera, 2006) reaches 4% of the eventual total weight gain of rehydration in 1 hour at 297 K (25 °C) and 100% RH (Vaniman and Chipera, 2006). The experimental rehydration time for amorphous hydrous Mg-sulfate to epsomite reported by Vaniman and Chipera (2006) is slightly (2-4 times) shorter than that determined by Wang et al. (2011), which suggests near-convergence at a dehydration time of ~10^0-10^1 hours at 50 °C. These timescales are at the low end of the range (hours to days) estimated for room-temperature lboratory conditions by Tosca and MSPG2 (2021). The hydration states of Mg-sulfates are known to vary to a much greater degree than the Ca-sulfates upon heating to 30 °C < T < 50 °C. The ability to perform the science investigations described in the preceding paragraph on Mg-sulfates could be impaired by heating in the same T range for hours or more.

Mineral habit (crystal shape - recall the story of the discovery of meridianiite, above), associations, paragenetic assemblages, and textures indicative of reaction relationships and temporal sequences of reactions, and O, S, and H isotope systematics of each paragenesis, are the solid-phase memory of the system's thermal and chemical history. Corresponding memory may exist ephemerally in hydrous Mg-sulfates on Mars and persist in recognizable form in the RSTA if temperature stays between 30 °C – 40 °C for less than three hours, or between 40°C – 50°C for less than one hour. Otherwise, all these memories will be lost in hours, like tears in the rain.

Timescales of deleterious effects

Wang et al. (2011) fit Arrhenius equations to experimental data. Interpolated times-to-completion in the range of interest to this study (30 °C < T < 50 °C) were calculated from the equations of Wang et al. (2011). Salient results (Table 13) include:

Dehydration of epsomite (7 water molecules per formula unit = pfu) to amorphous material (2 waters pfu; Wang et al., 2011) at r.h. <<0.1 evolves five molecules of water pfu of Mg-sulfate.

$MgSO_4 \cdot 7H_2O \rightarrow MgSO_4 \cdot 2H_2O + 5H_2O$

This reaction under these conditions is complete in ~28 min at 30 °C, ~6 min at 40 °C, and ~1 min at 50 °C. At higher relative humidity (RH = 11%), epsomite dehydrates to starkeyite in 36 days at 30 °C, 9 days at 40 °C, and 2 days at 50 °C.

Rehydration of starkeyite to hexahydrite or epsomite at any T of concern to this study takes 6-10 times longer at 59-64% RH than at 100% RH.

Table 13. Estimated timescales of hydrous Mg-sulfate dehydration and rehydration (Wang et al. 2011).

Reaction			Time to completion at			
		RH (%)	Units	30 °C	40 °C	50 °C
Dehydration						
Epsomite to starkeyite	$MgSO_4 \cdot 7H_2O \rightarrow MgSO_4 \cdot 4H_2O + 3H_2O$	11	days	36	9	2
Epsomite to amorphous	$MgSO_4 \cdot 7H_2O \rightarrow MgSO_4 \cdot 2H_2O + 5H_2O$	<<0.1	min	28	6	1
Rehydration						
Starkeyite to hexahydrite or epsomite	$MgSO_4 \cdot 4H_2O + 2\text{-}3H_2O \rightarrow MgSO_4 \cdot 6\text{-}7H_2O$	100	hours	52	26	14
Kieserite to hexahydrite or epsomite	$MgSO_4 \cdot H_2O + 5\text{-}6H_2O \rightarrow MgSO_4 \cdot 6\text{-}7H_2O$	100	days	5	4	3
Amorphous to hexahydrite or epsomite	$MgSO_4 \cdot 2H_2O + 4\text{-}5H_2O \rightarrow MgSO_4 \cdot 6\text{-}7H_2O$	100	hours	36	16	8
Starkeyite to hexahydrite or epsomite	$MgSO_4 \cdot 4H_2O + 2\text{-}3H_2O \rightarrow MgSO_4 \cdot 6\text{-}7H_2O$	59-64	days	8	5	4
			hours	188	126	86
Starkeyite to hexahydrite or epsomite	$MgSO_4 \cdot 4H_2O + 2\text{-}3H_2O \rightarrow MgSO_4 \cdot 6\text{-}7H_2O$	73-75	days	4	3	2
			hours	100	61	38
Starkeyite to hexahydrite or epsomite	$MgSO_4 \cdot 4H_2O + 2\text{-}3H_2O \rightarrow MgSO_4 \cdot 6\text{-}7H_2O$	100	hours	33	17	9

RH: Relative humidity.

Notice that dehydration of epsomite to amorphous material is nearly 30× faster at 50 °C than at 30 °C. Heating in the range of concern to this study could release additional water vapor to the closed-system RSTA internal atmosphere that could (1) rehydrate bassanite present at the time of sampling and thereby change the proportions of gypsum and bassanite in the heated sample in a matter of hours and (2) hydrate previously dry interlayers in smectite-group clay minerals (see section 3.8 below).

3.3.3. Fe-sulfates

3.3.3.1. Fe-sulfates and iMOST objectives

Data on dehydration of ferric and ferrous sulfates are available in the literature (Wang et al., 2019) and presented in Fig. 6. The probable occurrence of jarosite in returned Mars samples is anticipated based on orbital and in situ observations, including:

- K-Fe-sulfate occurs in at least some individual meteorites from each of the abundant groups of meteorites from Mars – shergottites, nakhlites, and chassignites (SNCs; see review by Velbel, 2012, references therein, and more recent references). Some may be part of the meteorite's mineral inventory on Mars (martian), but many are demonstrably terrestrial (formed by terrestrial weathering after the meteorite's fall). Ambiguity about this mineral group's origin in meteorites from Mars is one reason for the MSR campaign.
- Jarosite has been detected and quantified in 12 (80%) of the first 15 samples of fluviolacustrine sedimentary rocks analyzed as bulk drill-fine powders by MSL's CheMin XRD at Gale Crater (Rampe et al., 2020).
- Unspecified sulfate minerals have been detected from orbital MGS TES data in the Jezero watershed and Jezero crater (Salvatore et al., 2018).
- Jarosite has recently been reported in Jezero Crater from orbital spectroscopic data (Dundar et al., in review).

The MSR Campaign science to be built upon analyses of these minerals: High-priority iMOST Objectives, Sub-Objectives, Investigation Strategies and associated Measurement types – 1.1B, 1.2D, 1.3A, 1.4A, 1.4B, 1.4C, 1.5A.

Potassium jarosite – $KFe^{3+}{}_3(SO_4)_2(OH)_6$ – is a member of the alunite sulfate mineral group. As a host mineral for K, it contains a long-lived radioactive isotope of K. Measurements of isotopes, including the decay product of ^{40}K, enable K-Ar and especially Ar-Ar geochronology of jarosite. Jarosite forms by weathering and diagenesis (near-surface-ambient to subsurface conditions) and is therefore a promising and powerful tool for determining when it formed, constraining the age of its host rock and the paleoenvironmental conditions that existed at the time the jarosite precipitated on Mars. Jarosite is typically hydroxylated, with h bound in its crystal structure. It is not expected to dehydroxylate at temperatures of concern to this study (30 °C < T < 50 °C).

3.3.3.2. Fe-Sulfates - Deleterious effects of heating to (30 °C < T < 50 °C)

Dehydration and rehydration

In terrestrial laboratories jarosite loses little (Frost et al., 2005) or no (Chen, 2018) mass as H_2O at the proposed temperatures (30 °C < T < 50 °C), but that which is lost may be adsorbed (adventitious) terrestrial water vapor. For this reason, most noble gas laboratories intentionally heat terrestrial and meteoritic samples overnight at around 100–200 °C to drive off adsorbed terrestrial (contaminant) atmospheric gases. However, the adsorbed gases on returned samples would be martian, not terrestrial contaminants, so any heating at any time after sample acquisition could redistribute or remove the low-temperature fraction of this component. The noble gas record would likely not be compromised, and the derived Ar-Ar chronology for processes that occurred at low temperatures on Mars would likely be correct. Timescales of loss of adsorbed martian water from Fe-sulfates are seconds to minutes.

3.4. Nitrates

Nitrate has been detected on the martian surface (Stern et al. 2015). Under aqueous anoxic conditions, this nitrate may spontaneously react with Fe^{2+} and convert to nitrite and on to ammonium with the rate of reaction increasing dramatically with temperature (Summers and Chang 1993). Hence, a significant amount of the original nitrate may be lost as it reacts with ferrous iron. The ferrous iron could be derived from ferrous clay minerals or from primary mafic minerals (pyroxene, olivine, amphibole) that are contained in the sample. Isotopic effects of this reaction have so far not been investigated, but they are likely to be significant, given the large isotopic effects associated with biological

nitrate reduction. Hence, any efforts of constraining the primary N isotopic composition of the sample (including specific phases) could be compromised.

Nitrate may also assist the oxidation of sulfides either directly or indirectly using Fe^{3+} and either biologically or abiotically, with the latter occurring at slower rates (Hendrix et al. 2022).[MZ9][MS10] Sulfide oxidation would lead to the formation of sulfuric acid, which could significantly lower the pH of the solution. For example, in acid rock drainage on Earth the presence of sulfuric acid creates pH values around 2. The extent of this effect depends on the abundance of sulfide in the sample and on the buffering capacity of the remaining mineral assemblage. It needs to be verified what the influence of increasing temperature would be, but it likely enhances the abiotic reaction between nitrate and sulfides, similar to that which has been described for the reaction between nitrate and ferrous iron (Summers and Chang 1993).

3.5. Carbonates

3.5.1. Mg-carbonates

3.5.1.1. Mg-carbonates and iMOST objectives

The probable occurrence of hydrous Mg-carbonates in returned Mars samples is anticipated based on the following observational evidence:

- Orbital spectroscopy has detected properties consistent with Mg-carbonate magnesite ($MgCO_3$), which is anhydrous; however, the orbital spectra are also consistent with magnesite + hydromagnesite (Calvin et al., 1994; Ehlmann et al., 2008b; Horgan et al., 2020; Scheller et al., 2021).
- Unspecified carbonate has been tentatively identified in the Jezero crater from early *Perseverance* SuperCam VisNIR spectroscopy (Mandon et al., 2021).

The MSR Campaign science built upon analyses of these minerals: High-priority iMOST Objectives, Sub-Objectives, Investigation Strategies and associated Measurement types –1.1B, 1.1C, 1.2D, 1.2E, 1.3A,1.4A, 1.4B, 1.4C, 2.2A, 2.2F.

Hydrous Mg-carbonate minerals include hydromagnesite [$Mg_5(CO_3)4(OH)_2{\cdot}4H_2O$], nesquehonite [$Mg(HCO_3)(OH){\cdot}2H_2O$ = $MgCO_3{\cdot}3H_2O$], lansfordite ($MgCO_3{\cdot}5H_2O$), artinite [$Mg_2(CO_3)(OH)_2{\cdot}3H_2O$], pokrovskite [$Mg_2(CO_3)(OH)_2$], and dypingite [$Mg_5(CO_3)4(OH)_2{\cdot}5H_2O$]. Hydrous Mg-carbonates are sparsely distributed on Earth (Scheller et al., 2021) and occur naturally in cold climates in which dehydration kinetics are slow (Jull et al., 1988; Velbel et al., 1991; El-Shenawy et al., 2020) and in evaporitic lakes (Coshell et al., 1998; Russell et al., 1999). Hydrous carbonates contain H and O as structural water, and some also contain hydroxyl. Some hydrous Mg carbonates could be present in martian materials (Scheller et al. 2021) and may decompose to release H_2O.

El-Shenawy et al. (2020) explored the formation mechanism(s) of two previously identified generations (Antarctica and Houston) of terrestrial-weathering produced nesquehonite, which formed on the surface of the LEW 85320 ordinary chondrite. El-Shenawy et al. (2020) combined newly acquired carbon and oxygen isotopic data from recently extracted mineral samples with previously published data from decades ago (Gooding et al., 1988; Jull et al., 1988; Grady et al., 1989) and with oxygen isotope composition of melted ice from the Lewis Cliff Ice Tongue (the parent water of LEW carbonates) to produce the first nesquehonite-water oxygen isotope thermometer. From this, El-Shenawy et al. (2020) estimated the formation temperature of nesquehonite and observed a characteristic isotopic trend in both of the two generations consistent with formation of nesquehonite in the two generations by evaporation of water and coherent carbon isotope exchange between the parent liquid and the atmospheric CO_2. This mechanism has been shown to be directly applicable to interpretation of Mars meteorite carbonates and carbonate formation on Mars.

3.5.1.2. Mg-carbonates - Deleterious effects of heating to (30 °C < T < 50 °C)

Dehydration and rehydration

In a pure nitrogen atmosphere, both hydromagnesite and nesquehonite powder (grain size unspecified) begin to lose structural water at 313 K (40 °C) and 307 K (34 °C), respectively (Ren et al., 2014). Morgan et al. (2015) heated

nesquehonite to two temperatures, the lower of which was 50 °C. Under flowing dry CO_2 and N_2 (gas-flushed open system), nesquehonite decomposed completely in < 160 min (Morgan et al., 2015). The pH_2O in the RSTA will be crucial to the fate of these hydrous carbonate phases. If another phase in the RSTA acts as a sink for water evolved from a dehydrating hydrous salt, the dehydrating salt may completely decompose quickly. On the other hand, if another phase in the RSTA is simultaneously decomposing and evolving water rapidly enough to raise pH_2O in the RSTA, the nesquehonite would decompose more as slowly as pH_2O approached 0.04 atm, the condition at which nesquehonite would persist indefinitely (Morgan et al., 2015). Nesquehonite persistence would also be prolonged beyond 160 min if temperature were lower than 50 °C. An apparent Arrhenius activation energy (16 kcal mol^{-1}, 68 kJ mol^{-1}) was calculated for this study by way of the work of Morgan et al. (2015); it is between the activation energies of the last two steps of nesquehonite dehydration (~37 kJ mol^{-1} and ~128 kJ mol^{-1}) as determined by Ren et al. (2014).

Estimated amount of water

The amount of molecular water that could be released by complete dehydration of hydrous Mg-carbonates in fluvio-lacustrine sedimentary rock samples from Jezero crater after the RSTA is sealed cannot be estimated as for gypsum, because no Mg-carbonates, hydrous or anhydrous, were detected (and therefore quantified) by CheMin at Gale crater (Rampe et al., 2020).

Timescale of deleterious effect

The Arrhenius activation energy calculated from experiments (Morgan et al., 2015) permits extrapolation from the range of their experimental temperatures (50 °C < T < 100 °C) to temperatures in the range considered in this study (30 °C < T < 50 °C) (Table 14). At 30 °C, nesquehonite would persist >10 hrs in a dry (pH_2O = 0) closed-system RSTA. Nesquehonite persistence would decrease as temperature rises to 50 °C, at which it would take approximately two hours to allow complete dehydration.

Mineral habit (crystal shape), associations, paragenetic assemblages, and textures indicative of reaction relationships and temporal sequences of reactions, and O, C, and H isotope systematics of each paragenesis (for example, the paragenetic sequence preserved in the morphology of hydrous Mg-carbonates formed by Antarctic weathering and continued post-recovery alteration; Jull et al., 1988; Velbel et al., 1991; Velbel, 2014; El-Shenawy et al., 2020), are the solid-phase memory of the system's thermal and chemical history. Corresponding memory may exist ephemerally on Mars but, as with the onboard dehydration of gypsum in CheMin discussed above, will be lost by episodes of heating above 25 °C.

Table 14. Estimated timescales of nesquehonite dehydration (Morgan et al. 2015).

Reaction			Time to completion at				
		Units	10 °C	20 °C	30 °C	40 °C	50 °C
Dehydration	"Dry" - Paar environmental chamber, no water vapor, t to complete dehydration - Rietveld scale 0% of initial value						
Nesquehonite to poorly crystalline anhydrous Mg-carbonate	$MgCO_3 \cdot 3H_2O \rightarrow MgCO_3 + 2H_2O$	hours	88	33	13	5	2

Notice that dehydration of nesquehonite to amorphous material is at least six times faster at 50 °C than at 30 °C (Morgan et al. 2015). Heating in the range of concern to this study could release additional water vapor to the closed-system RSTA internal atmosphere that could (1) rehydrate bassanite and/or any of several less-hydrated Mg-sulfates

present at the time of sampling and thereby change the proportions of hydrous sulfates in the heated sample in a matter of hours and (2) hydrate dry interlayers in smectite-group clay minerals (see section 3.8).

3.5.2. Ca-carbonates

At near-freezing temperature, low-temperature pseudomorphs of carbonate (ikaite, vaterite) are favored, and these phases transition into calcite or aragonite at elevated temperatures. There is an upper temperature limit of +12 °C for ikaite stability, but a strong dependence on the fluid composition.

3.6. Chlorides

Halogenides (chorides, bromides, fluorides) are present in martian materials, and chlorides are the most abundant. Depending on RH, hydrated chlorides of Na, Ca, and Mg could partially or completely dehydrate below and within the +30 to +60 °C range (*e.g.*, Davila et al., 2010; Gough et al., 2019). Hydrohalite, $NaCl{\cdot}2H_2O$, is stable below ~265 K and typically forms through freezing of Na-Cl bearing solutions (*e.g.*, Marion and Kargel, 2008) and can form through hydration of NaCl by H_2O (g) well below 0 °C (Wise et al., 2012). Heating of martian samples above 0 °C suggests complete conversion of hydrohalite to halite:

$NaCl{\cdot}2H_2O \rightarrow NaCl + 2H_2O$[MZ11] (g).

$MgCl_2{\cdot}12H_2O$ and then $MgCl_2{\cdot}8H_2O$ dehydrate to bischofite ($MgCl_2{\cdot}6H_2O$) before the temperature reaches ~0 °C (Davila et al., 2010; Primm et al., 2017) (Fig. 8). At 30-60 °C, dehydration of $MgCl_2{\cdot}6H_2O$ to $MgCl_2{\cdot}4H_2O$ occurs at RH < ~3% (30 °C) and HR < ~6 (60 °C), (Xu et al., 2021) (Fig. 9). It follows that bischofite could survive the heating of returned samples if RH is maintained in the ~3-30 % range (*e.g.*, by dehydration of less thermally stable salts such as perchlorates, hydrohalite, etc.). Note that deliquescence of $MgCl_2{\cdot}6H_2O$ in this temperature range occurs at RH > 30% (Fig. 9).

Experimental data (*e.g.*, Gough et al., 2019) suggest dehydration of $CaCl_2{\cdot}6H_2O$ (antarcticite) to $CaCl_2{\cdot}4H_2O$ between 284 K and 255 K at RH of 2.9%, with warmer temperatures also expected to cause dehydration. This dehydration occurred in the order of minutes, once conditions were favorable. Dehydration of $CaCl_2{\cdot}4H_2O$ to $CaCl_2{\cdot}2H_2O$ occurs at RH < 15-18%, depending on the temperature (Gough et al., 2016; Wang et al., 2019). At T > 45 °C, $CaCl_2{\cdot}2H_2O$ is the stable phase at RH < ~5% (Fig. 7) or at HR < ~15% (Fig. 14) that could coexist with the corresponding brine at RH of 3-5% (Fig. 7) or at RH of ~15% (Fig. 14). At ~25-45 °C, $CaCl_2{\cdot}4H_2O$ is subjected to deliquescence at RH > 18-20% (Wang et al., 2019; Fig. 6), RH > 5-15%, (Gough et al., 2016, Fig. 7), and at RH > 15-27% (Fig. 14). In summary, $CaCl_2{\cdot}4H_2O$ present in samples at ~30 °C would dehydrate upon further heating in the range 30-60 °C, primarily if single digit RH values are present.

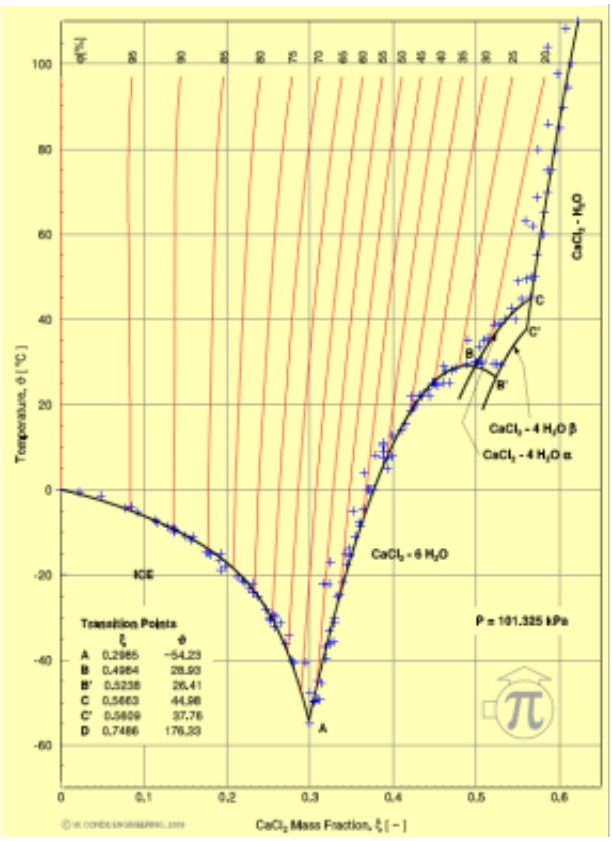

FIG. 14. Phase diagram $CaCl_2$-H_2O as a function of temperature and relative humidity. The area with red lines corresponds to liquid phase. http://www.mrc-eng.com/Downloads/CaCl2-H2O%20Relative%20Humidity.pdf

Even without dehydration, chloride minerals could undergo viscous deformations due to heating. On Earth, halite-rich deposits flow when exposed to moderate - high temperatures over millions of years. Deeply buried chloride deposits deform into salt diapirs. However, halite at 30 - 60 °C does not undergo such deformation in the suggested time scale.

Heating of chloride (*e.g.*, halite, NaCl) crystals may affect fluid inclusions in them (see Section 2.2.1.1). As temperatures approach ~60 °C, the outer portion of crystals may start to alter, resulting in stretched fluid inclusions. But the inner portions of crystals could retain original textures, preserving fluid inclusions. At long-term halite exposure to temperatures of ~90 °C, the outer parts of a crystal could alter to a clear, inclusion-free halite, and the innermost parts of the crystals have slightly stretched fluid inclusions. Shorter time exposure (hours and minutes) up to ~60 °C, as seen in preparation of halite thin sections, does not seem to alter halite and fluid inclusions.

3.7. Perchlorates

The results of evolved gas analysis experiments by the Sample Analysis at Mars instrument onboard the MSL rover suggest perchlorate is likely in the form of Ca-perchlorate at Gale Crater (Glavin et al., 2013). Clark et al. (2020) provided information on thermal decomposition and $HCl+O_2+H_2O$ formation upon heating of martian samples that contain perchlorate/chlorate salts. At the *Phoneix* landing site, both magnesium and calcium perchlorate may be present (Kounaves et al., 2014). Other perchlorate salts may exist, but here we focus on the potential phase transitions and decomposition of relevant hydrates of $Ca(ClO_4)_2$ and $Mg(ClO_4)_2$.

We assume that a brine phase will not be sampled, since deliquescence is not likely to actively occur at Jezero crater area. Therefore, the efflorescence phase transition (brine recrystallizing into a solid) is unlikely. These salts may be hydrated when sampled, however, and so dehydration is a potential concern.

For calcium perchlorate, the likely stable phase in the shallow subsurface is the tetrahydrate ($Ca(ClO_4)_2 \cdot 4H_2O$). This salt can dehydrate at any temperature provided the RH is sufficiently low. As seen in Fig. 15 (Martin-Torres et al., 2015), although the temperature range of interest in this report (+30 to +60 °C) is even warmer than what is plotted

here, a slight extrapolation shows that dehydration of the tetrahydrate at these elevated temperatures is only expected if the RH of the sample is less than 0.1%. Consistent with these theoretical results, Gough et al. (2019) performed dehydration experiments on $Ca(ClO_4)_2 \cdot 4H_2O$ and found that dehydration of hydrated $Ca(ClO_4)_2$ to the anhydrous phase only occurred at temperatures at or above 25 °C at RH < 1%. At these temperatures, dehydration took minutes to hours. Waters of hydration of $Ca(ClO_4)_2$ may be rapidly lost at temperatures above 25 °C if humidity is less than 1% RH.

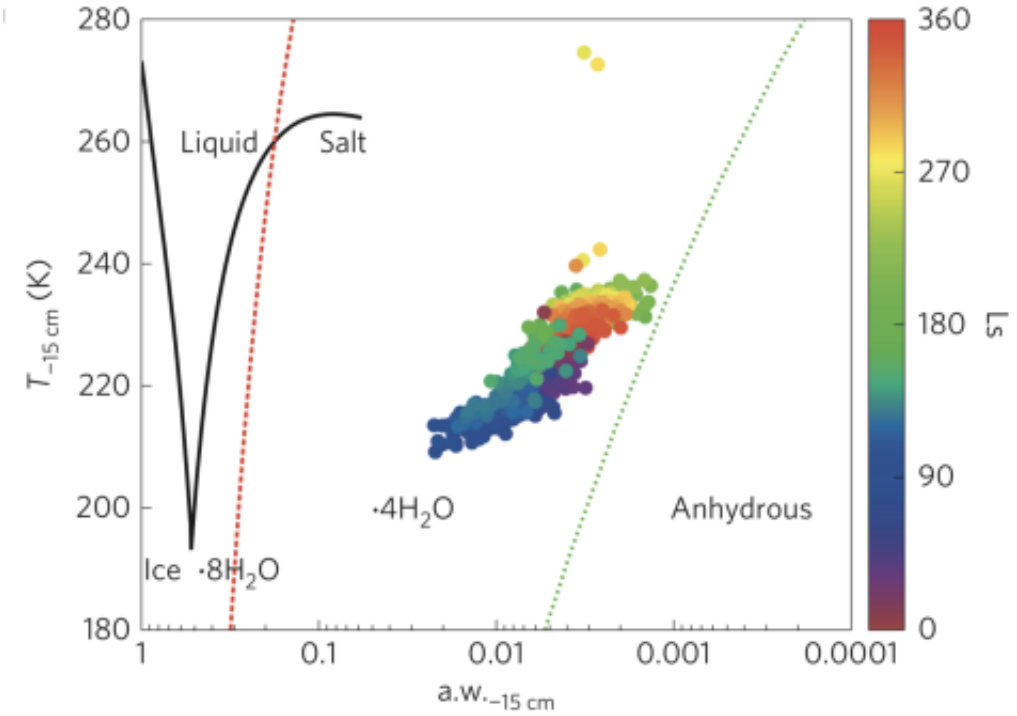

FIG. 15. Phase diagram of Ca-perchlorate (Martin-Torres et al., 2015). Crossing the theoretical dehydration phase transition boundary (green dotted line) requires very low RH values, especially at higher temperatures.

For magnesium perchlorate, data suggest that the stable form on Mars would be $Mg(ClO_4)_2 \cdot 6H_2O$ (Robertson and Bish, 2011). Environmental XRD experiments found no evidence of dehydration of this hexahydrate until the temperature was raised to at least 323 K. The dehydration kinetics depended on the RH and temperature. As an example, dehydration of the hexahydrate to the tetrahydrate took about 500 minutes at 90 °C and 2% RH. Exposure to the +30 to +60 °C temperature range on the timescale of hours or less is unlikely to affect the hydration state of $Mg(ClO_4)_2$.

Decomposition of perchlorate salts can occur at elevated temperatures. The SAM Evolved Gas Analyzer observed the major release of molecular oxygen from oxychlorine salts between 200 and 500 °C (Sutter et al., 2017). Thermal decomposition can start below these temperatures, however. When a hydrated perchlorate salt is heated, two possible types of reactions can take place. First, the salt may dehydrate (see above), leaving an anhydrous salt which can decompose to chloride and molecular oxygen. Alternatively, the water contained in the crystalline structure may hydrolyze the salt, leaving perchloric acid, water vapor, and a hydroxide or oxide product. The former occurs at higher temperatures, the latter at more moderate temperatures (Marvin and Woolaver, 1945). Calcium perchlorate appears to be stable in terms of either decomposition process below 200 °C. Hydrated magnesium perchlorate is more susceptible to hydrolysis, and this decomposition can begin to occur at temperatures just higher than 30 °C. Below 90 °C the extent of the reaction can be considered minor, with <5% decomposition (Marvin and Woolaver, 1945). Therefore, only negligible thermal decomposition of perchlorate salts will occur in the temperature range of +30 to +60 °C, although the detection of magnesium oxide or hydroxide products could suggest that some decomposition occurred during sample tube heating.

3.8. Phyllosilicates

3.8.1. Phyllosilicates and the iMOST objectives

Hydrous (and hydroxylated) phyllosilicates – including smectite-group clay minerals (Figure 12), vermiculite, and pillared (fixed-hydroy-interlayered) counterparts ("pedogenic" chlorite), and non-clay mineral phyllosilicates – are expected to occur in returned Mars samples based on the following evidence:

- Pre-terrestrial iddingsite (a mostly amorphous clay mineraloid of broadly smectitic composition formed by aqueous alteration of, mainly, olivine) occurs in almost all nakhlites (see review by Velbel, 2012, references therein, and more recent references). Iddingsite is part of the meteorite's mineral inventory on Mars (martian; formed before the meteorite's arrival at Earth).
- X-ray amorphous material is abundant (15-73 wt%) and more abundant than crystalline phyllosilicate (mean 12 wt%, maximum ~30 wt%; Rampe et al., 2020; Tu et al., 2021) in CheMin XRD analyses of fluvio-lacustrine sedimentary rocks at Gale crater. X-ray amorphous (non-crystalline) material compositionally similar to smectite may constitute a substantial fraction of the amorphous material (Rampe et al., 2020).
- Smectite-group clay minerals and a few non-smectite-group phyllosilicates have been identified in more than 2/3 of first 30 drillhole fines samples of fluviolacustrine sedimentary rocks analyzed as bulk powders by MSL's CheMin XRD at Gale crater (Tu et al., 2021).
- Unspecified clay- and other phyllosilicate minerals have been detected from orbital MGS TES data in the Jezero watershed and Jezero crater (Salvatore et al., 2018).
- Smectites have been spectroscopically detected at Jezero crater (Ehlmann et al., 2008a; Goudge et al., 2015; Horgan et al., 2020).
- Smectite-group clay minerals have been tentatively identified in Jezero crater from early *Perseverance* SuperCam VisNIR spectroscopy (Mandon et al., 2021).

The MSR Campaign science built upon analyses of these minerals: High-priority iMOST Objectives, Sub-Objectives, Investigation Strategies and associated measurement types – 1.1B, 1.2E, 1.3A, 1.3B, 1.3C, 1.3D, 1.4A, 1.4C, 1.4D, 1.5A, 2.2A, 2.2F.

Smectite-group minerals have been detected in more than half of the 30 samples from the Mt. Sharp stratigraphic succession at Gale crater discussed by Tu et al. (2021). The oxidation state of Fe, Mn, and other first-row transitions elements (FRTE) in clay minerals records the oxidation-reduction state of the environment in which the clay minerals formed. A complex trioctahedral mostly Fe^{3+}-bearing (but mixed Fe-valence, and with Fe^{3+} substitution for some tetrahedral Si) ferric (*sic*) saponite smectite has been identified in small amounts of crystalline and interstratified material in the iddingsite of the Lafayette nakhlite (Bridges et al., 2015). CheMin data from samples acquired low in the Gale crater stratigraphic succession were well-matched by a well-characterized trioctahedral Fe^{3+}-dominated mixed -valence ferrian saponite terrestrial analog (Treiman et al., 2014). Nontronite (dioctahedral Fe^{3+}-bearing smectite) occurs in at least one sample as indicated by SAM EGA data (Tu et al., 2021). Smectite-group clay minerals in samples from Jezero crater should be expected to preserve scientific information in the form of Fe, Mn, and other FRTE redox state about the redox conditions of the depositional (Hurowitz et al. 2017) or groundwater diagenetic (Rampe et al. 2017) environments within which they formed. Therefore, preservation of FRTE oxidation states in smectite-group clay minerals should be a high priority.

3.8.2. Phyllosilicates - Deleterious effects of heating to (30 °C < T < 50 °C)

Very few and minor deleterious consequences are expected between +30 °C and +50 °C, but the loss of rare occurrences of interlayer molecular water that does occur (as predicted from thermodynamics by Bish et al., 2003) would be a loss of a rare science opportunity. Loss of OH from phyllosilicates is not expected at the proposed sterilization temperatures (Velbel and others, 2022).

Regarding loss of molecular (interlayer) water (as distinct from structural hydroxyl): Collapsed smectite – that has lost most interlayer H_2O because of low humidity conditions – is the only smectite observed when using the CheMin instrument (Tu et al., 2021). Mars-relevant smectite-group minerals that lose a few weight % of their molecular interlayer water (out of a total of >20 wt%) over the temperature range of interest considered in this study (30 °C < T < 50 °C) include saponite (a trioctahedral smectite) (Kawano and Tomita, 1991), nontronite (a dioctahedral smectite), and Fe-smectite (Frost et al., 2000; "The term nontronite is used for dioctahedral smectites when Fe^{3+} is >3 mol% and when theayer charge originates from the tretrahedral sheet." Frost et al., 2000, p. 64), but this only matters if there is interlayer molecular water to lose in martian 2:1 layer-charged phyllosilicates. Che-Min XRD data from Gale crater

suggest very little molecular water associated with interlayer cations (*e.g.*, Vaniman et al., 2014, 2018; Bristow et al., 2015; Sutter et al., 2017; Tu et al., 2021), although a few samples at Gale crater evolved water between 100 °C and 300 °C in *Curiosity*'s SAM instrument; this was interpreted as interlayer water (Sutter et al., 2017). SAM analyses begin at 125°C (Mahaffy et al., 2012), so there is no knowledge from SAM of mass changes in clay minerals and other phyllosilicates in the temperature range of interest to this study. Given the considerable scientific value interlayer water H and O isotopes would have for characterizing ancient aqueous solutions and recent atmospheric water vapor with which smectite interacted (iMOST 2018; Beaty et al., 2019), appropriate caution would require anticipating that such minor interlayer water that may persist in the clay minerals of some sedimentary-rock samples might be partially depleted or lost during heating to the range of interest of this study. Hydroxylated cation-OH "pillars" in the interlayer sites of 2:1 pillared (hydroxy-interlayered) phyllosilicates (as in "pedogenic chlorite"; Sawhney, 1958, 1960 a,b) may occur in a few samples (*e.g.*, 1 of ~30 at Gale crater; Tu et al., 2021) but are generally not evolved below ~300-400°C (Sawhney, 1960a).

However, it must be noted that there may be little or no interlayer (exchangeable) molecular water in martian smectite now at Mars' present sample-able surface (Vaniman et al., 2014, 2018; Bristow et al., 2015; Sutter et al., 2017; Tu et al., 2021) and, thus, at the time of sample acquisition. The previous paragraphs' facts and inferences are for samples consisting entirely of clay minerals. However, samples from Mars (especially sedimentary rocks) are mixtures of many minerals and amorphous phases.

Experience with dehydration of hydrous sulfates during sample acquisition, transfer to the MSL onboard CheMin XRD instrument, and analysis demonstrate the need to consider hydrous sulfates as internal sources of molecular water in the closed system within each M2020 RSTA after its sealing. "It is evident from CheMin analyses of gypsum that the act of sampling and analysis can produce mineral transformations through dehydration. The transformation of gypsum to bassanite is clearly observed in CheMin XRD analyses. To relate observations within CheMin to mineralogy *in situ*, adjunct data are needed from thermal sensors within CheMin as well as data from the Rover Environmental Monitoring Station (REMS) Ground Temperature Sensor. ChemCam analyses of surface hydrogen abundances in veins and SAM evolved gas analyses support these interpretations. Multiple instrumentation is of great importance for sample analyses on Mars. *In situ* analyses and documentation will be even more important when returning martian samples to Earth. Simple dehydration is not the only process that must be considered; reactions between hydrous phases may also be driven by changes in temperature and relative humidity (*e.g.*, cation exchange reactions between clay minerals and Mg-sulfates in the absence of free-liquid H_2O, accompanied by formation of gypsum or bassanite where thin skins of water may have formed; Wilson and Bish 2011). Broader concerns such as this, and the limitations in ability to fully prevent any such transformations, are a concern recognized in sample return strategies for Mars. For the return of samples to Earth, encapsulation and monitoring of thermal history may not prevent mineral transformations but will provide a basis for unraveling such processes (Mars Exploration Planning Group - MEPAG 2008). Bringing mutable phases out of their "comfort zone" *in situ* provides new understanding of what transformations are likely. The CheMin experience with gypsum dehydration on Mars provides another empirical data point on the long path toward sample return from Mars to Earth." (Vaniman et al., 2018, p. 1018-1019)

Beginning upon drilling, and continuing during sample acquisition, transfer to *Perseverance's* onboard adaptive caching assembly (ACA), hermetic sealing, and post-sealing storage within and RSTA, each sample acquired by M2020 rover *Perseverance* will be exposed to temperature and relative humidity different from each sample's natural pre-sampling conditions. The interlayer hydration state of clay minerals and other similar phyllosilicates will likely change in response to the changes in temperature. "Orbital spectral data suggest that smectites at the martian surface are dehydrated, and these *in situ* measurements likely confirm this hypothesis … however the relative humidity inside CheMin is lower than the martian surface … and therefore some uncertainty remains." (Tu et al., 2021, p. 25). "The potential prevalence of collapsed smectites observed by CheMin suggests planned samples collected by *Perseverance* from smectite-bearing terrains in Jezero may also have collapsed smectite. These samples would have to be kept under desiccating conditions after collection and return to Earth to prevent hydration and cation exchange, which is critical to sample preservation. Similarly, samples that contain hydrated minerals (*e.g.*, gypsum) will need to be kept under specific temperature and relative humidity conditions to prevent dehydration. This may be difficult to achieve within the sample tubes after collection and caching on the martian surface. Diurnal and temperature fluctuations may cause the dehydration of some phases and the adsorption of H_2O by others, like smectite." (Tu et al., 2021, p. 28).

It is more likely that clay minerals will serve as sinks rather than sources of water in the multiphase closed-system RSTA (Tu et al., 2021).

3.8.3. Estimated capacity for incorporation of water

The amount of molecular water that could be released by complete dehydration of gypsum in fluvio-lacustrine sedimentary rock samples from Jezero crater after the RSTA is sealed has been discussed above. Complete dehydration of the gypsum in mudstones and mafic sandstones evolves ~250 – 350 mg of water into other phases – likely including clay-mineral interlayer sites – in the sealed, closed-system RSTA. Higher proportions of gypsum in the rock would yield higher abundances of water.

The smectite clay minerals in a polymineralic sample could acquire interlayer water, introduced as water of dehydration evolved from co-occurring minerals (*e.g.*, hydrous sulfates) in the (sealed, closed-system) RSTA. The amount of molecular water that could be incorporated into the smectite-group clay-mineral fraction of fluvio-lacustrine sedimentary rock samples from Jezero crater after the RSTA is sealed can be estimated. The preliminary estimate here uses the weight % of interlayer water in hydrated smectites; 7 – 18 wt.%, depending on whether the specific smectite is dioctahedral or trioctahedral, its layer charge and structural siting of the charge-producing ions, and the interlayer cation(s) (most of which are not well-constrained by CheMin data). Other terms include the maximum known abundance of clay minerals in similar rocks by CheMin at Gale crater (34 wt%; Tu et al., 2021), and the same estimated densities of sedimentary rock types and volume of a nominal cylindrical sample in an RSTA used in the counterpart calculations for gypsum above. From these values and assumptions, complete hydration of interlayer sites of smectite-group clay minerals in mudstones and mafic sandstones could incorporate ~400 – 1,400 mg of water from dehydration of gypsum and other phases in the sealed, closed-system RSTA.

Such post-acquisition interlayer water would compromise the pre-acquisition state of the smectite. Addition of interlayer water would facilitate closed-system in-RSTA redox reactions of structural (octahedral) Fe^{2+} and Mn^{2+} and the electron donors and electron acceptors involved. The loss of information about FRTE oxidation state in the smectites would not be compensated for by the closed-system-sourced interlayer water recording the equilibrium/steady-state relative humidity and change in mass (abundance) and stable H and O isotopes of molecular interlayer water sourced from other phases in the RSTA between sealing and opening the RSTA (cf Tosca et al., 2021).

The smectite clay minerals in a polymineralic sample could acquire interlayer water, introduced as water of dehydration evolved from co-occurring minerals (*e.g.*, Mg-sulfates) in the (sealed, closed-system) sample RSTA. Such post-acquisition interlayer water would compromise the pre-acquisition state of the smectite – for example, facilitating closed-system in-RSTA redox reactions of structural (octahedral) Fe^{2+} and Mn^{2+} and the electron donors and electron acceptors involved. The loss of information about FRTE oxidation state in the smectites would not be compensated for by the closed-system-sourced interlayer water recording the equilibrium/steadystate relative humidity and change in mass (abundance) and stable H and O isotopes of molecular interlayer water sourced from other phases in the RSTA between sealing and opening the RSTA (cf. Tosca et al., 2021).

3.8.4. Timescale of deleterious effect

Experimentally determined interlayer diffusion coefficients of deuterated water (HDO) in damp pellets of Li-montmorillonite (Cebula et al., 1981) and of tritiated water (HTO) in compacted pellets of Ca- and Na-bentonite (Choi and Oscarson, 1996) are within approximately one order of magnitude or less of the tracer- or self-diffusion coefficients for diffusion of solvated cations and molecular water through water and unconsolidated sediment (Li and Gregory, 1974).

The effective diffusion coefficients of HDO in saturated compacted pellets of Na-bentonite were determined both parallel and perpendicular to the oriented fabric of the clay-mineral platelets at four temperatures of direct relevance to this study (25°C, 40°C, 50°C, and 60°C; Suzuki et al., 2004). All effective HDO diffusion coefficients are within one order of magnitude or less of the tracer- or self-diffusion coefficients for solvated-cation diffusion and molecular water through water and unconsolidated sediment (Li and Gregory, 1974). The D_e values increase (diffusion becomes faster) by ~2.2× - 2.7× from 25 to 60°C (Suzuki et al., 2004).

Structural expressions of changes (interlayer expansion or contraction) upon clay-mineral interlayer-cation water of solvation can be measured in < 1 s at cryo-TEM conditions (Whittaker et al., 2019).

At a diffusion coefficient of $D = 1 \times 10^{-5}$ cm^2 s^{-1} (the upper limit for interlayer diffusion in and through compact clay-

rich materials), water (evolved from any source, alone or as water of cation solvation) would diffuse along and through grain boundaries or through a water-saturated (micro)porous medium and penetrate up to a few hundred microns in an hour. However, at diffusion coefficients for molecular and Knudsen diffusion in unsaturated microporous media (*e.g.*, Mars-dry sandstones, unconsolidated regolith, and, especially, mudstones consisting by definition of intrinsically small discrete crystallites and particles) with $D = 1 \times 10^{-3}$ to 1×10^{-0} cm^2 s^{-1} (Lerman, 1979; Reinecke and Sleep, 2002), molecular water vapor would penetrate the entire radius of the sample core in minutes to seconds.

Rehydration of dehydrated interlayers in smectites is slower than dehydration (*e.g.*, Huang et al., 1994). Consequently, rehydration of smectites like those examined by CheMin on Mars (Tu et al., 2021) may have to overcome a kinetic barrier to initial prising open of interlayer sites at the edges of the dry smectite crystallites. However, once initiated, diffusion of water from the newly expanded edge to the interior of the crystallite would likely be rapid (9 min at 40°C; Huang et al., 1994) and limited only by the availability of molecular water.

3.9. Amorphous material

X-ray amorphous material is abundant (15-73 wt%) and more copious than crystalline phyllosilicate (mean 12 wt%, maximum ~30 wt%; Rampe et al., 2020; Tu et al., 2021) in CheMin XRD analyses of fluvio-lacustrine sedimentary rocks at Gale crater. Some X-ray amorphous material may consist of volcanic glass, some of amorphous hydrated silica and ferric O-bearing phases, some of non-crystalline smectite-precursors, and some of amorphous hydrous sulfates or hydrous carbonates. Metal-sulfate phases may be either amorphous or mixtures of crystalline sulfates that were individually below the CheMin detection limit. Durations of dehydration and rehydration reactions vary (Table 15). Dehydration of epsomite to amorphous material is nearly 30× and 6× faster at 50 °C and 40 °C (respectively) than at 30°C. Dehydration of nesquehonite to amorphous material is more than 6× and 2× faster at 50 °C and 40 °C (respectively) than at 30°C. Rehydration of amorphous material to starkeyite or epsomite is more than 4× and 2× faster at 50 °C and 40 °C (respectively) than at 30 °C. Mobilization of water vapor among (evolution from or incorporation into) nearby amorphous and hydrated phases will be substantially accelerated, and timescales of deleterious effects substantially shorter (< to <<10 hrs), at T > 30 °C, with potentially severe consequences for the closed-system contents of the RSTA and associated loss of science.

Table 15. Dehydration and rehydration reactions and their times to completion (from Tables 13 and 14).

Reactions		Time to completion at			
		Units	30°C	40°C	50°C
Dehydration					
Epsomite to amorphous	$MgSO_4 \cdot 7H_2O \rightarrow MgSO_4 \cdot 2H_2O + 5H_2O$	min	28	6	1
Nesquehonite to poorly crystalline anhydrous Mg-carbonate	$MgCO_3 \cdot 3H_2O \rightarrow MgCO_3 + 3H_2O$	hours	13	5	2
Rehydration					
Amorphous to hexahydrite or epsomite	$MgSO_4 \cdot 2H_2O + 4\text{-}5H_2O \rightarrow MgSO_4 \cdot 6\text{-}7H_2O$	hours	36	16	8
Starkeyite to hexahydrite or epsomite	$MgSO_4 \cdot 4H_2O + 2\text{-}3H_2O \rightarrow MgSO_4 \cdot 6\text{-}7H_2O$	hours	33	17	9

3.10 Summary on Inorganic Materials

Inorganic materials expected in many to-be-returned Mars samples constitute a system rich in metastable volatile-bearing phases. Heating could overprint the entire inventory of volatile-hosting minerals and amorphous materials in the as-sampled phase assemblage in the RSTA with an equilibrium-in-the-tube assemblage. This is unlikely by design in the expected (Table 1) multi-years of onboard caching on Mars. However, thermal deterioration of important measurable properties of samples is likely at a range of shorter-duration heating episodes. Many, though not all, additional known or possible higher-temperature excursions (30 °C < T < 50 °C) are identified and their durations described in Table 1.2. These include temperature excursions to higher than 30 °C (30 °C < T < 50 °C) during drilling the core (less than ten minutes), sealing the RSTA (less than twenty minutes), depot caching (years), transfer to the Orbiting Sample (OS) (months), and sterilization or other thermal excursions during sealing in the OS (hours).

If one volatile-redistribution process happens on the timescale of the transient heating-cooling episode, other phases may be affected. Such effects would follow from mass transfer from a dehydrating hydrous mineral to the chamber atmosphere and then from the tube atmosphere to an initially less-hydrous or anhydrous but potential hydratable material, such low-hydration-state Ca- or Mg-sulfates (Vaniman et al., 2018) or carbonates, or the Mars-dry as-sampled interlayers of smectite-group clay mineral at Gale crater (Vaniman et al., 2018; Tu et al., 2021). At diffusion coefficients for molecular and Knudsen diffusion in unsaturated microporous media (e.g., Mars-dry sandstones, unconsolidated regolith, and, especially, mudstones consisting by definition of intrinsically small discrete crystallites and particles) of $D = 1 \times 10^{-3}$ to 1 × 10-0 $cm^2\ s^{-1}$ (Lerman, 1979; Reinecke and Sleep, 2002), molecular water vapor would penetrate the entire radius of the sample core in minutes to seconds. Such mass transfer could continue until either the clay-mineral interlayer sites are fully saturated (which depends in part on the abundance of clay minerals in the sample), or the dehydrating hydrous mineral is fully exhausted of its water. Either end-state would have changed the distribution of water molecules and their isotopes from their as-sampled state on Mars – the state in which the sample preserves evidence of the Mars conditions under which it formed – to a no-longer-Mars state, an RSTA closed system at a hitherto not experienced temperature and vapor pressure. This is potentially a serious loss of iMOST-anticipated measurable properties.

Most of the phenomena identified in this section as deleterious to high-priority iMOST science objectives are critical at thermal-excursion (30 °C < T < 50 °C) durations of days, and some are critical at durations of hours or even minutes (*e.g.*, hydrous Mg-sulfate dehydration in minutes; Mg-sulfate rehydration and hydrous Mg-carbonate dehydration in hours). Furthermore, because the volatiles are mobile as vapor in the closed-system RSTA, a fast change in a critical sample property of a phase evolving or consuming volatiles may likely affect other phases in the tube. Phases in the sample that will be especially vulnerable to volatiles evolved by others are those that were "dry" at Mars surface conditions but are exposed to higher-than-Mars-surface-ambient vapor evolved by the rapidly dehydrating co-existing phase in the closed-system RSTA. This is especially true for samples of regolith and samples of porous sedimentary rock.

Higher-temperature excursions (30 °C < T < 50 °C) during drilling the core (less than ten minutes), sealing the RSTA (less than twenty minutes), depot caching (years), transfer to the OS (months), MAV launch (minutes), sealing-brazing and sterilization in the OS (months), and Entry Descent and Landing (EDL) at Earth (tens of minutes) (durations from Table 1) would impose new thermal conditions on the phases inside the RSTA and cause corresponding losses of scientific information and value.

The Statement of Task provided to the Temperature-Time Tiger Team by the NASA and ESA Mars Sample Return Program designated MSR Objectives 1 and 2 (iMOST, 2018; Beaty et al., 2019) as highest priority. These include:

- sub-objective 2.2 – biosignature-ancient – of the iMOST Level 1 Objective 2 – Life – and
- four of the five sub-objectives of the iMOST Level 1 Objective 1 – Interpret the primary geologic processes and history that formed the martian geologic record, with an emphasis on the role of water – on which Objective 2 depends

Almost all investigation strategies in sub-objectives of iMOST Objective 2 – the carbon and life objective – identify "(s)amples listed from environments listed in Objective 1 that contain" carbon or organic matter, or "(a)ll samples collected as a part of Objective 1" as being sought for advancing the iMOST investigation strategies. There are 73 iMOST-identified measurement types in Objective 1. Of these, at minimum 38 (listed in supplemental Table S1) would very likely be compromised if the sample materials to be measured are modified by transient episodic heating to the temperature range of concern to this study (30°C < T < 50°C). In conclusion, most of the potential investigations in

both two highest-priority Objectives would be compromised or irreversibly damaged and lost to highest-priority science if the volatiles hosted in even one inorganic phase in the RSTA are mobilized between 30°C < T < 50°C and induce "far-field" effects on other phases elsewhere in the RSTA closed system.

The matter of how conditions in a heating RSTA atmosphere affect organic molecules and potential biosignatures – directly or in tandem with changes in the inorganic phases – is addressed in the next section.

4. Organic Materials

4.1. Impacts of temperature on organic matter

There is a strong motivation for limiting the heating of samples to avoid sample degradation induced by instantaneous temperature excursions above a certain level. Additionally, even for samples that have been exposed to higher temperatures there is still a significant science benefit to limiting further exposure to higher temperatures because chemical reaction rates for the samples inside the closed environment of the tubes are directly tied to temperature.

4.2. Thermal effects

Organic matter in returned samples may be hosted in several forms (Fig. 16), and each will have a different susceptibility to modification by elevated temperature. Volatiles can be present as free gases in pore spaces. Volatiles can be adsorbed on the surfaces of minerals or organic matter. Semi volatiles (liquids at ambient temperature and pressure) can also be present in pore spaces or on mineral or organic matter surfaces. High molecular weight organic matter (*e.g.*, like terrestrial kerogen or insoluble organic matter in chondritic meteorites) takes the form of clasts intermixed with, or coated on, minerals. More complex hosting styles also exist, and organic materials may be occluded within i) other organic matter (Watson et al. 2010) or ii) closed mineral voids (Steele et al., 2012).

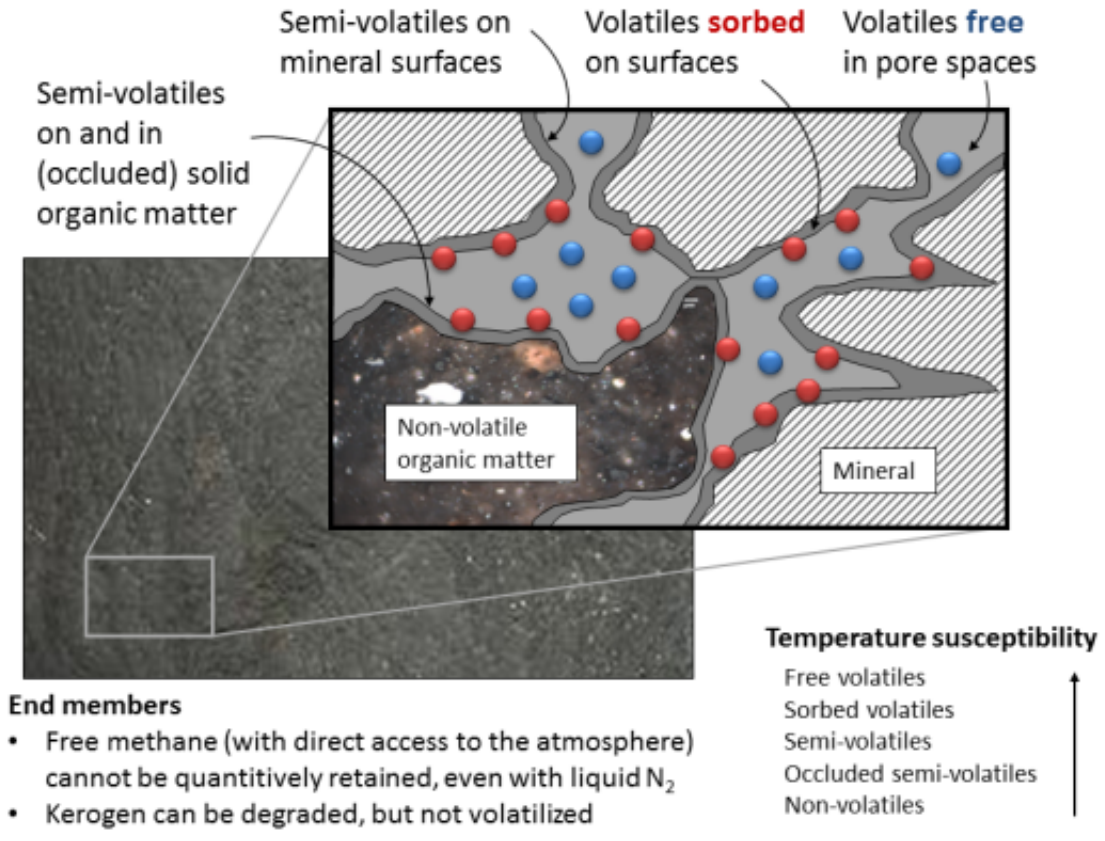

FIG. 16. Carbon based compounds and their hosting by rocks.

Rock types are highly variable in both their porosity and permeability, but all pores on the outside of a fresh core or fragmented rock will have access to the atmosphere and increased volatile loss from their host phases. Adsorbed volatiles can be lost from their host phases more gradually as they equilibrate with the surrounding free gases.

Eventually, all volatiles can be redistributed from their host phases. Semi-volatiles can be lost from their host phases by evaporation when subjected to heat or agitation by fluid flow. At terrestrial room temperature and pressure, the process can lead to the loss from their host phases of semi volatiles up to octadecane (n-C_{18}) or phenanthrene (Sephton et al., 2001), although it must be noted that temperature and pressure are different on Mars relative to Earth's surface. Higher molecular weight organic matter is relatively immovable. Yet some information can still be lost at relatively low temperatures. The three-dimensional (tertiary and quaternary) structure of proteins is determined by weak bonds that are sensitive to heat and proteins denature above 40 °C.

4.3. Thermochemical effects

Organic matter in returned samples may be juxtaposed with other materials, and the assemblage can initiate chemical reactions. Higher temperatures would lead to faster chemical reaction rates and, therefore, greater sample alteration and chemical degradation the longer they are exposed to higher temperatures. One of the compounding factors for organic compound preservation is the presence of strong oxidants, such as Mn oxides, H_2O_2 and ClO_4^- inthe martian surface. Such reactions are strongly temperature dependent and result in the unrecoverable loss of organic compounds (see Section 2.2, and Table 8). Hydrocarbons are expected in the samples and are known to be destroyed by oxidation. For example, the peroxide destruction of aliphatic hydrocarbons at 60 °C is 16x faster than at 30°C (oxidation of hexadecane is 300 vs. 4800 $M^{-1}s^{-1}$ respectively; Koreck et al. 1972). To minimize chemical alteration of the sample, both the maximum and average temperature should be as low as reasonably possible. The rate of destruction is based on the concentration of oxidant, organic, and temperature (Fig. 17).

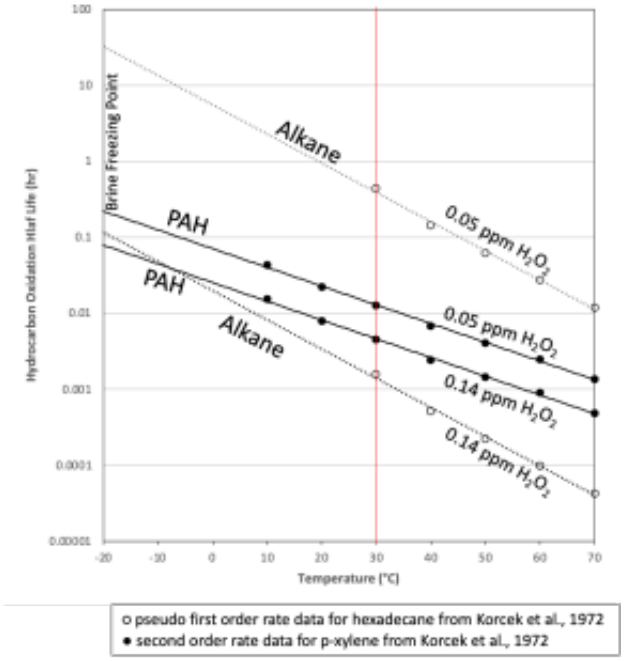

FIG. 17. Temperature impacts on reaction rates. Example decomposition rates of two classes of plausible martian organic compounds from hydrogen peroxide (Koreck et al. 1972). Reactions are assumed to occur in aqueous inclusions or films, and hydrogen peroxide concentration range (0.05-0.14 ppm or 1.5-4.1 μM) is taken from those observed in the analogous Atacama desert environment (Navarro-Gonzalez et al. 2003). Reactions are based on the physical or gas contact of solutes with brine, and this particular reaction will effectively stop below the brine freezing point. Alkane reactions are assumed to be pseudo first order as the SAM/*Curiosity* detection of ~10 ppm (~40 nM for hexadecane) alkanes is much lower than the hydrogen peroxide concentration. The PAH concentration was taken from martian meteorite ALH 84001 (1 ppm or about 6 μM for chrysene; Becker et al. 1997).

For the organic matter-perchlorate oxidative degradation reaction, the influence of the relative abundance of chemical reactants has been studied, and there is a critical ratio (>9.6) above which where the amount of reduced organic matter is too great and simply exhausts the oxidant (Royle et al. 2018).

Carboxyl carbon is susceptible to dissolved inorganic carbon exchange reactions (Filipe et al., 2005). Hydrogen isotope exchange reactions (likely with H in water) may begin at the higher end of the +30 °C to +60 °C temp range, especially for tertiary carbon centers. Moreover, increased water activity and lowered pH, both effects induced by heating of inorganic materials as described above, can promote the cleavage of ester linkages in organic compounds

(Speight 2017). Stereochemical rearrangements (enantiomer changes from less stable to more stable forms; racemic amino acids, etc.) are also initiated by increases in temperature, and the record contained within organic architectures can be degraded.

5. Microorganisms

The MSR Campaign is not designed as a life-detection mission, and planned handling of the samples is not conducive to maximum preservation of biological material. However, an opportunity exists that the returned samples may still contain terrestrial contaminants or putative martian life, which will be also targeted by Sample Safety Assessment.

Chemically reactive minerals that have been detected on Mars may change the microenvironments within the sampled core. For example, several minerals in martian samples could dehydrate (Sections 2.2.1.3 and 3.1). As explained above, different types of sampled material may exhibit different levels of susceptibility to alteration due to the heating intervals that will occur during the drilling, sealing of the core tube(s), storage on Mars, and transport of samples at the surface of Mars. The tubes containing material that has significantly changed due to maximum heating to 60 °C may release enough moisture to damage potentially present biological material. Changes in temperature due to diurnal variations and mission operations will cause freezing and thawing of the core samples. The freeze-thaw process in hydrated biological material can physically damage nucleic acids by shearing due to ice crystals formation. Additionally, the freeze-thaw process may form transient microenvironments with various concentrations of dissolved solutes released from the surrounding mineral matrix. Such microenvironments may increase or decrease the pH of the solution (Section 2.2.1.5). Changes in pH could damage cells; for example, lowering pH may cause acid depurination, while more alkaline pH could influence hydrolysis of sugar phosphate backbone. Further oxidative damage by metal ions, for example, the release of Fe^{2+} in microenvironments, could lead to a reaction in which Fe^{2+} and H_2O_2 will react (Table 8; Section 2.2.1.5), form OH^- ion and hydroxyl radicals, and promote oxidative damage of nucleic acids is a possibility, as in Fenton reaction. Other metal ions, such as Cu, could react similarly in these conditions (Burg and Meyerstein, 2012).

If, for most of the time, temperature variations are kept at a lower possible scale, this means that less water structurally trapped in minerals would be released so that the freeze-thawing process might be less damaging to terrestrial or hypothetical martian organisms. A valuable example or organismal resistance to temperature changes in Mars simulated conditions had been observed in desiccated extremophiles set as experiments on board of the International Space Station (ISS) (Rabbow et al., 2012, Wassmann et al., 2012, Onofri et al., 2015). In particular, the ESA-EXPOSE-E remained in space for 1.5 years and exposed astrobiology-relevant samples to simulate martian surface conditions (tray 2). Data on temperature, solar ultraviolet (UV), and cosmic radiation were measured every 10 s. The mission temperature (measured by six temperature sensors) fluctuated between -21.71 °C and 42.95 °C, most of the time temperature fluctuations were between –15 to 20 °C and 40 °C. Once a high-temperature excursion of 59.61 °C to 61 °C for about an hour was recorded (Fig. 18; Rabbow et al., 2012). The martian conditions in the carriers of the tray 2 were simulated by low-pressure martian-like atmosphere and quartz filters used to cut extreme UV radiation. Below the radiation exposed carriers, an additional set of carriers were kept in the dark.

The ADAPT I, PROTECT, and LIFE experiments were performed to test the effects of martian surface conditions on microorganisms (Rabbow et al., 2012). The ADAPT I experiment exposed spores of a UV resistant *Bacillus subtilis* strain to space and simulated Mars conditions (Wassmann et al., 2012). The PROTECT experiment exposed endospores of *Bacillus pumilus* and *B. subtilis* to the same conditions (Horneck et al., 2012). The LIFE experiment exposed cryptoendolithic microorganisms from Antarctica to Mars-like conditions (Onofri et al., 2015). All three experiments had the same set of organisms set in dark conditions.

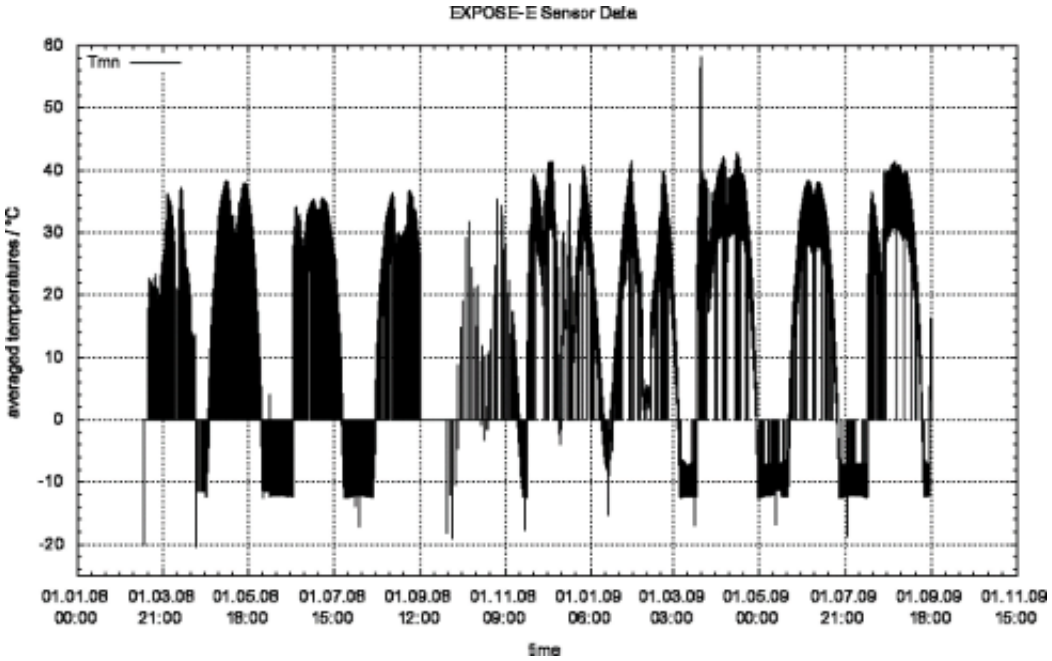

FIG. 18. Temperature variations during the EXPOSE-E mission as averaged from the measurements of the six temperature sensors (from Rabbow et al., 2012).

The ADAPT I revealed that spores of the UV-resistant strain of *B. subtilis*, kept in the dark martian atmosphere and subjected to thermal stresses, were not affected by these conditions. The PROTECT dark experiment revealed that endospores of a different strain of *B. subtilis* and *B. pumilus* exhibited 70/75% survival. During the LIFE experiment, the Antarctic cryptoendolithic black fungi *Cryomyces antarcticus* and *C. minteri* showed low survival in Mars dark conditions (measured 60 % of undamaged cells). However, desiccated Antarctic rock colonized by cryptoendolithic communities were exposed to space and simulated martian conditions. More than 70% of undamaged cells were reported, and the two organisms able to grow after the experiments were identified as *Stichococcus* sp. (green alga) and *Acarospora* sp. (lichenized fungal genus) (Onofri et al. 2015; Scalzi et al., 2012)

Within the ESA-EXPOSE-E, another interesting experiment contained a natural phototroph's biofilm with cyanobacteria and algae; the biofilm was augmented with akinetes of *Anabaena cylindrica* and vegetative cells of *Nostoc commune* and *Chroococcidiopsis*. In space-exposed dark experiments, two algae (*Chlorella* and *Rosenvingiella* spp.), a cyanobacterium (*Gloeocapsa* sp.) and two bacteria associated with the natural community survived. Among the augmented organisms, cells of *A. cylindrica* and *Chroococcidiopsis* survived, but no cells of *N. commune*. The best survival results have been obtained in dark conditions simulated in space (Cockell et al., 2011). These results indicate that some of the extremophiles exhibit good resistance after being exposed to dark martian simulated atmospheric conditions and subjected to temperature fluctuations from -15/20 to 40 °C (up to 61 °C) and dehydrated, during 559-day exposure on the ISS.

The EXPOSE-R2 ISS facility exposed (BIOMEX experiment, 2014-2016) samples to dark Mars simulated conditions. The cyanobacterium *Chroococcidiopsis*, mixed with martian regolith simulant, showed 0.01-0.04% viability based on colony forming units (Billi et al., 2019). Under the same conditions, *C. antarcticus* showed about 50% viability (Onofri et al., 2019). Temperature oscillations are shown in the literature (Fig. 19; Rabbow et al., 2017).

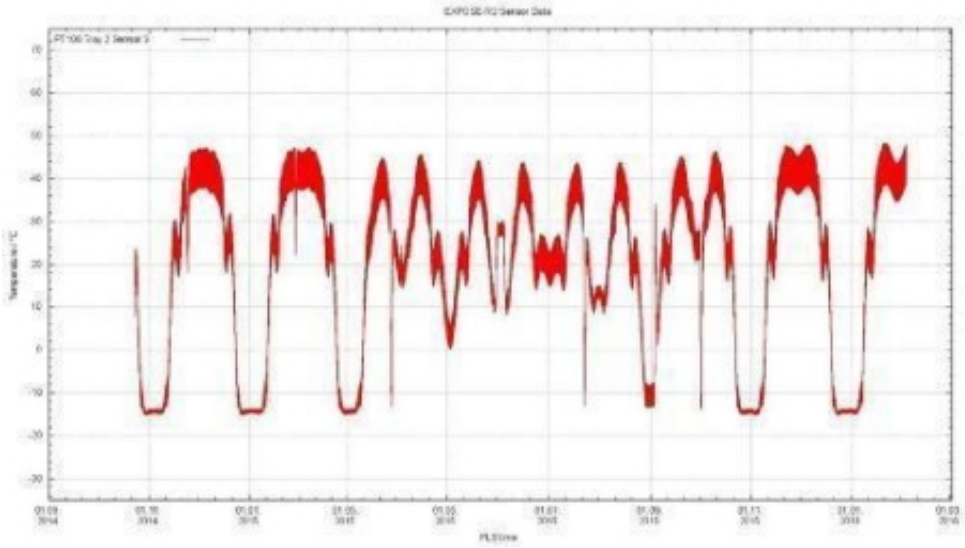

FIG. 19. The temperature profiles from October 23, 2014. to February 2, 2016. for ISS EXPOSE-R2 (from Rabbow et al., 2017).

Microorganisms and organic compounds within fluid inclusions in chemical sediments or diagenetic phases may be insulated from maximum temperatures by their host mineral. Terrestrial halite, in particular, has proven to preserve unaltered microorganisms in fluid inclusions for hundreds of millions of years at burial depths with estimated temperatures up to ~60 °C (Lowenstein et al 2011; Roedder 1984; Benison 2019).

Currently, these data are the closest analogs to the conditions that the core samples on Mars are set to experience until they are returned to Earth. A time span of 1.5 years is much shorter, and the organisms are preselected as potentially resistant and desiccated to avoid freeze-thaw damages. Based on current data, we know that most terrestrial organisms would not survive heating-cooling conditions +30 to +60 °C for an extensive period. However, the data collected from ISS experiments conducted on some of the most resistant extremophiles indicate that we cannot dismiss a possibility that some very resistant extremophiles, terrestrial or putative martian, could survive the conditions of sample retrieval procedures planned for the MSR campaign. Once the organisms die, decomposition of the organics takes place, and the rate of degradation is governed by the processes outlined above.

Additional knowledge of the temperature limits for microorganisms is provided by analogue environments on Earth such as Antarctica. The Antarctic Dry Valleys are considered reliable analogues of Mars; fossilized cryptoendolithic communities, including algae, fungi, and bacteria, have been described in sedimentary rocks (Wierzchos and Ascaso 2002). These fossils resisted in recognizable morphological shape to freeze-thawing cycles (possibly from 25 to -50 °C), rehydrated cyclically by melting snow (Nienow and Friedmann, 1993), making possible the hypothesis of their conservation if they exist in the subsurface of Mars.

It is widely reported in the literature that most mesophilic microorganisms in metabolically active state are killed or could resist a few seconds to 60 °C, but it must be taken into account that very few microorganisms are in vegetative status at activity of water less than or just above 0.70, thus at RH lower than 70% are very likely unable to activate microorganisms (Grant, 2004). Our calculations above reveal that dehydration of gypsum could result in 40% RH in the tube, which on its own is not enough for activating microorganisms with terrestrial-like metabolism. At low RH (*e.g.*, <30%), there is some faint possibility of life preservation, decreasing with increasing temperature, but preservation of morphological biosignatures is more likely. In any case, putative microorganisms surviving in Mars conditions should be very resistant and in dormant state (*e.g.*, spores).

6. The consequence-based risk-matrix

The Tiger Team deliberated the potential science represented by the samples, the susceptibility of potential science to changes in temperature, and established a consequence-based risk-matrix to inform the review of potential waiver requests.

For inorganic materials and the records they represent, over both long time scales (hours to days) and short time scales (minutes to hours), no temperature excursion above 30 °C could be accommodated without loss of science (Fig. 20). While there will be some robust constituents (feldspars, quartz, pyroxenes, etc.) that are unaffected, there will also be

some less robust constituents (salts, phyllosilicates, strong gaseous oxidants, radicals, etc.) that are affected across all temperature ranges ≤60 °C.

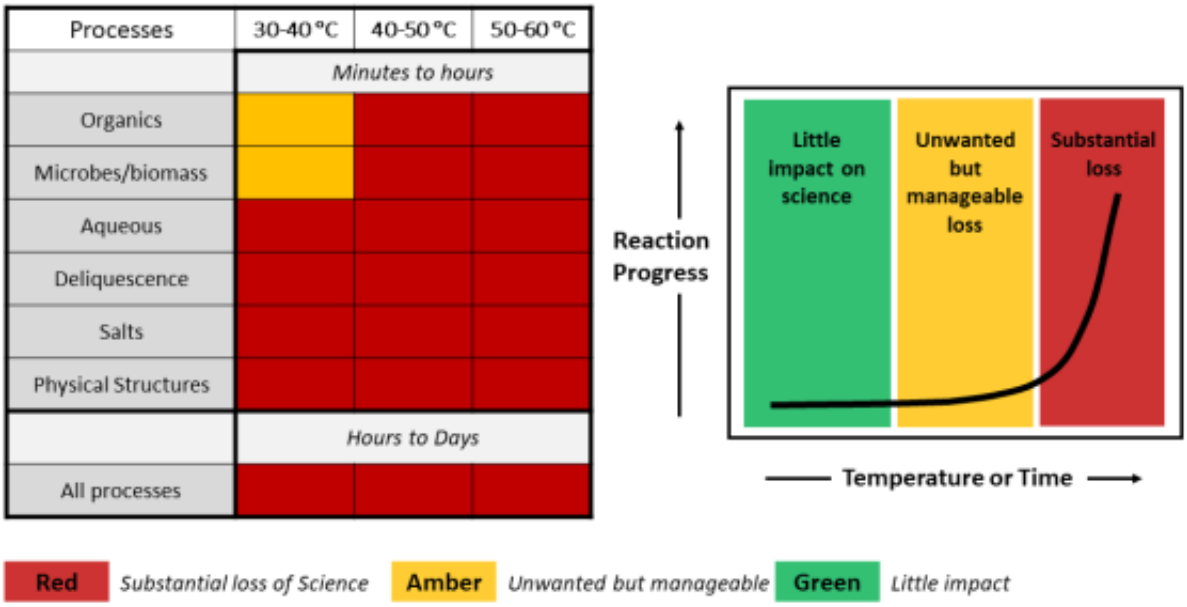

FIG. 20. A consequence-based risk-matrix displaying the impact on science, related to inorganic and organic materials, of temperatures in the range of +30 °C to +60 °C for samples returning from Mars. Note that the relationship between science impact and temperature is not linear.

For organic materials and, in particular, potential organic biosignatures, the risks reflect that preservation is reliant on a number of processes and change in one component within a sample tube can lead to effects on another (Fig. 21).

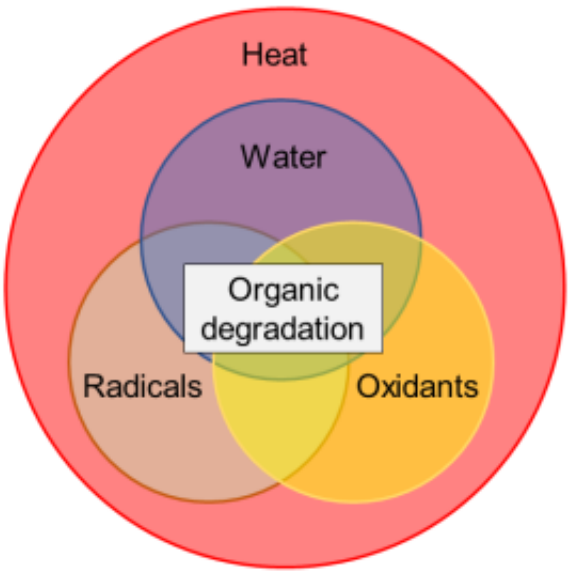

FIG. 21. The multiple processes that are initiated by rising temperatures can affect organic-based records either alone or in combination.

For organic materials and the records that they represent over long time scales (hours to days), no temperature excursion above 30 °C could be accommodated without loss of science (Fig. 20), but over short time scales (minutes to hours) raising the temperature to 40 °C could be manageable without major disruption to science, while temperatures

above 40 °C would lead to significant losses.

Acknowledgements

The decision to implement Mars Sample Return will not be finalized until NASA's completion of the National Environmental Policy Act (NEPA) process. This document is being made available for planning and information purposes only. The authors would like to express thanks for the following support: MAS (UK Space Agency grants ST/N000560/1, ST/V002732/1, ST/V006134/1 and ST/W002264/1), EES (NERC grant NE/V010824/1), KCB (NASA grant 80NSSC20K0235), BC A portion of this work was carried out at the Jet Propulsion Laboratory, California Institute of Technology, under a contract with the National Aeronautics and Space Administration (80NM0018D0004) , RCP (NSERC) and JPD (NASA). For the purpose of open access, the author has applied a Creative Commons Attribution (CC BY) license to any Author Accepted Manuscript version arising. The authors are extremely grateful for the detailed suggestions of two anonymous reviewers.

Appendix A

Abbreviations and acronyms used in this report.

Abbreviation / acronym	Definition
ACA	Adaptive Caching Assembly
AFT	Allowable Flight Temperature
ALH	Allan Hills, Antarctica (a meteorite recovery area)
APXS	Alpha Particle X-Ray Spectrometer (aboard MSL rover *Curiosity*)
CheMin	Chemistry and Mineralogy (XRD instrument aboard MSL rover *Curiosity*)
CHNOPS	Carbon, hydrogen, nitrogen, oxygen, phosphorous, sulfur (important elements for life)
CRISM	Compact Reconnaissance Imaging Spectrometer for Mars (aboard Mars Reconnaissance Orbiter)
DRH	Deliquescence relative humidity
EDL	Entry, Descent, and Landing
EGA	Evolved Gas Analyzer (one instrument in the MSL SAM tool)
ERH	Efflorescence relative humidity
ESA	European Space Agency
FRTE	First-row transition elements
iMOST	International MSR Objectives and Samples Team
ISS	International Space Station
LEW	Lewis Cliff, Antarctica (a meteorite recovery area)
M2020	Mars 2020 (NASA mission)

MAV	Mars Ascent Vehicle
MEPAG	Mars Exploration Planning and Analysis Group
MER	Mars Exploration Rovers (NASA mission)
MGS	Mars Global Surveyor
MSL	Mars Science Laboratory (NASA mission)
MSPG2	Mars Sample Return Science Planning Group Phase 2
MSR	Mars Sample Return
NASA	National Aeronautics and Space Administration
NEPA	National Environmental Policy Act
OMEGA	**O**bservatoire pour la **M**ineralogie, l'**E**au, les **G**laces et l'**A**ctivite (spectrometer on ESA Mars Express orbiter)
OS	Orbiting Sample
pfu	Per formula unit
PHX	*Phoneix* Mars Lander (NASA mission)
PIXL	Planetary Instrument for X-ray Lithochemistry
REMS	Rover Environmental Monitoring Station (weather instruments aboard MSL rover *Curiosity*)
RH	Relative humidity
ROS	Reactive oxygen species
RSSB	Return Sample Science Board
RSTA	Returned Sample Tube Assembly
SAM	Sample Analysis at Mars (three instruments aboard MSL rover *Curiosity*)
SHERLOC	Scanning Habitable Environments with Raman & Luminescence for Organics & Chemicals (instrument aboard M2020 rover *Perseverance*)
SNC	Shergottite, nakhlite, chassignite (names of the three groups of the most abundant and longest-studied Mars meteorites)
SuperCam	VisNIR spectrometer aboard M2020 rover *Perseverance*
T4	Temperature-Time Tiger Team
TE	Temperature, eutectic
TEM	Transmission electron microscope
TES	Thermal Emission Spectrometer
TI	Thermal inertia

UV	Ultraviolet
VisNIR	Visible and near-infrared spectroscopy
WATSON	Wide Angle Topographic Sensor for Operations and eNgineering (supports SHERLOC)
WCH	Worst-case heating
XRD	X-ray diffraction

References

Alpers, C.N., Nordstrom, D.K. and Ball, J.W. (1989) Solubility of jarosite solid solutions precipitated from acid mine waters, Iron Mountain, California, *U.S.A. Sciences Géologiques Bull* 42: 281-298.

Arvidson, R.E., Squyres, S.W., Bell, J.F. III, Catalano, J.G., Clark, B.C., Crumpler, L.S., de Souza, P.A. Jr., Fairén, A.G., Farrand, W.H., Fox, V.K., and others. (2014) Ancient aqueous environments at Endeavour Crater, Mars. *Science* 343: 1–8. https://doi.org/10.1126/science.1248097

Aubrey, A., Cleaves, H.J., Chalmers, J.H., Skelley, A.M., Mathies, R.A., Grunthaner, F.J., Ehrenfreund, P., Bada, J.L. (2006) Sulfate minerals and organic compounds on Mars. *Geology* 34: 357–360. https://doi:10.1130/G22316.1

Bao, H. and Koch, P. L. (1999) Oxygen isotope fractionation in ferric oxide–water systems: Low temperature synthesis. *Geochimica et Cosmochimica Acta* 63: 599–613. https://doi.org/10.1016/S0016-7037(99)00005-8

Beaty D. W., Grady M. M., McSween H. Y., et al. (2019) The potential science and engineering value of samples delivered to Earth by Mars sample return: International MSR Objectives and Samples Team (iMOST). *Meteoritics and Planetary Science* 54: S3-S152. https://doi.org/10.1111/maps.13232

Becker, L., Glavin, D.P., Bada, J.L. (1997) Polycyclic aromatic hydrocarbons (PAHs) in Antarctic Martian meteorites, carbonaceous chondrites, and polar ice. *Geochimica et Cosmochimica Acta* 61: 475–481. https://doi.org/10.1016/S0016-7037(96)00400-0

Benison, K.C. (2019) How to search for life in martian chemical sediments and their fluid and solid inclusions using petrographic and spectroscopic methods. *Frontiers in Environmental Science* 7: 108. https://doi.org/10.3389/fenvs.2019.00108

Benison, K.C., Bowen, B.B., Oboh-Ikuenobe, F. E., Jagniecki, E.A., Laclair, D.A., Story, S.L., Mormile, M. R., Hong, B.-Y. (2007) Sedimentology of acid saline lakes in Southern Western Australia: newly described processes and products of an extreme environment. *Journal of Sedimentary Research* 77: 366-388. https://doi.org/10.2110/jsr.2007.038

Billi, D., Staibano, C., Verseux, C., Fagliarone, C., Mosca, C., Baqué, M., et al. (2019) Dried biofilms of desert strains of Chroococcidiopsis survived prolonged exposure to space and Mars-like conditions in low Earth orbit. *Astrobiology* 19: 1008–1017. https://doi.org/10.1089/ast.2018.1900

Bing, H., He, P., Zhang, Y. (2015) Cyclic freeze–thaw as a mechanism for water and salt migration in soil. *Environ Earth Sci* 74: 675-681. https://doi.org/10.1007/s12665-015-4072-9

Bish, D.L. and Duffy, C. J. (1990) Thermogravimetric analysis of minerals. In Thermal analysis in clay science, In: Thermal Analysis in Clay Science, Workshop Lectures, Volume 3, edited by J.W. Stucki, D.L. Bish, and F.A. Mumpton, The Clay Minerals Society, Boulder, Colorado, USA, pp. 96-157. https://doi.org/10.1346/CMS-WLS-3.4

Bish, D.W., Carey, J.W., Vaniman, D.T. and Chipera, S.J. (2003) Stability of hydrous minerals on the martian surface. *Icarus* 164: 96-103. https://doi.org/10.1016/S0019-1035(03)00140-4

Boogerd, F.C., Van Den Beemd, C., Stoelwinder, T. and Bos, P, (1991) Relative contributions of biological and chemical reactions to the overall rate of pyrite oxidation at temperatures between 30 °C and 70 °C. *Biotechnology and Bioengineering* 38: 109-115. https://doi.org/10.1002/bit.260380202

Brass, G.W. (1980). Stability of brines on Mars. *Icarus* 42: 20–28. https://doi.org/10.1016/0019-1035(80)90237-7

Bridges, J.C., Schwenzer, S.P., Leveille, R., Westall, F., Wiens, R.C., Mangold, N., Bristow, T., Edwards, P., and Berger, G., (2015) Diagenesis and clay mineral formation at Gale Crater, Mars, *Journal of Geophysical Research: Planets* 120: 1–19. https://doi.org/10.1002/2014JE004757

Bristow, T. F., Bish, D.L., Vaniman, D.T., Morris, R.V., Blake, D.F., Grotzinger, J.P., Rampe, E.B., Crisp, J.A., Achilles, C.N., Ming, D.W., Ehlmann, B.L., King, P.L., Bridges, J.C., Eigenbrode, J.L., Sumner, D.Y., Chipera, S.J., Michael Moorokian, J., Treiman, A.H., Morrison, S.M., Downs, R.T., Farmer, J.D., Des Marais, D., Sarrazin, P., Floyd, M.M., Mischna, M.A., McAdam, A.C., (2015) The origin and implications of clay minerals from Yellowknife Bay, Gale crater, Mars. *American Mineralogist* 100: 834-836. https://doi.org/10.2138/am-2015-5077CCBYNCND

Burg, A., Meyerstein, D,. (2012) Chapter 7 – The chemistry of monovalent copper in aqueous solutions, In Advances in Inorganic Chemistry, edited by Eldik, R. van, Ivanović-Burmazović, I., Academic Press, pp. 219–261. https://doi.org/10.1016/B978-0-12-396462-5.00007-6

Calvin, W.M., King, T.V.V., and Clark, R.N., (1994) Hydrous carbonates on Mars?: Evidence from Mariner 6/7 infrared spectrometer and ground-based telescopic spectra. *Journal of Geophysical Research: Planets* 99: 14659-14675. https://doi.org/10.1029/94JE01090

Cebula, D.J., Thomas, R.K., and White, J.W., (1981) Diffusion of water in Li-montmorillonite studied by quasielastic neutron scattering. *Clays and Clay Minerals* 29: 241-248. https://doi.org/10.1346/CCMN.1981.0290401

Che, C., Glotch, T.D., Bish, D.L., Michalski, J.R., and Xu, W. (2011) Spectroscopic study of the dehydration and/or dehydroxylation of phyllosilicate and zeolite minerals. *Journal of Geophysical Research: Planets*, 116: E05007. https://doi.org/10.1029/2010JE003740

Chen, L. (2018) Thermal decomposition characterization of supergene potassium-jarosite and sodium-jarosite minerals from the northern Tibetan Plateau, China. *Physicochem Probl Miner Process* 54: 459-466.

Chipera, S.J., and Vaniman, D.T. (2007) Experimental stability of magnesium sulfate hydrates that may be present on Mars. *Geochimica et Cosmochimica Acta* 71: 241–250, https://doi.org/10.1016/j.gca.2006.07.044

Chipera, S. J., Vaniman, D. T., Rampe, E. B., Bristow, T. F., Martínez, G., Tu, V. M., et al. (2023) Mineralogical investigation of Mg-sulfate at the Canaima drill site, Gale crater, Mars. *Journal of Geophysical Research: Planets*, 128, e2023JE008041. https://doi.org/10.1029/2023JE008041

Choi, J-W. and Oscarson D.W. (1996) Diffusive transport through compacted Na-and Ca-bentonite. *Journal of Contaminant Hydrology* 22:189-202. https://doi.org/10.1016/0169-7722(95)00081-X

Chou, I-M., Seal, R.R. II, and Wang, A. (2013) The stability of sulfate and hydrated sulfate minerals near ambient conditions and their significance in environmental and planetary sciences. *Journal of Asian Earth Sciences* 62: 734–758. https://doi.org/10.1016/j.jseaes.2012.11.027

Chyou, S.D., Shih, H.C., and Chen, T.T. (1993) On the corrosion characterization of titanium nitride in sulphuric acid. *Corrosion Science* 35:337-347. https://doi.org/10.1016/0010-938X(93)90165-D

Clark, B. C., A. K. Baird, R. J. Weldon, D. M. Tsusaki, L. Schnabel, and M. P. Candelaria (1982) Chemical composition of Martian fines, *Journal of Geophysical Res.,* 87: 10059–10067. https://doi.org/10.1029/JB087iB12p10059.

Clark, J.V., Sutter, B., McAdam, A.C., Rampe, E.B., Archer, P.D., Ming, D.W., et al. (2020) High-temperature HCl evolutions from mixtures of perchlorates and chlorides with water-bearing phases: Implications for the SAM instrument in Gale crater. Mars. *Journal of Geophysical Research : Planets* 125: e2019JE006173. https://doi.org/10.1029/2019JE006173

Clark, J., Sutter, B., Archer, P.D., Jr., Ming, D., Rampe, E., McAdam, A., Navarro-González, R., Eigenbrode, J., Glavin, D., Zorzano, M.-P., et al. (2021) A review of sample analysis at Mars-Evolved Gas Analysis Laboratory analog work supporting the presence of perchlorates and chlorates in Gale Crater, Mars. *Minerals* 11: 475. https://doi.org/10.3390/min11050475

Cockell, C., Rettberg, P., Rabbow, E. et al. (2011) Exposure of phototrophs to 548 days in low Earth orbit: microbial selection pressures in outer space and on early Earth. *The ISME Journal* J5: 1671–1682. https://doi.org/10.1038/ismej.2011.46

Cornell, R.M. and Schwertmann, U. (1996) The Iron Oxides: Structure, Properties, Reactions, Occurrence, and Uses, Weinheim: Wiley–VCH.

Cornell, R.M., Giovanoli, R., and Schneider, W. (1989) Review of the Hydrolysis of Iron(III) and the Crystallization of Amorphous Iron(III) Hydroxide Hydrate, *J Chem Technol Biotechnol* 46: 115–134. https://doi.org/10.1002/jctb.280460204

Coshell, L., Rosen, M.R., and McNamara, K.J. (1998) Hydromagnesite replacement of biomineralized aragonite in a new location of Holocene stromatolites, Lake Walynugup, Western Australia. *Sedimentology* 45: 1005-1018. https://doi.org/10.1046/j.1365-3091.1998.00187.x

Davila, A.F. et al. (2010) Hygroscopic salts and the potential for life on Mars. *Astrobiology* 10: 617–628. https://doi.org/10.1089/ast.2009.0421

Dos Santos, E.C., de Mendonça Silva, J.C. and Duarte, H.A. (2016) Pyrite oxidation mechanism by oxygen in aqueous medium. *The Journal of Physical Chemistry C 120:* 2760-2768. https://doi.org/10.1021/acs.jpcc.5b10949Dundar, M., Ehlmann, B.L., and Leask, E.K. (2021) Machine-Learning-Driven New Geologic Discoveries at Mars Rover Landing Sites: Jezero and NE Syrtis. *Geophysical Research Letters*, in review. https://doi.org/10.48550/arXiv.1909.02387

Ehlmann, B.L., Mustard, J.F., Fassett, C.I., et al. (2008a) Clay minerals in delta deposits and organic preservation potential on Mars. *Nature Geoscience* 1: 355-358. https://doi.org/10.1038/ngeo207

Ehlmann, B.L., Mustard, J.F., Murchie, S.L., et al. (2008b) Orbital identification of carbonate-bearing rocks on Mars. *Science* 322: 1828-32. https://doi.org/10.1126/sciadv.abo3399

El-Shenawy, M.I., Niles, P.B., Ming, D.W., et al. (2020) Oxygen and carbon stable isotope composition of the weathering Mg-carbonates formed on the surface of the LEW 85320 ordinary chondrite: Revisited. *Meteoritics and Planetary Science* 55: 1884-1898. https://doi.org/10.1111/maps.13553

Felipe, M.A., Kubicki, J.D., Freeman, K.H. (2005). A mechanism for carbon isotope exchange between aqueous acetic acid and CO_2/HCO_3^-: An ab initio study. *Organic Geochemistry* 36: 835–850. https://doi.org/10.1016/j.orggeochem.2005.01.012

Fischer, E., Martínez, G.M., Elliott, H.M., Rennó, N.O. (2014) Experimental evidence for the formation of liquid saline water on Mars. *Geophys Research Letters* 41: 4456–4462. https://doi.org/10.1002/2014GL060302

Fischer, E., Martínez, G.M. and Renno, N.O. (2016) Formation and persistence of brine on Mars: experimental simulations throughout the diurnal cycle at the *Phoneix* landing site. *Astrobiology* 16: 937–948. https://doi.org/10.1089/ast.2016.1525

Frost, R.L., Ruan H., Kloprogge J.T., et al. (2000) Dehydration and dehydroxylation of nontronites and ferruginous smectite. *Thermochimica Acta* 346: 63-72. https://doi.org/10.1016/S0040-6031(99)00366-4

Frost, R.L., Weier, M.L., and Martens, W. (2005) Thermal decomposition of jarosites of potassium, sodium and lead. *Journal of Thermal Analysis and Calorimetry* 82: 115-118. https://doi.org/10.1007/s10973-005-0850-z

Garrels, R.M. and Mackenzie, F.T. (1967) Origin of the Chemical Composition of Some Springs and Lakes. In Equilibrium Concepts in Natural Water Systems, Chap. 10, edited by W. Stumm, American Chemical Society, Washington DC, pp 222-242.

Gendrin, A., Mangold, N., Bibring, J.-P., Langevin, Y., Gondet, B., Poulet, F., Bonello, G., Quantin, C., Mustard, J., Arvidson, R., and LeMouélic, S. (2005) Sulfates in Martian layered terrains: The OMEGA/Mars Express view. *Science* 307: 1587-1581. https://doi.org/10.1126/science.1109087

Georgiou, C.D., Zisimopoulos, D., Kalaitzopoulou, E., and Quinn, R.C. (2017) Radiation-driven formation of reactive oxygen species in oxychlorine-containing Mars surface analogues. *Astrobiology* 17: 319–336. https://doi.org/10.1089/ast.2016.1539

Gislason, S.R. and Eugster, H.P. (1987) Meteoric water-basalt interactions: I. A laboratory study. *Geochimica et Cosmochimica Acta* 51: 2827–2840. https://doi.org/10.1016/0016-7037(87)90161-X

Glavin, D.P. et al. (2013) Evidence for perchlorates and the origin of chlorinated hydrocarbons detected by SAM at the Rocknest aeolian deposit in Gale Crater. *Journal of Geophysical Research: Planets* 118: 1955-1973. https://doi.org/10.1002/jgre.20144

Goldstein, R.H., and Reynolds, T.J. (1994). *Systematics of Fluid Inclusions in Diagenetic Minerals: SEPM Short Course Notes* (Tulsa, OK: SEPM Society for Sedimentary Geology).

Golombek, M., Grant, J., Kipp, D., et al. (2012) Selection of the Mars Science Laboratory Landing Site. *Space Science Reviews* 170: 641-737. https://doi.org/10.1007/s11214-012-9916-y

Gooding, J.L. (1992) Soil mineralogy and chemistry on Mars: Possible clues from salts and clays in SNC meteorites. *Icarus* 99: 28-41. https://doi.org/10.1016/0019-1035(92)90168-7

Goudge, T.A., Mustard, J.F., Head, J.W., et al. (2015) Assessing the mineralogy of the watershed and fan deposits of the Jezero crater paleolake system, Mars. *Journal of Geophysical Research Planets* 120: 775-808. https://doi.org/10.1002/2014JE004782

Gough, R.V., Chevrier, V.F., Baustian, K. J., Wise, M.E. and Tolbert, M.A. (2011) Laboratory studies of perchlorate phase transitions: support for metastable aqueous perchlorate solutions on Mars. *Earth and Planetary Science Letters* 312: 371–377. https://doi.org/10.1016/j.epsl.2011.10.026

Gough, R.V., Chevrier, V.F., Tolbert, M.A. (2014) Formation of aqueous solutions on Mars via deliquescence of chloride-perchlorate binary mixtures. *Earth and Planetary Science Letters* 393: 73–82. https://doi.org/10.1016/j.epsl.2014.02.002

Gough, R.V., Chevrier, V.F., Tolbert, M.A. (2016) Formation of liquid water at low temperatures via the deliquescence of calcium chloride: Implications for Antarctica and Mars. *Planetary and Space Science* 131: 79–87. https://doi.org/10.1016/j.pss.2016.07.006

Gounelle, M. and Zolensky, M.E. (2001) A terrestrial origin for sulfate veins in CI1 chondrites. *Meteoritics and Planetary Science 3*6: 1321–1329. https://doi.org/10.1111/j.1945-5100.2001.tb01827.x

Grady M.M., Gibson Jr E.K., Wright I.P., et al. (1989) The formation of weathering products on the LEW 85320 ordinary chondrite: Evidence from carbon and oxygen stable isotope compositions and implications for carbonates in SNC meteorites. *Meteoritics* 24: 1-7. https://doi.org/10.1111/j.1945-5100.1989.tb00934.x

Grant J.A., Golombek M.P., Wilson S.A., et al. (2018) The science process for selecting the landing site for the 2020 Mars rover. *Planetary and Space Science*, 164: 106-126. https://doi.org/10.1016/j.pss.2018.07.001

Grant, W. D. (2004) Life at low water activity. *Philosophical Transactions of the Royal Society of London. Series B: Biological Sciences*, 359: 1249-1267. https://doi.org/10.1098/rstb.2004.1502

Grim, R.E. (1953) Clay Mineralogy. McGraw-Hill, New York, pp. 384.

Hayakawa, A., Hatakeyama, M., Asano, R., Ishikawa, Y., and Hidaka, S. (2013) Nitrate reduction coupled with pyrite oxidation in the surface sediments of a sulfide-rich ecosystem. *Journal of Geophysical Research: Biogeosciences* 118: 639– 649. https://doi.org/10.1002/jgrg.20060

Hendrix, K. Bleyen, N., Mennecart, T., Bruggeman, C. Valcke, E. (2019) Sodium azide used as microbial inhibitor

caused unwanted by-products in anaerobic geochemical studies. *Journal of Applied Geochemistry* 107: 120-130. https://doi.org/10.1016/j.apgeochem.2019.05.014

Herkenhoff, K.E., Squyres, S.W., Arvidson, R., Bass, D.S., Bell, J.F., III, Bertelsen, P., Ehlmann, B.L., Farrand, W., Gaddis, L., Greeley, R., and others (2004) Evidence from Opportunity's Microscopic Imager for water on Meridiani Planum. *Science* 306: 1727-1730. https://doi.org/10.1126/science.1105286

Hill, A.E. (1937) The Transition Temperature of Gypsum to Anhydrite. *Journal of the American Chemical Society* 59: 2242–2244. https://doi.org/10.1021/ja01290a039

Holm, N. G., Oze, C., Mousis, O., Waite, J. H., & Guilbert-Lepoutre, A. (2015). Serpentinization and the Formation of H_2 and CH_4 on Celestial Bodies (Planets, Moons, Comets). Astrobiology, 15(7), 587–600. https://doi.org/10.1089/ast.2014.1188

Horgan, B.H.N., Anderson, R.B., Dromart G., et al. (2020) The mineral diversity of Jezero crater: Evidence for possible lacustrine carbonates on Mars. *Icarus* 339: 113526. https://doi.org/10.1016/j.icarus.2019.113526

Huang, W.-L., Bassett, W.A. and Wu, T.-C. (1994) Dehydration and hydration of montmorillonite at elevated temperatures and pressures monitored using synchrotron radiation. *American Mineralogist* 79: 683–691.

Hudson-Edwards, K.A., Schell, C., Macklin, M.G. (1999) Mineralogy and geochemistry of alluvium contaminated by metal mining in the Rio Tinto area, southwest Spain. *Applied Geochemistry* 14:1015-1030. https://doi.org/10.1016/S0883-2927(99)00008-6

Hurowitz, J.A., Grotzinger, J.P., Fischer, W.W., McLennan, S.M., Milliken, R.E., Stein, N., Vasavada, A.R., Blake, D.F., Dehouck, E., Eigenbrode, J.L., Fairén, A.G., Frydenvang, J., Gellert, R., Grant, J.A., Gupta, S., Herkenhoff, K.E., Ming, D.W., Rampe, E.B., Schmidt, M.E., Siebach, K.L., Stack-Morgan, K., Sumner, D.Y., Wiens, R.C. (2017) Redox stratification of an ancient lake in Gale crater, Mars. *Science* 356: 6849. https://doi.org/10.1126/science.aah6849

iMOST (International MSR Objectives and Samples Team) (2018) The potential science and engineering value of samples delivered to Earth by Mars Sample Return, (co-chairs D. W. Beaty, M. M. Grady, H. Y. McSween, E. Sefton-Nash; documentarian B.L. Carrier; plus 66 co-authors), 186 p. white paper. Posted August, 2018 by MEPAG at https://mepag.jpl.nasa.gov/reports.cfm.

Johnson, J.E., Savalia, P., Davis, R., Kocar, B.D., Webb, S.M., Nealson, K.H., Fischer, W.W. (2016) Real-Time Manganese Phase Dynamics during Biological and Abiotic Manganese Oxide Reduction. *Environmental Science and Technology* 50:4248-58. https://doi.org/10.1021/acs.est.5b04834

Jull, A.J.T., Cheng, S., Gooding, J. L., and Velbel, M.A. (1988) Rapid growth of magnesium-carbonate weathering products in a stony meteorite from Antarctica. *Science* 242: 417-419. https://doi.org/10.1126/science.242.4877.417

Kawano, M. and Tomita, K. (1991) Dehydration and rehydration of saponite and vermiculite. *Clays and Clay Minerals* 39: 174-183. https://doi.org/10.1346/CCMN.1991.0390209

Kempe, S. and Kazmierczak, J. (1997) A terrestrial model for an alkaline martian hydrosphere. *Planetary and Space Science* 45: 1493-1499. https://doi.org/10.1016/S0032-0633(97)00116-5

Kempe, S., and Kaźmierczak, J. (2011) Soda Lakes: In Encyclopedia of Geobiology, edited by V. Thiel and J. Reitner, Springer.

Korcek, S. Chenier, J. H. B., Howard, J. A. and Ingold. K. U. (1972) Absolute rate constants for hydrocarbon autoxidation. XXI. Activation energies for propagation and the correlation of propagation rate constants with Carbon–Hydrogen bond strengths. *Canadian Journal of Chemistry* 50: 2285-2297. https://doi.org/10.1139/v72-365

Kounaves, S.P., Chaniotakis, N.A., Chevrier, V.F., Carrier, B.L., Folds, K.E., Hansen, V.M., McElhoney, K.M., O'Neil, G.D., Weber, A.W. (2014) Identification of the perchlorate parent salts at the *Phoneix* Mars landing site and possible implications. *Icarus* 232: 226–231. https://doi.org/10.1016/j.icarus.2014.01.016

Langevin Y., Poulet F., Bibring J.P., Gondet B. (2005) Sulfates in the north polar region of Mars detected by OMEGA/Mars Express. *Science* 307:1584-6. https://doi.org/10.1126/science.1109091

Lanza, N. L., et al. (2014) High manganese concentrations in rocks at Gale crater, Mars, *Geophysical Research Letters* 41: 5755– 5763. https://doi.org/10.1002/2014GL060329

Lasne, J., Noblet, A., Szopa, C., Navarro-González, R., Cabane, M., Poch, O., Stalport, F., François, P., Atreya, S.K. and Coll, P., (2016) Oxidants at the surface of Mars: a review in light of recent exploration results. *Astrobiology*, 16: 977-996. https://doi.org/10.1089/ast.2016.1502

Lerman A. (1979) Geochemical Processes – Water and Sediment Environments. New York, Wiley, pp 481.

Li, L. Sheerwood Lollar, B., Li, H., Wortmann, U.G., Lacrampe-Couloume G. (2012) Ammonium stability and nitrogen isotope fractionations for NH_3(aq)–NH_3(gas) systems at 20–70 °C and pH of 2–13: applications to habitability and nitrogen cycling in low-temperature hydrothermal systems. *Geochimica et Cosmochimica Acta* 84: 280-296. https://doi.org/10.1016/j.gca.2012.01.040

Li Y.-H. and Gregory S. (1974) Diffusion of ions in sea water and in deep-sea sediments. *Geochimica et Cosmochimica Acta* 38: 703-714. https://doi.org/10.1016/0016-7037(74)90145-8

Lowenstein, T. K., Schubert, B. A., and Timofeeff, M. N. (2011). Microbial communities in fluid inclusions and long-term survival in halite. *GSA Today* 21: 4-9. https://doi.org/10.1130/GSATG81A.1

Machel, H.G. (2001) Bacterial and thermochemical sulfate reduction in diagenetic settings — old and new insights. *Sedimentary Geology* 140: 143-175. https://doi.org/10.1016/S0037-0738(00)00176-7

Marion, G.M., Kargel, J.S., (2008) Cold Aqueous Planetary Geochemistry with FREZCHEM: From Modeling to the Search for Life at the Limits. Springer, Berlin/Heidelberg. https://doi.org/10.1007/978-3-540-75679-8

Marion, G.M., Catling, D.C., Kargel, J.S. (2009) Br/Cl partitioning in chloride minerals in the Burns formation on Mars. *Geochimica et Cosmochimica Acta* 200: 436-445. https://doi.org/10.1016/j.icarus.2008.12.004

Marion, G.M., Catling, D.C., Zahnle, K.J., Claire, M.W. (2010) Modeling aqueous perchlorate chemistries with applications to Mars. *Icarus* 207: 675–685. https://doi.org/10.1016/j.icarus.2009.12.003

Marvin, G.G. and Woolaver, L.B. (1945) Thermal decomposition of perchlorates. *Industrial and Engineering Chemistry Analytical Edition* 17:474–476.

Mahaffy, P. R., Webster, C.R., Cabane M., et al. (2012) The Sample Analysis at Mars Investigation and Instrument Suite. *Space Science Reviews* 170: 401–478. https://doi.org/10.1007/s11214-012-9879-z

Mandon, L., Royer, C., Beck, P., et al. (2021) Spectral diversity of rocks and regolith at Jezero crater, Mars, as seen by the SuperCam VISIR spectrometer onboard *Perseverance*. American Geophysical Union Fall Meeting 2021 Abstract P22B-04.

McCollom, T. M., Donaldson C. (2016) Generation of hydrogen and methane during experimental low-temperature reaction of ultramafic rocks with water. *Astrobiology* 16: 389–406. https://doi.org/10.1089/ast.2015.1382.

McLennan, S.M., Bell, J.F., III., Calvin, W.M., Christensen, P.R., Clark, B.C., de Souza, P.A., Farmer, J., Farrand, W.H., Fike, D.A., Gellert, R., et al. (2005) Provenance and diagenesis of the evaporite-bearing Burns formation, Meridiani Planum, Mars. *Earth and Planetary Science Letters* 240: 95-121. https://doi.org/10.1016/j.epsl.2005.09.041

MEPAG (Mars Exploration Program Analysis Group) (2008) Science Priorities for Mars Sample Return *Astrobiology* 8: 489–535. https://doi.org/10.1089/ast.2008.0759

Meslin P.-Y., Forni O., Beck P., Cousin A., Beyssac O., et al. (2022) Evidence for Perchlorate and Sulfate Salts in Jezero Crater, Mars, from Supercam Observations. Lunar and Planetary Science Conference LIII, Abstract #2694. https://www.hou.usra.edu/meetings/lpsc2022/pdf/2694.pdf

Milliken, R.E., Grotzinger, J.P., Thomson, B.J., (2010) Paleoclimate of Mars as captured by the stratigraphic record in Gale Crater. *Geophysical Research Letters* 37. https://doi.org/10.1029/2009GL041870

Moeller, R.C., Jandura, L., Rosette, K. et al. (2021) The Sampling and Caching Subsystem (SCS) for the Scientific Exploration of Jezero Crater by the Mars 2020 *Perseverance* Rover. *Space Science Reviews* 217: 5 https://doi.org/10.1007/s11214-020-00783-7

Molenda, M., Stengler, J., Linder, M., Worner, A. (2013) Reversible hydration behavior of $CaCl_2$ at high H_2O partial pressures for thermochemical energy storage, *Thermochim Acta* 560: 76–81. https://doi.org/10.1016/j.tca.2013.03.020

Moody, J.B., 1976. Serpentinization: a review. *Lithos*, 9: 125-138. https://doi.org/10.1016/0024-4937(76)90030-X

Morgan B., Wilson S. W., Madsen I. C., Gozukara Y. M., and Habsuda J. (2015) Increased thermal stability of nesquehonite ($MgCO_3 \cdot 3H_2O$) in the presence of humidity and CO_2: Implications for low-temperature CO_2 storage. *International Journal of Greenhouse Gas Control* 39: 366–376. https://doi.org/10.1016/j.ijggc.2015.05.033

Moses, C.O. and Herman, J.S. (1991) Pyrite oxidation at circumneutral pH. *Geochimica et Cosmochimica Acta* 55: 471–482. https://doi.org/10.1016/0016-7037(91)90005-P

Navarro-González, R., Rainey, F.A., Molina, P., Bagaley, D.R., Hollen, B.J., de la Rosa, J., Small, A.M., Quinn, R.C., Grunthaner, F.J., Cáceres, L., Gomez-Silva, B., McKay, C.P. (2003) Mars-Like Soils in the Atacama Desert, Chile, and the Dry Limit of Microbial Life. *Science* 302, 1018–1021. https://doi.org/10.1126/science.1089143

Neal, C.R. (2000) Issues involved in a Martian sample return: Integrity preservation and the Curation and Analysis Planning Team for Extraterrestrial Materials (CAPTEM) position. *Journal of Geophysical Research: Planets*, 105: 22487-22506. https://doi.org/10.1029/1999JE001185Neubeck, A., Duc, N.T., Bastviken, D. et al. (2011) Formation of H_2 and CH_4 by weathering of olivine at temperatures between 30 and 70°C. *Geochem Trans* 12: 6. https://doi.org/10.1186/1467-4866-12-6

Nienow, J.A., Friedmann, E.I. (1993). Terrestrial lithophytic (rock) communities. In: Friedmann E.I. (ed.) Antarctic Microbiology. Wiley-Liss, New York, pp 343–412.

Novak, K., Daimaru, T., & Bhandari, P. (2022). Final Thermal Design of the Mars 2020 Sample Tube. 51st International Conference on Environmental Systems, 10-14 July 2022, St. Paul, Minnesota.

Nuding, D., Rivera-Valentin, E., Davis, R., Gough, R., Chevrier, V., Tolbert, M. (2014) Deliquescence and efflorescence of calcium perchlorate: An investigation of stable aqueous solutions relevant to Mars. *Icarus* 243: 420–428. https://doi.org/10.1016/j.icarus.2014.08.036

Ohmoto, H., Lasaga, A. L. (1982) Kinetics of reactions between aqueous sulfates and sulfides in hydrothermal systems. *Geochimica et Cosmochimica Acta* 46:1727–1745. https://doi.org/10.1016/0016-7037(82)90113-2

Onofri, S., de Vera, J.P., Zucconi, L., Selbmann, L., Scalzi, G., Venkateswaran, K.J., Rabbow, E., de la Torre, R., Horneck, G. (2015) Survival of Antarctic cryptoendolithic fungi in simulated Martian conditions on board the international space station. *Astrobiology* 15: 1052-1059. https://doi.org/10.1089/ast.2015.1324

Parente M., Bishop J. L., Saranathan A. M., Szynkiewicz A., and Fenton L. (2022) Detection of Bassanite in the North Polar Dunes of Mars and Implications for Aqueous Activity. Lunar and Planetary Science Conference LIII, Abstract #2342. https://www.hou.usra.edu/meetings/lpsc2022/pdf/2342.pdf

Peterson, R.C., and Wang, R. (2006) Crystal molds on Mars: Melting of a possible new mineral species to create Martian chaotic terrain. *Geology* 34: 957–960. https://doi.org/10.1130/G22678A.1

Peterson, R.C., Nelson, W., Madu, B., and Shurvell, H.F. (2007) Meridianiite: A new mineral species observed on Earth and predicted to exist on Mars. *American Mineralogist*, 92: 1756-1759. https://doi.org/10.2138/am.2007.2668

Poppe, L.J., Paskevich, V.F., Hathaway, J.C., and Blackwood, D.S. (2001) A Laboratory Manual for X-Ray Powder Diffraction. U. S. Geological Survey Open-File Report 01-041. https://pubs.usgs.gov/of/2001/of01-041/

Price, L.C. (1993) Thermal stability of hydrocarbons in nature - Limits, evidence, characteristics, and possible controls. *Geochimica et Cosmochimica Acta* 57: 3261–3280. https://doi.org/10.1016/0016-7037(93)90539-9

Primm, K.M., Gough, R.V., Chevrier, V. F. and Tolbert, M.A. (2017). Freezing of perchlorate and chloride brines under mars-relevant conditions. *Geochimica et Cosmochimica Acta* 212: 211–220. https://doi.org/10.1016/j.gca.2017.06.012

Quinn, R.C., Martucci, H. F., Miller, S.R., Bryson, C.E., Grunthaner, F.J., and Grunthaner, P.J. (2013) Perchlorate radiolysis on Mars and the origin of martian soil reactivity. *Astrobiology*, 13: 515-520. https://doi.org/10.1089/ast.2013.0999

Rabbow, E., Rettberg, P., Barczyk, S., Bohmeier, M., Parpart, A., Panitz, C., Horneck, G. von, Heise-Rotenburg, R., Hoppenbrouwers, T., Willnecker, R., Baglioni, P., Demets, R., Dettmann, J., and Reitz, G. (2012) EXPOSE-E: an ESA astrobiology mission 1.5 years in space. *Astrobiology* 12: 374–386. https://doi.org/10.1089/ast.2011.0760

Rabbow, E., Rettberg, P., Parpart, A., Panitz, C., Schulte, W., Molter, F., Jaramillo, E., Demets, R., Weiß, P., Willnecker, R. (2017) EXPOSE-R2: The Astrobiological ESA Mission on Board of the International Space Station. *Frontiers in Microbiology* 15;8:1533. https://doi.org/10.3389/fmicb.2017.01533

Rampe, E.B., Ming, D.W., Blake, D. F., et al. (2017) Mineralogy of an ancient lacustrine mudstone succession from the Murray formation, Gale crater, Mars. *Earth and Planetary Science Letters*, 471: 172-185. https://doi.org/10.1016/j.epsl.2017.04.021

Rampe, E.B., Blake, D.F., Bristow, T.F., et al. (2020) Mineralogy and geochemistry of sedimentary rocks and eolian sediments in Gale crater, Mars: A review after six Earth years of exploration with *Curiosity*. *Geochemistry* 80: 125605. https://doi.org/10.1016/j.chemer.2020.125605

Rampe, E.B., Bristow, T.F., Blake, D.F., Vaniman, D.T., Chipera, S.J., et al. (2022) Mineralogical trends over the clay-sulfate transition in Gale Crater from the Mars Science Laboratory CheMin instrument. LPSCLIII Abstract #1532.

Redmond, M., Sherman, S., Bhandari, P., and Novak, K. (2017) Thermal Design, Analysis, and Sensitivity of a Sample Tube on the Martian Surface. 47th International Conference on Environmental Systems 16-20 July 2017, Charleston, SC, ICES-2017-115.

Reinecke, S.A. and Sleep, B.E. (2002) Knudsen diffusion, gas permeability, and water content in an unconsolidated porous medium, *Water Resources Research*38: 1280. https://doi.org/10.1029/2002WR001278

Ren, H., Chen, Z., Wu, Y., Yang, M., Chen J., Hu H.., and Liu J. (2014). Thermal characterization and kinetic analysis of nesquehonite, hydromagnesite, and brucite, using TG–DTG and DSC techniques. *Journal of Thermal Analysis and Calorimetry* 115: 1949–1960. https://doi.org/10.1007/s10973-013-3372-0

Returned Sample Science Board (RSSB) (2018) Summary of sample quality standards for returned Martian samples. 49th Lunar and Planetary Science Conference, abstract #1516. https://www.hou.usra.edu/meetings/lpsc2018/pdf/1516.pdf

Ritterbach L. and Becker P. (2020) Temperature and humidity dependent formation of $CaSO_4 \cdot xH_2O$ (x = 0…2) phases. *Global and Planetary Change* 187: 103132. https://doi.org/10.1016/j.gloplacha.2020.103132

Robertson, K., and Bish, D. (2011), Stability of phases in the $Mg(ClO_4)_2 \cdot nH_2O$ system and implications for perchlorate occurrences on Mars. *Journal of Geophysical Research* 116: E07006. https://doi.org/10.1029/2010JE003754

Roedder E (1984) The fluids in salt. *American Mineralogist* 69: 413–39.

Royle, S.H., Oberlin, E., Watson, J.S., Montgomery, W., Kounaves, S.P., and Sephton, M.A. (2018) Perchlorate-driven combustion of organic matter during pyrolysis-gas chromatography-mass spectrometry: Implications for organic matter detection on Earth and Mars. *Journal of Geophysical Research: Planets* 123: 1901–1909. https://doi.org/10.1029/2018JE005615

Russell, M.J., Ingham, J.K., Zedef V., et al. (1999) Search for signs of ancient life on Mars: expectations from hydromagnesite microbialites, Salda Lake, Turkey. *Journal of the Geological Society (London)* 156: 869-888.

https://doi.org/10.1144/gsjgs.156.5.0869

Sawhney, B. L. (1958) Aluminium lnterlayers in Soil Clay Minerals, Montmorillonite and Vermiculite. *Nature* 182: 1595-1596. https://doi.org/10.1038/1821595a0

Sawhney, B. L. (1960a) Weathering and Aluminum Interlayers in a Soil Catena: Hollis — Charlton — Sutton — Leicester. *Soil Science Society of America Proceedings* 24: 221-226. https://doi.org/10.2136/sssaj1960.03615995002400030028x

Sawhney, B.L. (1960b) Aluminium lnterlayers in Clay Minerals, Montmorillonite and Vermiculite: Laboratory Synthesis. *Nature* 187: 261-262. https://doi.org/10.1038/187261a0

Salvatore, M.R., Goudge T.A., Bramble, M.S., Edwards C.S., Bandfield J.L., Amador E.S., Mustard, J.F., and Christen, P.R. (2018) Bulk mineralogy of the NE Syrtis and Jezero crater regions of Mars derived through thermal infrared spectral analyses. *Icarus* 301: 76–96. https://doi.org/10.1016/j.icarus.2017.09.019

Scalzi, G., Selbmann, L., Zucconi, L., Rabbow, E., Horneck, G., Albertano, P., and Onofri, S. (2012) LIFE experiment: isolation of cryptoendolithic organisms from Antarctic colonized sandstone exposed to space and simulated Mars conditions on the International Space Station. *Orig Life Evol Biosph* 42: 253–262. https://doi.org/10.1007/s11084-012-9282-5

Scheller, E.L., Swindle, C., Grotzinger, J., Barnhart, H., Bhattacharjee, S., Ehlmann, B.L., et al. (2021). Formation of magnesium carbonates on Earth and implications for Mars. *Journal of Geophysical Research: Planet*s, 126, e2021JE006828. https://doi.org/10.1029/2021JE006828

Scheller E.L., Razzell Hollis J., Cardarelli E.L., Steele A., Beegle L.W., et al. (2022) First-Results from the Perseverance SHERLOC Investigation: Aqueous Alteration Processes and Implications for Organic Geochemistry in Jezero Crater, Mars. Lunar and Planetary Science Conference LIII Abstract #1652. https://www.hou.usra.edu/meetings/lpsc2022/pdf/1652.pdf

Schmidt M.E., Allwood, A. Clark, B.C. et al. (2021) Naltsos, First Rock Examined by the M2020 PIXL Instrument: Rock Components and Dust Characteristics. American Geophysical Union Fall Meeting 2021 Abstract #P21B-07.

Sephton, M.A., Pillinger, C.T., Gilmour, I. (2000) Aromatic moieties in meteoritic macromolecular materials: Analyses by hydrous pyrolysis and $\delta^{13}C$ of individual compounds. *Geochimica Cosmochimica Acta* 64: 321–328. https://doi.org/10.1016/S0016-7037(99)00282-3

Sephton, M.A., Pillinger, C.T., Gilmour, I. (2001) Normal alkanes in meteorites: molecular $\delta^{13}C$ values indicate an origin by terrestrial contamination. *Precambrian Research* 106: 47-58. https://doi.org/10.1016/S0301-9268(00)00124-8

Smith, A.M.L., Hudson-Edwards, K.A., Dubbin, W.E., Wright, K. (2006) Dissolution of jarosite [$KFe_3(SO_4)_2(OH)_6$] at pH 2 and 8: Insights from batch experiments and computational modelling. *Geochimica et Cosmochimica Acta* 70: 608–621. https://doi.org/10.1016/j.gca.2005.09.024

Speight, J.G., 2017. Chapter 3 - Industrial Organic Chemistry, in: Speight, J.G. (Ed.), Environmental Organic Chemistry for Engineers. Butterworth-Heinemann, pp. 87–151. https://doi.org/10.1016/B978-0-12-804492-6.00003-4

Squyres, S.W., Arvidson, R.E., Bell, J.F., III, Brückner, J., Cabrol, N.A., Calvin, W., Carr, M.H., Christensen, P.R., Clark, B.C., Crumpler, L., and others (2004) The Opportunity Rover's Athena science investigation at Meridiani Planum, Mars. *Science* 306: 1698-1703. https://doi.org/10.1126/science.1106171

Steele, A., McCubbin, F.M., Fries, M., Kater, L., Boctor, N.Z., Fogel, M.L., et al. (2012) A reduced organic carbon component in Martian basalts. *Science* 337: 212–215. https://doi.org/10.1126/science.1220715

Steiger, M., Linnow, K., Ehrhardt,D., Rohde, M. (2011) Decomposition reactions of magnesium sulfate hydrates and phase equilibria in the $MgSO_4$–H_2O and Na^+–Mg^{2+}–Cl–SO_4^{2-} -H_2O systems with implications for Mars. *Geochimica et Cosmochimica Acta* 75: 3600-3626. https://doi.org/10.1016/j.gca.2011.03.038

Stern, J.C., Sutter, B., Freissinet, C., Navarro-González, R., McKay, C.P., Archer, P.D., et al. (2015) Evidence for Indigenous Nitrogen in Sedimentary and Aeolian Deposits from the *Curiosity* Rover Investigations at Gale Crater, Mars. *Proceedings of the National Academy of Science USA* 112, 4245–4250. https://doi.org/10.1073/pnas.1420932112

Stopar, J.D., Taylor, G.J., Velbel, M.A., et al. (2013) Element abundances, patterns, and mobility in nakhlite Miller Range 03346 and implications for aqueous alteration. *Geochimica et Cosmochimica Acta* 112: 208-225. https://doi.org/10.1016/j.gca.2013.02.024

Summers, D., Chang, S. (1993) Prebiotic ammonia from reduction of nitrite by iron (II) on the early Earth. *Nature* 365 : 630–633. https ://doi.org/10.1038/365630a0

Sutter, B., McAdam, A.C., Mahaffy, P.R., et al. (2017) Evolved gas analyses of sedimentary rocks and eolian sediment in Gale Crater, Mars: Results of the *Curiosity* rover's sample analysis at Mars instrument from Yellowknife Bay to the Namib Dune. *Journal of Geophysical Research: Planets* 122: 2574-2609. https://doi.org/10.1002/2016JE005225

Suzuki, S., Sato, H., Ishidera, T., and Fujii, N. (2004) Study on anisotropy of effective diffusion coefficient and activation energy for deuterated water in compacted sodium bentonite. *Journal of Contaminant Hydrology* 68: 23–37. https://doi.org/10.1016/S0169-7722(03)00139-6

Tan, J.S.W. and Sephton, M. A. (2020) Organic Records of Early Life on Mars: The Role of Iron, Burial, and Kinetics on Preservation. *Astrobiology* 20: 53-72. https://doi.org/10.1089/ast.2019.2046

Tan J.S.W., Royle S.H., Sephton M.A. (2021) Artificial Maturation of Iron- and Sulfur-Rich Mars Analogues: Implications for the Diagenetic Stability of Biopolymers and Their Detection with Pyrolysis-Gas Chromatography-Mass Spectrometry. *Astrobiology* 21: 199-218. https://doi.org/10.1089/ast.2019.2211

Tan, J.S.W. and Sephton, M.A. (2021) Quantifying Preservation Potential: Lipid Degradation in a Mars-Analog Circumneutral Iron Deposit. *Astrobiology* 21: 638-654. https://doi.org/10.1089/ast.2020.2344

Toner, J.D. and Catling D. C. (2018) Chlorate brines on Mars: Implications for the occurrence of liquid water and deliquescence. *Earth and Planetary Science Letters* 497: 161-168. https://doi.org/10.1016/j.epsl.2018.06.011

Tosca, N.J., Agee, C.B., Cockell, C.S., Glavin, D.P., Hutzler, A., Marty, B., McCubbin, F.M., Regberg, A.B., Velbel, M.A., Kminek, G., Meyer, M.A., Beaty, D.W., Carrier, B.L., Haltigin, T., Hays, L.E., Busemann, H., Cavalazzi, B., Debaille, V., Grady, M.M., Hauber, E., Pratt, L.M., Smith, A.L., Smith, C.L., Summons, R.E., Swindle, T.D., Tait, K.T., Udry, A., Usui, T., Wadhwa, M., Westall, F., Zorzano, M.-P., 2022. Time-Sensitive Aspects of Mars Sample Return (MSR) Science. *Astrobiology* 22, S-81 – S-111. https://doi.org/10.1089/ast.2021.0115

Treiman, A. H., et al. (2014) Ferrian saponite from the Santa Monica Mountains (California, U.S.A., Earth): Characterization as an analog for clay minerals on Mars with application to Yellowknife Bay in Gale Crater, *American Mineralogist* 99: 2234–2250. https://doi.org/10.2138/am-2014-4763

Tu, V.M., Rampe, E.B., Bristow, T.F., Thorpe, M.T., Clark, J.V., Castle, N., Fraeman, A.A., Edgar, L.A., McAdam, A., Bedford, C., et al. (2021) A Review of the Phyllosilicates in Gale Crater as Detected by the CheMin Instrument on the Mars Science Laboratory, *Curiosity* Rover. *Minerals* 11: 847. https://doi.org/10.3390/min11080847

Vaniman, D.T. and Chipera, S.J. (2006) Transformations of Mg- and Ca-sulfate hydrates in Mars regolith. *American Mineralogist* 91: 1628-1642. https://doi.org/10.2138/am.2006.2092

Vaniman, D.T., Bish, D.L. and Chipera, S.J. (2008) Calcium sulfate hydration, stability, and transformation on Mars. Lunar and Planetary Science XXXIX, Abstract #1816. https://www.lpi.usra.edu/meetings/lpsc2008/pdf/1816.pdf

Vaniman, D.T., Bish, D.L., Ming, D.W., Bristow, T.F., Morris, R.V., Blake, D.F., Chipera, S.J., Morrison, S.M., Treiman, A.H., Rampe, E.B., Rice, M., Achilles, C.N., Grotzinger, J.P., McLennan, S.M., Williams, J., Bell III, J.F., Newsom, H.E., Downs, R.T., Maurice, S., Sarrazin, P., Yen, A.S., Morookian, J.M., Farmer, J.D., Stack, K., Milliken, R.E., Ehlmann, B.L., Sumner, D.Y., Berger, G., Crisp, J.A., Hurowitz, J.A., Anderson, R., Des Marais, D.J., Stolper, E.M., Edgett, K.S., Gupta, S., Spanovich N., and MSL Science Team (2014) Mineralogy of a Mudstone at Yellowknife Bay, Gale Crater, Mars. *Science* 343: 1243480. https://doi.org/10.1126/science.1243480

Vaniman, D.T., Martinex, G.M., Rampe, E.B., Bristow, T.F., Blake, D.F., Yen, A.S., Ming, D.W., Rapin, W., Meslin, P.Y., Morookian, J.M., et al. (2018) Gypsum, basanite, and anhydrite at Gale crater, Mars. *American Mineralogist* 103: 1011–1020. https://doi.org/10.2138/am-2018-6346

Velbel, M.A. (2012) Aqueous alteration in Martian meteorites: Comparing mineral relations in igneous-rock weathering of Martian meteorites and in the sedimentary cycle of Mars. In Grotzinger, J., and Milliken, R. (eds.) Sedimentary Geology of Mars, SEPM – Society for Sedimentary Geology Special Publication 102: 97-117. https://doi.org/10.2110/pec.12.102.0097 http://sp.sepmonline.org/content/sepsp102/1.toc

Velbel, M.A. (2018) Crystallography on Mars – *Curiosity*'s Bragging right. (Highlights and Breakthroughs: Invited) *American Mineralogist* 103: 837-838. https://doi.org/10.2138/am-2018-6468CCBYNCND

Velbel, M.A., and Zolensky, M.E. (2021). Thermal metamorphism of CM chondrites: A dehydroxylation-based peak-temperature thermometer and implications for sample return from asteroids Ryugu and Bennu. *Meteoritics and Planetary Science*, v. 56, p. 546-585. https://onlinelibrary.wiley.com/doi/full/10.1111/maps.13636

Velbel, M.A., Long, D.T., and Gooding J.L. (1991) Terrestrial weathering of Antarctic stone meteorites: Formation of Mg-carbonates on ordinary chondrites. *Geochimica et Cosmochimica Acta* 55: 67-76. https://doi.org/10.1016/0016-7037(91)90400-Y

Velbel, M.A., Beaty, D.W., Carrier, B.L., Cockell, C.S., Glavin, D.P., Marty, B., Regberg, A.B., Smith, A.L., Tosca, N.J., Wadhwa, M., Kminek, G., Meyer, M.A., Haltigin, T., Hays, L. E., Agee, C., Busemann, H. Cavalazzi, B., Debaille, V., Grady, M.M., Hauber, E., Hutzler, A., McCubbin, F. M., Pratt, L.M., Smith, C.L., Summons, R.E. Swindle, T.D., Tait, K.T., Udry, A., Usui, T., Westall, F., and Zorzano, M.-P., and the MSPG2 (2022) Planning Implications Related to Sterilization-Sensitive Science Investigations Associated with Mars Sample Return (MSR). *Astrobiology* 22: S-112 – S-164. https://doi.org/10.1089/ast.2021.0113

Wang, A., Freeman, J.J. and Jolliff, B.L. (2009) Phase transition pathways of the hydrates of magnesium sulfate in the temperature range 50°C to 5°C: Implication for sulfates on Mars, *Journal of Geophysical Research* 114: E04010. https://doi.org/10.1029/2008JE003266

Wang, A., Freeman, J. J., Chou, I.-M. and Jolliff, B. L. (2011), Stability of Mg-sulfates at −10°C and the rates of dehydration/rehydration processes under conditions relevant to Mars, *Journal of Geophysical Research* 116: E12006. https://doi.org/10.1029/2011JE003818

Wang, A., Ling, Z., Yan, Y., McEwen, A.S., Mellon, M.T., Smith, M.D., Jolliff, B.L., and Head, J. (2019) Subsurface Cl-bearing salts as potential contributors to recurring slope lineae (RSL) on Mars. *Icarus* 333: 464–480. https://doi.org/10.1016/j.icarus.2019.06.024

Wassmann, M., Moeller, R., Rabbow, E., Panitz, C., Horneck, G., Reitz, G., Douki, T., Cadet, J., Stan-Lotter, H., Cockell, C.S., and Rettberg P. (2012). Survival of spores of the UV-resistant Bacillus subtilis strain MW01 after exposure to low-earth orbit and simulated martian conditions: data from the space experiment ADAPT on EXPOSE-E. *Astrobiology* 12: 498–507. https://doi.org/10.1089/ast.2011.0772

Watson, J., Sephton, M., and Gilmour, I. (2010). Thermochemolysis of the Murchison meteorite: Identification of oxygen bound and occluded units in the organic macromolecule. *International Journal of Astrobiology* 9: 201-208. https://doi.org/10.1017/S1473550410000194

Wentworth, S.J., Gibson, E.K., Velbel, M.A., and McKay, D.S. (2005) Antarctic Dry Valleys and Indigenous Weathering in Mars Meteorites: Implications for Water and Life on Mars. *Icarus* 174: 382-395. http://dx.doi.org/doi:10.1016/j.icarus.2004.08.026

Whittaker, M.L., Lammers, L.N., Carrero, S., Gilbert, B., and Banfield, J. F. (2019) Ion exchange selectivity in clay is controlled by nanoscale chemical–mechanical coupling. *Proceedings of the National Academy of Science USA*, 116: 22052-22057. https://doi.org/10.1073/pnas.1908086116

Wilson S. A. and Bish D. L. (2012) Stability of Mg-sulfate minerals in the presence of smectites: Possible mineralogical controls on H_2O cycling and biomarker preservation on Mars. *Geochimica et Cosmochimica Acta* 96:

120-133. https://doi.org/10.1016/j.gca.2012.08.008

Wierzchos, J., and Ascaso, C. (2002) Microbial fossil record of rocks from the Ross Desert, Antarctica: implications in the search for past life on Mars. *International Journal of Astrobiology* 1: 51-59. https://doi.org/10.1017/S1473550402001052

Wise, M.E., Baustian, K.J., Koop, T., Freedman, M.A., Jensen E.J., Tolbert, M.A. (2012) Depositional ice nucleation onto crystalline hydrated NaCl particles: a new mechanism for ice formation in the troposphere. *Atmos Chem Phys* 12: 1121–1134. https://doi.org/10.5194/acp-12-1121-2012

Wray, J.J., Squyres, S.W., Roach, L.H., Bishop, J.L., Mustard, J.F. and NoeDobrea, E.Z. (2010). Diverse aqueous conditions on Mars from new orbital detections of carbonate and sulfate. *Icarus* 209: 416–421.

Xu, J., Li, T., Yan, T., Chao, J., and Wang, R. (2021) Dehydration kinetics and thermodynamics of magnesium chloride hexahydrate for thermal energy storage. *Solar Energy Materials and Solar Cells* 219: 110819. https://doi.org/10.1016/j.solmat.2020.110819

Yen, A.S., Kim, S.S., Hecht, M.H., Frant, M.S., and Murray, B. (2000) Evidence that the reactivity of the Martian soil is due to superoxide ions. *Science* 289: 1909-1912. https://doi.org/10.1126/science.289.5486.1909

Zent, A.P. and McKay, C.P. (1994) The chemical reactivity of the martian soil and implications for future missions. *Icarus* 108: 146-157. https://doi.org/10.1006/icar.1994.1047.

Zhang, J., Quay, P. D., and Wilbur, D. O. (1995) Carbon isotope fractionation during gas-water exchange and dissolution of CO_2. *Geochimica et Cosmochimica Acta* 59: 107–114. https://doi.org/10.1016/0016-7037(95)91550-D

Zorzano, M.P., Mateo-Martí, E., Prieto-Ballesteros, O., Osuna, S., Renno, N. (2009) Stability of liquid saline water on present day Mars. *Geophysical Research Letters* 36, L20201. https://doi.org/10.1029/2009GL040315

[MZ1]Removed italics to be consistent with the rest of the text.

[MZ2]Combine with preceding paragraph.

[MZ3]These are redundant statements (see the moved text above). Consider consolidation (delete this nitrate text and refer to the text above).

[MZ4]Maybe it is tome to update wording and references (in was written in early 2022)?

[VM5]If this were a review paper, then I would concur. However, a major role of this paper is preserve for the easily accessible public (science community) record the basis of the advice that T4 gave to Campaign leadership in March 2022.

[MS6]The addition of the last paragraph before section 1.4 now keeps all this clear and in line.

[MZ7]Format: wt.% or wt% (next line)?

[VM8]I redirect this question to Sherry.

[MZ9]This text of nitrates is redundant as well.

[MS10]I've also reworded the comments so that each mention is different.

[MZ11]Different format in the middle